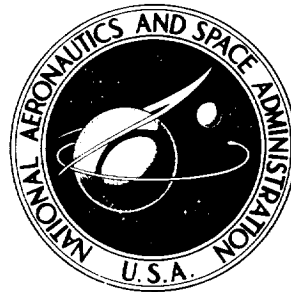


NASA TECHNICAL NOTE



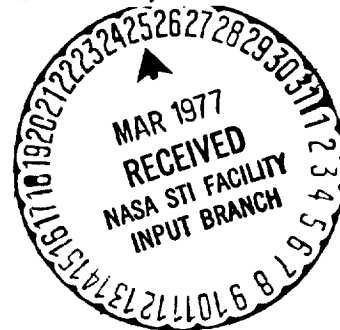
NASA TN D-8430

NASA TN D-8430

(NASA-TN-D-8430) REVISED FORTRAN PROGRAM  
FOR CALCULATING VELOCITIES AND STREAMLINES  
ON THE HUB-SHROUD MIDCHANNEL STREAM SURFACE  
OF AN AXIAL-, RADIAL-, OR MIXED-FLOW  
TURBOMACHINE OR ANNULAR DUCT. 1: USER'S

N77-18992  
HC A06  
MF A01  
Unclas  
21299

H1/01



REVISED FORTRAN PROGRAM FOR  
CALCULATING VELOCITIES AND STREAMLINES  
ON THE HUB-SHROUD MIDCHANNEL STREAM  
SURFACE OF AN AXIAL-, RADIAL-, OR  
MIXED-FLOW TURBOMACHINE OR ANNULAR DUCT

I - User's Manual

*Theodore Katsanis and William D. McNally*

*Lewis Research Center*

*Cleveland, Ohio 44135*



1. Report No. NASA TN D-8430		2. Government Accession No.		3. Recipient's Catalog No.	
4. Title and Subtitle REVISED FORTRAN PROGRAM FOR CALCULATING VELOCITIES AND STREAMLINES ON THE HUB-SHROUD MIDCHANNEL STREAM SURFACE OF AN AXIAL-, RADIAL-, OR MIXED-FLOW TURBOMACHINE OR ANNULAR DUCT I - USER'S MANUAL				5. Report Date March 1977	
				6. Performing Organization Code	
7. Author(s) Theodore Katsanis and William D. McNally				8. Performing Organization Report No. E-8734	
				10. Work Unit No. 505-04	
9. Performing Organization Name and Address Lewis Research Center National Aeronautics and Space Administration Cleveland, Ohio 44135				11. Contract or Grant No.	
				13. Type of Report and Period Covered Technical Note	
12. Sponsoring Agency Name and Address National Aeronautics and Space Administration Washington, D. C. 20546				14. Sponsoring Agency Code	
15. Supplementary Notes Supersedes NASA TN D-7343 (FORTRAN Program for Calculating Velocities and Streamlines on the Hub-Shroud Mid-Channel Flow Surface of an Axial- or Mixed-Flow Turbomachine, 1973)					
16. Abstract A FORTRAN-IV computer program has been developed that obtains a detailed subsonic or shock-free transonic flow solution on the hub-shroud midchannel stream surface of a turbomachine. The blade row may be fixed or rotating, and the blades may be twisted and leaned. Flow may be axial, mixed, or radial. This program is a revision of a previous program and this report supersedes NASA TN D-7343. Upstream and downstream flow variables may vary from hub to shroud, and provision is made to correct for loss of stagnation pressure. The results include velocities, streamlines, and flow angles on the stream surface as well as approximate blade surface velocities. Subsonic solutions are obtained by a finite-difference, stream-function solution. Transonic solutions are obtained by a velocity-gradient method that uses information from a finite-difference, stream-function solution at a reduced mass flow.					
17. Key Words (Suggested by Author(s)) Meridional plane; Turbomachine flow; Midchannel stream surface; Axial-flow turbomachine; Mixed-flow turbomachine; Transonic flow; Radial-inflow turbine; Centrifugal compressor			18. Distribution Statement Unclassified - unlimited STAR Category 01		
19. Security Classif. (of this report) Unclassified		20. Security Classif. (of this page) Unclassified		21. No. of Pages 105	22. Price* A06

\* For sale by the National Technical Information Service, Springfield, Virginia 22161



# CONTENTS

	Page
<u>SUMMARY</u> . . . . .	1
<u>INTRODUCTION</u> . . . . .	2
<u>METHOD OF ANALYSIS</u> . . . . .	5
BASIC ASSUMPTIONS . . . . .	5
SOLUTION BY COMBINATION OF METHODS . . . . .	6
SUBSONIC STREAM-FUNCTION SOLUTION . . . . .	6
TRANSONIC VELOCITY-GRADIENT APPROXIMATE SOLUTION . . . . .	8
BLADE SURFACE VELOCITIES . . . . .	9
<u>APPLICATION OF PROGRAM</u> . . . . .	9
<u>DESCRIPTION OF INPUT AND OUTPUT</u> . . . . .	10
INPUT . . . . .	11
Input Dictionary . . . . .	17
Special Instructions for Preparing Input . . . . .	25
(a) Units of measurement . . . . .	26
(b) Damping factors FNEW and DNEW . . . . .	26
(c) Hub and shroud flow channel geometry . . . . .	26
(d) Orthogonal mesh . . . . .	27
(e) Upstream and downstream flow conditions . . . . .	27
(f) Mean blade surface and thickness coordinates . . . . .	28
(g) How to specify points for spline curves . . . . .	29
(h) Requests for output data . . . . .	29
(i) Incompressible flow . . . . .	31
(j) Straight infinite cascade . . . . .	31
(k) Choosing a value for REDFAC . . . . .	31
(l) Choosing a value for ANGROT . . . . .	31
OUTPUT . . . . .	31
Printed Output . . . . .	32
Plotted Output . . . . .	52
Error Messages . . . . .	66
<u>NUMERICAL EXAMPLE</u> . . . . .	70

APPENDIXES

A - GOVERNING EQUATIONS . . . . .	73
B - DERIVATION OF STREAM-FUNCTION EQUATION . . . . .	77
C - DERIVATION OF VELOCITY-GRADIENT EQUATION . . . . .	85
D - LOSS CORRECTIONS . . . . .	90
E - DEFINING REDUCED-MASS-FLOW PROBLEM . . . . .	92
F - INCIDENCE AND DEVIATION CORRECTIONS. . . . .	93
G - BLADE SURFACE VELOCITIES AND BLADE-TO-BLADE AVERAGE DENSITIES . . . . .	95
H - SYMBOLS. . . . .	98
<u>REFERENCES</u> . . . . .	101

REVISED FORTRAN PROGRAM FOR CALCULATING VELOCITIES AND  
STREAMLINES ON THE HUB-SHROUD MIDCHANNEL STREAM  
SURFACE OF AN AXIAL-, RADIAL-, OR MIXED-FLOW  
TURBOMACHINE OR ANNULAR DUCT  
I - USER'S MANUAL \*

by Theodore Katsanis and William D. McNally

Lewis Research Center

SUMMARY

A FORTRAN-IV computer program has been developed that obtains a detailed subsonic or transonic flow solution on the hub-shroud midchannel stream surface of a single blade row of a turbomachine. A solution can also be obtained for an annular duct without blades. The flow must be essentially subsonic, but there may be locally supersonic flow. The solution is for two-dimensional, adiabatic shock-free flow. The blade row may be fixed or rotating, and the blades may be twisted and leaned. The flow may be axial, mixed, or radial. Upstream and downstream flow conditions can vary from hub to shroud, and provision is made for an approximate correction for loss of stagnation pressure. Viscous forces are neglected along solution mesh lines running from hub to tip.

The present program is a revision of a previous program and this report supersedes NASA TN D-7343. The primary revisions are to extend the program to handle nonaxial flows without restriction, to handle annular ducts without blades, to allow for any specified streamwise loss distribution, and to make numerous detailed improvements for more accurate and efficient calculations.

The basic analysis is based on the stream function and consists of the solution of the simultaneous, nonlinear, finite-difference equations of the stream function. This basic solution, however, is limited to strictly subsonic flow. When there is locally supersonic flow, a transonic solution must be obtained. The transonic solution is obtained by a combination of a finite-difference, stream-function solution and a velocity-gradient solution. The finite-difference solution at a reduced mass flow provides information that is used to obtain a velocity-gradient solution at the full mass flow.

The program is reported in two volumes, with part I as the user's manual and part II as the programmer's manual. This report, part I, contains all the information necessary to use the program as it is. It explains the equations involved and the method of solution and gives a numerical example to illustrate the use of the program. Part II includes the complete program listing and a detailed program procedure.

---

\*Supersedes NASA TN D-7343.

## INTRODUCTION

The design of blades for compressors and turbines ideally requires methods for analyzing unsteady, three-dimensional, turbulent viscous flow through a turbomachine. Clearly, such solutions are impossible at the present time, even on the largest and fastest computers. The usual approach at present is to analyze only steady flows and to separate inviscid solutions from viscous solutions. Three-dimensional inviscid solutions are just beginning to be obtained with the present generation of computers, but they require excessive computer time. So, at present, inviscid analyses usually involve a combination of several two-dimensional solutions on intersecting families of stream surfaces to obtain what is called a quasi-three-dimensional solution.

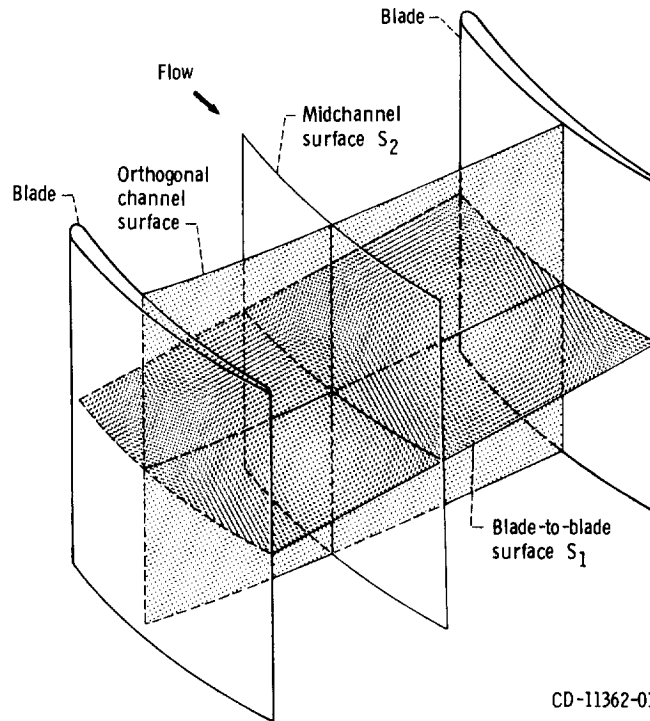
Since there are several choices of two-dimensional surfaces to analyze and many ways of combining them, there are many approaches to obtaining a quasi-three-dimensional solution. Most two-dimensional solutions are either on a blade-to-blade surface of revolution (Wu's  $S_1$  surface, ref. 1) or on the meridional or midchannel stream surface between two blades (Wu's  $S_2$  surface). However, when three-dimensional effects are most important, significant information can often be obtained from a solution on a passage cross-sectional surface (normal to the flow). This is called a channel solution (fig. 1).

In this report a solution to the equations of flow on the meridional  $S_2$  surface is carried out. This solution surface is chosen when the turbomachine under consideration has significant variation in flow properties in the hub-shroud direction, especially when input is needed for use in blade-to-blade calculations. The solution can be obtained either by the quasi-orthogonal method, which solves the velocity-gradient equation from hub to shroud on the meridional stream surface (ref. 2), or by a finite-difference method, which solves a finite-difference equation for stream function on the same stream surface. The quasi-orthogonal method is efficient in many cases and can obtain solutions into the transonic regime. However, there is difficulty in obtaining a solution when blade aspect ratios are above 1. Difficulties are also encountered with curved passages and low-hub-tip-ratio blades. For such cases, the most promising method is the finite-difference solution, but this solution is limited to completely subsonic flows.

Finite-difference programs for flow on the midchannel surface of a turbomachine have been reported in the literature. However, many of these programs are proprietary or are of limited generality. The program reported herein is very general and has been thoroughly tested and refined as the result of extensive usage at the NASA Lewis Research Center.

The program described in this report uses both the finite-difference and the quasi-orthogonal (velocity gradient) methods, combined in a way that takes maximum advantage of both. The finite-difference method is used to obtain a subsonic-flow solution.





CD-11362-01

Figure 1. - Two-dimensional analysis surfaces in a turbomachine.

The velocity-gradient method is then used if necessary to extend the range of solutions into the transonic regime.

A computer program called MERIDL has been written to perform these calculations. This program was written for an axial-, mixed-, or radial-flow turbomachine blade row, either a compressor or turbine, or for an annular duct. Upstream and downstream flow conditions can vary from hub to shroud. The solution is for compressible, shock-free flow or for incompressible flow. An approximate correction for loss of stagnation pressure through the blade row is provided. The blade row may be either fixed or rotating. The blades may be twisted and leaned and can have high aspect ratio and arbitrary thickness distribution.

The solution obtained by this program also provides the information necessary for a more detailed blade-shape analysis on blade-to-blade surfaces (fig. 1). A useful program for this purpose is TSONIC (ref. 3). Information needed to prepare all the input for TSONIC is calculated and printed by MERIDL.

The MERIDL program reported herein is a revision of the program described in

references 4 and 5. Two types of changes were made: first, extension of the program's capability to handle cases beyond those originally offered; and second, revisions to improve the accuracy and efficiency of the program. Although the input form has been extended to handle additional input where required, any input that was satisfactory for the original MERIDL program is still satisfactory for the revised MERIDL program. The following major extensions and revisions were made to the program (additional internal changes are documented in part II):

(1) The program has been extended to handle nonaxial flow configurations, including both radial turbines and centrifugal compressors.

(2) The program has been extended to handle an annular duct without blades.

(3) The program has been extended to permit the user to specify an arbitrary streamwise distribution of loss within the blades. This is in addition to the original provision for hub-shroud loss distribution.

(4) The program has been modified so that the blade thickness can be specified precisely by a set of tangential (circumferential) thickness coordinates. The original program required specification of thickness normal to the mean camber line on an input blade section. This normal thickness was influenced by blade lean, camber, and non-parallel blade surfaces and was difficult to specify accurately for some blade shapes.

(5) If desired the leading- and trailing-edge, mean-camber-line tangent angles can be specified as input. This simplifies the specification of some blade shapes.

(6) Output quantities have been added to station-line output to give absolute velocity components and to give static as well as absolute and relative total temperature, density, and pressure.

(7) Several informational messages have been added to the output.

(8) Additional error messages have been provided.

(9) Upstream and downstream boundary conditions have been changed to improve both the convergence and the quality of the solution near these boundaries.

(10) Interpolation and calculation procedures near the leading and trailing edges have been improved to give better convergence and smoother solutions in these regions.

(11) Numerous small changes have been made to improve the accuracy and efficiency of the program.

The MERIDL program has been implemented on the NASA Lewis time-sharing IBM-TSS/360-67 computer. For the numerical example of this report, the storage of variables required 60 000 words for a  $21 \times 41$  grid of 861 points. The amount of variable storage could be easily reduced by equivalencing of variables or by using a coarser mesh. Storage requirements for the program code depend on the computer system and compiler being used. Run times for the program range from 3 to 15 minutes on IBM-TSS/360-67 equipment.

The MERIDL program is reported in two volumes, with part I as the user's manual

and part II (ref. 6) as the programmer's manual. This report, part I, contains all the information necessary to use the program. It explains the method of solution, describes the input and output, gives a numerical example to illustrate the use of the program, and derives the equations used (in appendixes A to G.) Symbols are defined in appendix H. Part II includes a complete program listing, detailed program procedure, and appendixes that derive the special numerical techniques used.

## METHOD OF ANALYSIS

### BASIC ASSUMPTIONS

It is desired to determine the flow distribution through a stationary or rotating cascade of blades on a midchannel hub-shroud stream surface. The following simplifying assumptions are used in deriving the equations and in obtaining a solution:

- (1) The flow relative to the blade is steady.
- (2) The fluid is a perfect gas with constant specific heat  $C_p$ .
- (3) The only forces along a hub-shroud orthogonal mesh line are those due to momentum and pressure gradient.
- (4) There is no heat transfer.
- (5) The midchannel surface is a stream surface that has the same shape as the blade mean-camber surface, except near the leading and trailing edges, where an arbitrary correction is made to match the free-stream flow.
- (6) The velocity varies linearly between blade surfaces.
- (7) The relative stagnation pressure loss is known through the blade row.
- (8) The upstream and downstream boundaries of the solution region are orthogonal to the streamlines.

The flow may be axial, mixed, or radial. Whirl, stagnation pressure, and stagnation temperature may vary from hub to shroud, both upstream and downstream of the blade row. The blade row may be either fixed or rotating, with leaned and twisted blades; or there may be no blades at all. Within the given assumptions, no terms are omitted from the equations.

In connection with assumption 3, the viscous forces along a hub-shroud orthogonal mesh line are neglected, since these forces are usually very small. The viscous forces in the streamwise direction are much larger. The effects of these streamwise viscous forces are considered indirectly by specifying a streamwise total-pressure-loss distribution.

## SOLUTION BY COMBINATION OF METHODS

A flow analysis on the meridional stream surface can be obtained either by the velocity-gradient method or by the finite-difference method. The finite-difference method is limited to subsonic flow; the velocity-gradient method is limited to relatively low-aspect-ratio blades. The most accurate solution is obtained by the finite-difference technique, so that this method is used where possible (i.e., for subsonic flow). With locally supersonic flow, the finite-difference solution is first obtained at a reduced mass flow (appendix E) for which the flow field is completely subsonic. The streamline curvatures and flow angles throughout the passage that are obtained from this solution provide the information necessary to obtain an approximate velocity-gradient solution at full mass flow, regardless of aspect ratio.

### SUBSONIC STREAM-FUNCTION SOLUTION

The stream-function equation (eq. (A1), appendix A) is a partial differential equation on a midchannel hub-shroud stream surface (assumption 5, p. 5). It is in one unknown (the stream function) as a function of two variables and is derived from Wu's momentum equation (eq. (96), ref. 1) on what he calls an  $S_2$  surface. Equation (A1) is

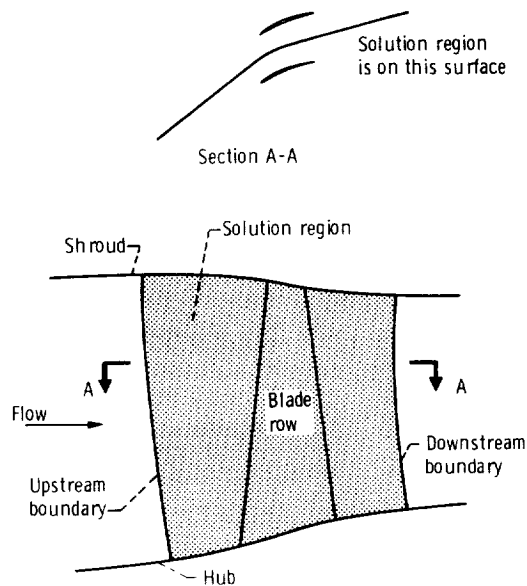


Figure 2. - Solution region.

nonlinear but can be solved iteratively by the finite-difference method when the flow is completely subsonic.

A finite region (as indicated in fig. 2) is considered for the solution of equation (A1). It is assumed that the upstream and downstream boundaries are sufficiently far from the blade so as to have a negligible effect on the solution. Equation (A1) is elliptic for subsonic flow. Therefore, when the flow is entirely subsonic, equation (A1) can be solved when proper boundary conditions are specified on the entire boundary of the region. These conditions are the values of the stream function or its normal derivative on all four boundaries. The stream function is zero on the hub and 1 at the shroud. On the upstream and downstream boundaries, the derivative of the stream function normal to the boundary is assumed to be zero. This is equivalent to assuming that the upstream and downstream boundaries are orthogonal to the streamlines (assumption 8, p. 5).

The numerical solution of equation (A1) is obtained by the finite-difference method. A grid must be used for the finite-difference equations. The type of grid that was chosen is an orthogonal mesh that is generated by the program. The method used to generate the grid follows that reported in reference 7. The space between the hub and the shroud is divided into equal increments along several hub-shroud lines. Spline curves are then fit through the resulting points to obtain the streamwise orthogonals (fig. 3). The normal orthogonals are obtained by a predictor-corrector technique. This technique is analogous to the second-order Runge-Kutta method for solving ordinary differential equations, which is known also as the improved Euler method or Heun's method (ref. 8). The distances along orthogonal mesh lines are  $s$  and  $t$ . The  $s$ -distance is in the streamwise direction and the  $t$ -distance is normal to this, as indicated in figure 3. With the mesh determined, the finite-difference equations on the orthogonal mesh are given in part II of this report (ref. 6). Note that the orthogonal mesh is not used as a coordinate system.

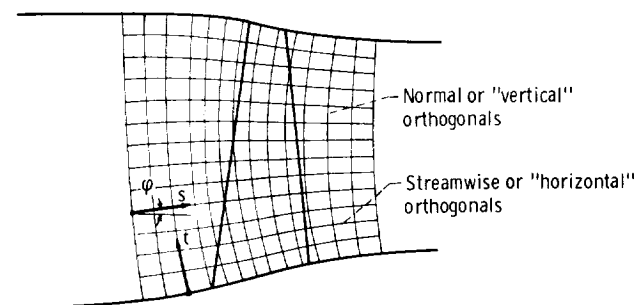


Figure 3. - Orthogonal finite-difference mesh on solution region.

The finite-difference equations are nonlinear since the original equation (A1) is nonlinear. These equations can be solved iteratively. On the first iteration an initial density is assumed; this linearizes some of the terms. The remaining nonlinear terms are omitted for the first iteration so that the finite-difference equations are entirely linearized. These linearized equations are then solved to obtain the first approximate solution for the stream function. This solution provides information that is used to obtain a better estimate of the density and an estimate of the other nonlinear terms. The equations are then solved again to obtain an improved solution. This process is repeated, and by iteration a final converged solution can be obtained if the flow is subsonic.

For each step of this iteration the linearized finite-difference equations must be solved. The method used to solve the equations is successive overrelaxation (ref. 9) with an optimum overrelaxation factor. Since this is also an iterative method, we have two levels of iteration. The overrelaxation is performed in the "inner iteration," and the corrections to the nonlinear terms are made in the "outer iteration." The inner iteration is internal to the program, so the only iteration apparent to the user is the outer iteration. When an iteration is mentioned in this report, it is always the outer iteration.

After the stream function is obtained, the velocity distribution is found by numerical partial differentiation of the stream function and by using equations (A5) and (A6). The details of the numerical procedure and programming technique are described in part II (ref. 6).

#### TRANSONIC VELOCITY-GRADIENT APPROXIMATE SOLUTION

For the case where there is locally supersonic flow, equation (A1) is no longer elliptic in the entire region but is hyperbolic in the region of supersonic flow (ref. 10). This changes the boundary conditions and means that there will probably be shock losses in going from supersonic to subsonic flow. The finite-difference method cannot be used with locally supersonic flow. However, an approximate solution can be obtained by getting a reduced-flow solution with the finite-difference method and extending this to the full flow by using the velocity-gradient method. This technique is described in reference 3.

The velocity-gradient equations are equations (A7) to (A11). Equation (A7) is solved as an initial-value problem, where the velocity  $W$  is specified at the hub for any given vertical mesh line running from hub to tip. By finding several solutions for varying values of  $W$  at the hub, a solution satisfying the specified mass flow (eq. (A12)) will be found. When equation (A7) has been solved, subject to giving the

correct mass flow, for every hub-shroud mesh line in the region, the entire velocity distribution at full mass flow has been obtained.

## BLADE SURFACE VELOCITIES

The solution that is obtained by either the finite-difference or velocity-gradient method is for the midchannel surface between the blades. When there are blades, the blade surface velocities are of greater interest. These can be estimated since the blade loading is dependent on the rate of change of whirl. By assuming a linear variation of velocity between blade surfaces, equation (A13) can be derived for calculating the blade surface velocities.

## APPLICATION OF PROGRAM

The program can be used both for analysis and as a design tool. When it is used for design, other programs should be used with this program. For axial compressors, reference 11 describes a program that will give blade mean-camber-line coordinates and thicknesses for an axial compressor blade. This blade design can be checked by using the MERIDL program to analyze the flow distribution in detail. Usually, changes must be made to the blade design to achieve a desirable flow distribution. These changes may involve more than just the blade shape; for example, hub and shroud profile, inlet and outlet whirl distribution, and loss distribution may have to be changed. Of course, the accuracy of the MERIDL solution depends on the accuracy of the boundary conditions used.

When a reasonable flow pattern is achieved by the MERIDL flow analysis on the midchannel stream surface, more-detailed blade surface velocities can be obtained by flow analyses on various blade-to-blade stream surfaces. A useful program for this purpose is TSONIC (ref. 3). Most of the information required to compute input for TSONIC is calculated and printed directly by MERIDL. Item 12 of the section Printed Output (p. 50) explains how to obtain and use this output from MERIDL. Further changes in blade shape or whirl distribution may be considered at this time. Reference 12 (ch. VII) gives information on incidence and deviation for good designs and for off-design conditions.

For cases where the flow is well guided in the channel but has large variations, both from blade to blade and from hub to shroud, the CHANEL program (ref. 13) is useful. The CHANEL program obtains a solution on a channel cross-section surface.

The CHANEL program is particularly useful for calculating choking mass flow through a blade row.

### DESCRIPTION OF INPUT AND OUTPUT

The principal block of input required for the program is a geometric description of the blade row to be analyzed. The geometry is given in cylindrical coordinates, as shown in figure 4. The blade shape is given as a series of blade sections from hub to shroud. Each blade section is described by a set of  $z$  and  $r$  mean-camber-line coordinates and two sets of blade-shape coordinates on any general, smooth surface of

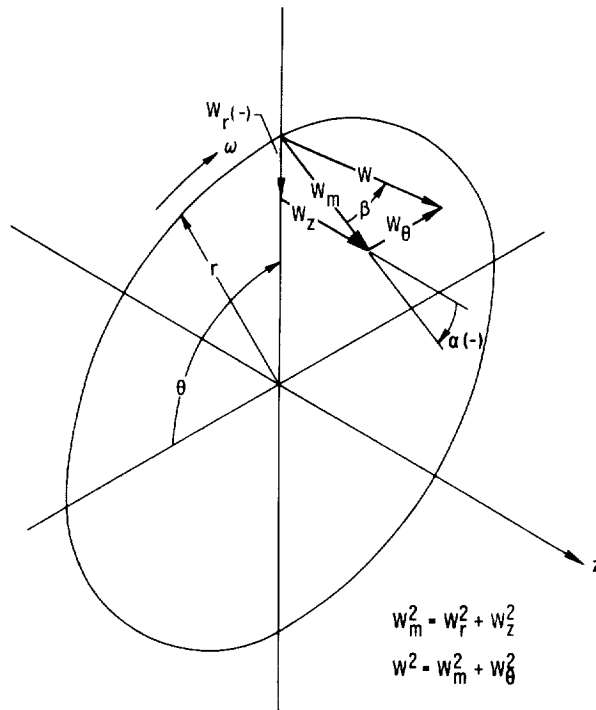


Figure 4. - Cylindrical coordinate system and velocity components.



revolution. Other inputs include upstream and downstream flow conditions, a geometric description of hub and shroud, appropriate gas constants, operating conditions such as mass flow and rotational speed, and a description of the finite-difference solution mesh. There are also input variables to indicate the desired blocks of output data.

Output is given at any or all of three principal geometric locations: (1) on all mesh points of the orthogonal solution mesh, (2) along user-designated streamlines through the blade row, or (3) along user-designated lines from hub to shroud (station lines). Output consists mainly of z- and r-coordinates and velocity components and angles. At station lines more output is given, including density, temperature, and pressure.

## INPUT

Figure 5 shows the input variables as they are punched on the data cards. The first input data card is for a title, which serves for problem identification. Any information may be put in the 80 columns of this card.

All the numbers on the three input cards beginning with MBI, LSFR, and IMESH are integers (no decimal point) in a five-column field (fig. 5). These must be all right adjusted. The input variables on all other data cards are real numbers (punch decimal point) in 10-column fields.

Figure 5 indicates that several options exist for specifying upstream and downstream flow conditions. First, the user can specify these conditions either as a function of the stream function (SFIN and SFOUT) or as a function of radius (RADIN and RADOUT). Next, the user can specify either whirl (LAMIN and LAMOUT) or absolute tangential velocity (VTHIN and VTHOUT). At the downstream input station either absolute total pressure (PROP) or fractional loss of total pressure (LOSOUT) may be given. Finally, a loss distribution (PERLOS) within the blade may be specified. If the loss distribution through the blade is not given, the loss is assumed to vary linearly between the leading and trailing edges.

Input variables are both geometric and nongeometric. The geometric input variables are shown in figures 6 to 10. Further information concerning the input variables is given in the section Special Instructions for Preparing Input (pp. 25 to 31).

1	5	6	10	11	15	16	20	21	25	26	30	31	35	36	40	41	45	46	50	51	55	56	60	61	65	66	70	71	75	76	80
TITLE																															
GAM		AR		MSFL		OMEGA		REDFAC		VELTOL		FNEW		DNEW																	
MBO		MHT		NBL		NHUB		NBLPL		NSTAT		NSL		NLOSS																	
LTP		LROT		LBLAD		LETEAN																									
ANGROT																															
ZOMIN		ZOMBI		ZOMBO		ZOMOUT		ROMIN		ROMBI		ROMBO		ROMOUT																	
ZHUB (1 to NHUB)																															
RHUB (1 to NHUB)																															
ZTIP (1 to NTIP)																															
RTIP (1 to NTIP)																															
ZHIN		ZTIN		RHIN		RTIN																									
SFIN (1 to NIN) or RADIN (1 to NIN)																															
TIP (1 to NIN)																															
PRIP (1 to NIN)																															
LAMIN (1 to NIN) or VTHIN (1 to NIN)																															
ZHOUT		ZTOUT		RHOUT		RTOUT																									
SFOUT (1 to NOUT) or RADOUT (1 to NOUT)																															
PROP (1 to NOUT) or LOSOUT (1 to NOUT)																															

REPRODUCIBILITY OF THE ORIGINAL PAGE IS POOR

LAMOUT (1 to NOUT) or VTHOUT (1 to NOUT)																				
ZBL (1 to NPPP by 1 to NBLPL)																				
RBL (1 to NPPP by 1 to NBLPL)																				
THBL (1 to NPPP by 1 to NBLPL) or THIBL (1 to NPPP by 1 to NBLPL)																				
TNBL (1 to NPPP by 1 to NBLPL) or TNBL (1 to NPPP by 1 to NBLPL) or TH2BL (1 to NPPP by 1 to NBLPL)																				
* BETALE (1 to NBLPL)																				
* BETATE (1 to NBLPL)																				
* ZHST (1 to NOSTAT)																				
* RHST (1 to NOSTAT)																				
* ZTST (1 to NOSTAT)																				
* RTST (1 to NOSTAT)																				
* FLR (1 to NSL)																				
* PERCRD (1 to NLOSS)																				
* PERLOS (1 to NLOSS)																				
JMESH			ISLINE			ISTATL			IPLOT			ISUPER			JTSON			IDEBUG		

← Omit these cards if there are no blades →

Figure 5. - Input form. (Cards denoted by asterisks are optional. See Input Dictionary.)

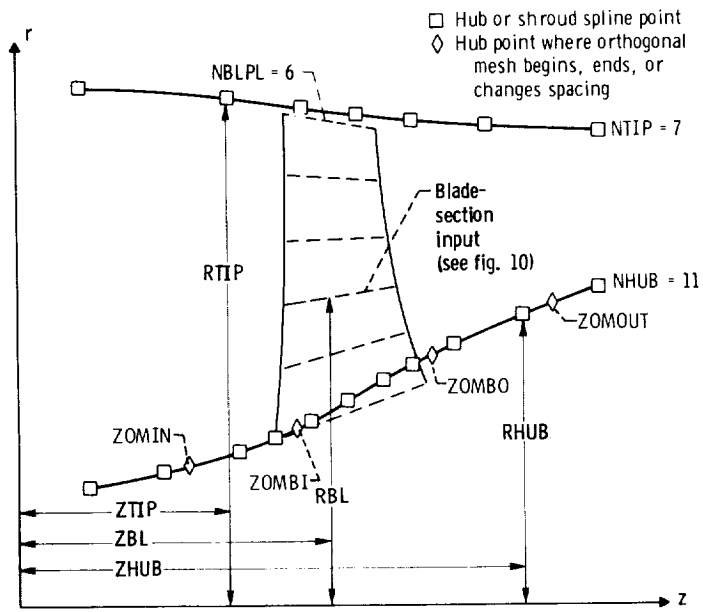


Figure 6. - Input variables - hub, shroud, and blade sections.

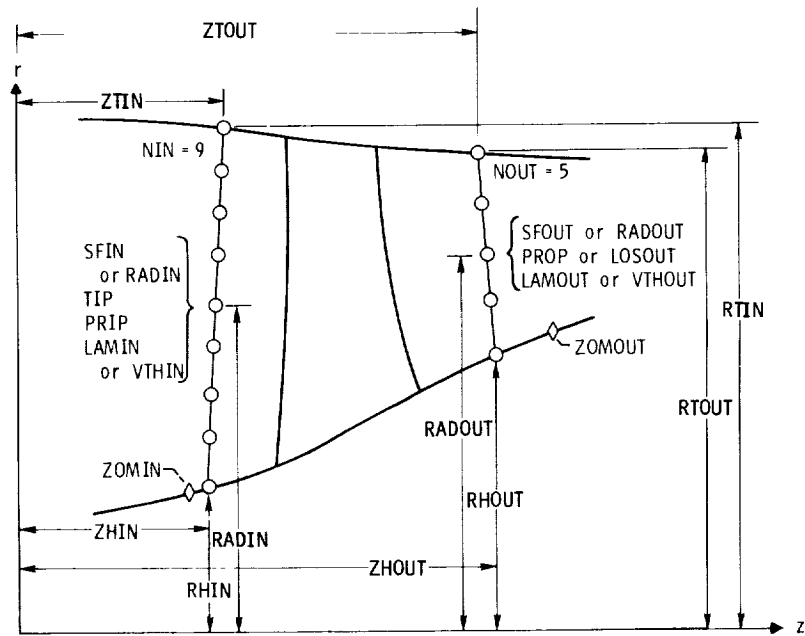
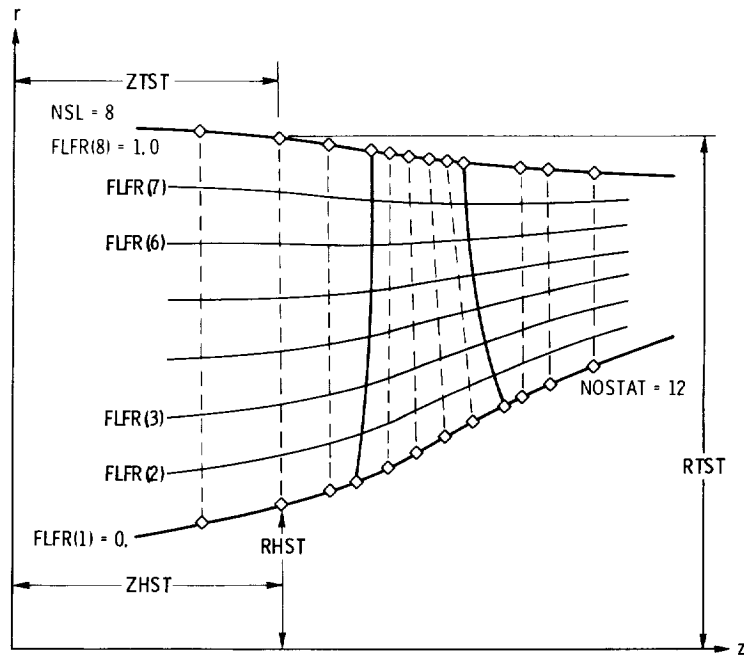
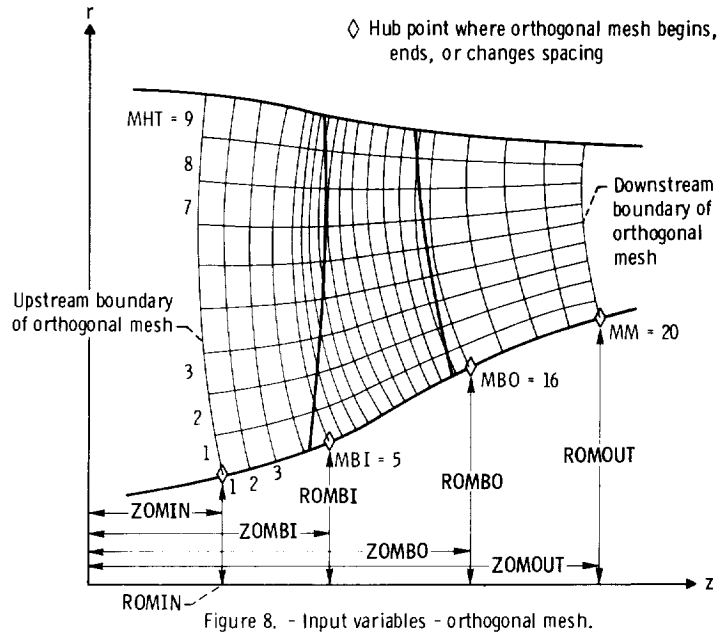


Figure 7. - Input variables - upstream and downstream flow variables.



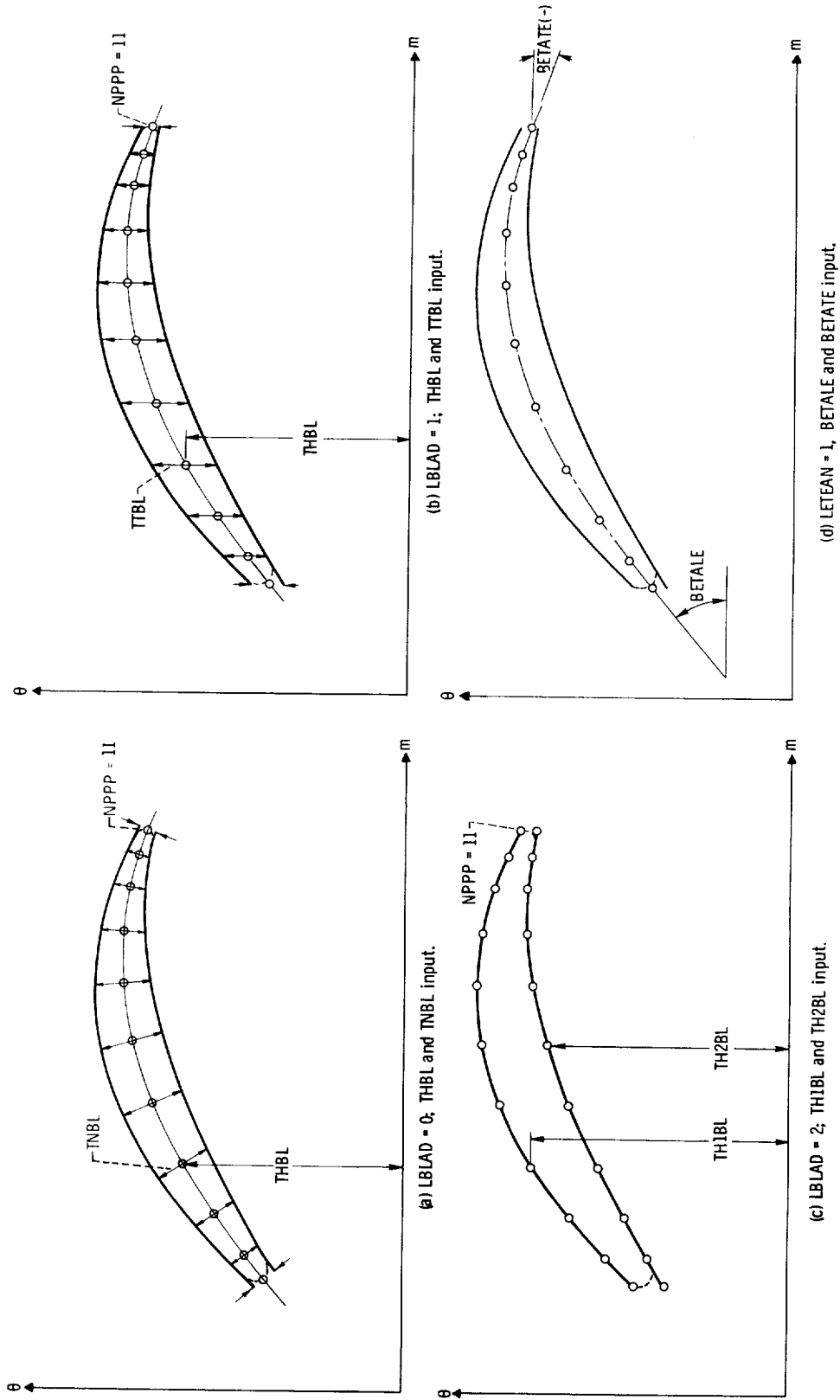


Figure 10. - Input variables - blade section. (RBL and ZBL must be given at each location (see fig. 6).) (TNBL is given in meters. THBL, TTBL, TH1BL, and TH2BL are given in radians.)

## Input Dictionary

The input variables are described in terms of a consistent set of SI units: newtons, kilograms, meters, joules, kelvins, and seconds. The program, however, will run with input in any consistent set of units.

The input variables, in the order that they appear in figure 5, are the following:

GAM	Specific-heat ratio, $\gamma$
AR	Gas constant, J/(kg)(K)
MSFL	Total mass flow through entire circumferential annulus of blade row, kg/sec
OMEGA	Rotational speed, $\omega$ , rad/sec. Note that $\omega$ is negative if rotation is in opposite direction of that shown in fig. 4.
REDFAC	Factor by which mass flow (MSFL) must be reduced in order to assure subsonic flow throughout flow passage. REDFAC may be left blank, in which case a value of 1.0 will be used. See section (k), p. 31.
VELTOL	Convergence tolerance on maximum velocity change in each iteration, over all mesh points, for reduced-mass-flow solution. VELTOL may be left blank, and a value of 0.01 will be used by the program. Whatever value is given is multiplied by the minimum of FNEW and DNEW before it is printed and subsequently used by the program. A value of 0.001 for VELTOL is a tight tolerance, 0.01 is a medium tolerance, and 0.1 is a loose tolerance.
FNEW	Damping factor on calculation of $F_t$ from iteration to iteration. A value of 0.5 is suggested for FNEW. FNEW may be left blank, in which case the program will use a value of 0.5. See section (b), p. 26.
DNEW	Damping factor on calculation of $\partial(rV_\theta)/\partial t$ within blade row from iteration to iteration. DNEW may be left blank, and the program will use a value of 0.5. DNEW does not have to be equal to FNEW. See section (b), p. 26.
MBI	Number of vertical mesh lines from left boundary of orthogonal mesh (ZOMIN) to point of first mesh-size change (ZOMBI). Use MBI = 0 if there are no blades. See fig. 8 and section (d), p. 27.

MBO	Total number of vertical mesh lines from left boundary of orthogonal mesh (ZOMIN) to point of second mesh-size change (ZOMBO). Use MBO = 0 if there are no blades. See fig. 8 and section (d), p. 27.
MM	Total number of vertical mesh lines from left to right boundaries of orthogonal mesh (ZOMIN to ZOMOUT), maximum of 100. See fig. 8 and section (d), p. 27.
MHT	Total number of horizontal mesh spaces from hub to shroud of orthogonal mesh, maximum of 100. See fig. 8 and section (d), p. 27.
NBL	Number of blades in total circumference of blade row. Use NBL = 1 if there are no blades.
NHUB	Number of spline points given in ZHUB and RHUB arrays, maximum of 50. See fig. 6 and section (c), p. 26.
NTIP	Number of spline points given in ZTIP and RTIP arrays, maximum of 50. See fig. 6 and section (c), p. 26.
NIN	Number of data points given in upstream arrays of flow properties (SFIN, RADIN, TIP, PRIP, LAMIN, VTHIN), maximum of 50. See fig. 7 and section (e), p. 27.
NOUT	Number of data points given in downstream arrays of flow properties (SFOUT, RADOUT, PROP, LOSOUT, LAMOUT, VTHOUT), maximum of 50. See fig. 7 and section (e), p. 27.
NBLPL	Number of blade planes or blade sections on which data (ZBL, RBL, etc.) are given to describe mean blade shape and blade thickness, maximum of 50. See fig. 6 and section (f), p. 28.
NPPP	Number of data points per blade section or blade plane in ZBL, RBL, etc., arrays, maximum of 50. See fig. 10 and section (f), p. 28.
NOSTAT	Number of stations from hub to shroud (located by coordinates in ZHST and ZTST) at which output is desired, maximum of 50. See fig. 9 and section (h), p. 29. NOSTAT may be left blank, in which case no input cards should be included for ZHST, ZTST, RHST, and RTST arrays.
NSL	Number of streamlines from hub to shroud (designated by values in FLFR) at which output is desired, maximum of 50. See fig. 9. NSL may be left blank, in which case no cards should be included



for FLFR array. If NSL is left blank, the program will set it equal to 11 and print requested streamline output on 11 streamlines that vary by 10 percent of total flow (i. e., 0, 10, 20, ..., 100 percent).

- NLOSS            Number of points at which fractional loss (PERLOS) is specified, maximum of 50. If NLOSS is zero or left blank, the program will use a linear loss distribution in the streamwise direction. In this case, no input cards should be included for PERCRD or PERLOS arrays.
- LSFR            Integer (0 or 1) indicating whether upstream and downstream flow conditions are given as a function of stream function (0) or radius (1).
- LTPL            Integer (0 or 1) indicating whether downstream total pressure (0) or fractional loss of stagnation pressure (1) is given as input.
- LAMVT           Integer (0 or 1) indicating whether upstream and downstream whirl (0) or tangential velocity (1) is given as input.
- LROT            Integer (0 or 1) indicating whether coordinate rotation (ANGROT) is necessary (1) for hub and shroud spline fit curves. See section (l), p. 31.
- LBLAD           Integer (0, 1, or 2) indicating which two blade-shape coordinates are given as input. If LBLAD = 0, mean blade shape  $\theta$  (THBL) and normal thickness  $t_n$  (TNBL) are given. If LBLAD = 1, mean blade shape  $\theta$  (THBL) and tangential  $\theta$ -thickness  $t_\theta/r$  (TTBL) are given. If LBLAD = 2, upper blade surface  $\theta_1$  (TH1BL) and lower blade surface  $\theta_2$  (TH2BL) are given. See fig. 10 and section (f), p. 28.
- LETEAN          Integer (0 or 1) indicating whether leading- and trailing-edge mean blade-shape angles  $\beta_{1e}$  and  $\beta_{te}$  (BETALE and BETATE) are specified (1). See fig. 10 and section (f), p. 28.
- ANGROT          Rotation angle of axis used for all streamwise spline fit curves, deg. Omit this card if LROT is (0). See section (l), p. 31.
- ZOMIN           z-Coordinate of intersection of left boundary of orthogonal mesh with hub profile, m. See figs. 6 and 8 and section (d), p. 27.
- ZOMBI           z-Coordinate of intersection of vertical mesh line with hub profile where first change in mesh spacing occurs (MBI), m. See figs. 6 to 8 and section (d), p. 27. Set ZOMBI and ZOMBO to zero for no blades case.

ZOMBO	z-Coordinate of intersection of vertical mesh line with hub profile where second change in mesh spacing occurs (MBO), m. See figs. 6 and 8 and section (d), p. 27.
ZOMOUT	z-Coordinate of intersection of right boundary of orthogonal mesh (MM) with hub profile, m. See figs. 6 and 8 and section (d), p. 27.
ROMIN, ROMBI, ROMBO, and ROMOUT	r-Coordinates corresponding to ZOMIN, ZOMBI, ZOMBO, and ZOMOUT, m. Leave these spaces blank if LROT = 0.
ZHUB	Array of z-coordinates of input points defining hub or bottom boundary of flow channel, m. See fig. 6 and section (c), p. 26.
RHUB	Array of r-coordinates of input points defining hub or bottom boundary of flow channel, m. See fig. 6 and section (c), p. 26.
ZTIP	Array of z-coordinates of input points defining shroud or top boundary of flow channel, m. See fig. 6 and section (c), p. 26.
RTIP	Array of r-coordinates of input points defining shroud or top boundary of flow channel, m. See fig. 6 and section (c), p. 26.
ZHIN	z-Coordinate of intersection with hub profile of line on which upstream flow conditions are given, m. Leave this entire card blank if LSFR = 0, LAMVT = 0, and MBI $\neq$ 0. See fig. 7 and section (e), p. 27.
ZTIN	z-Coordinate of intersection with shroud profile of line on which upstream flow conditions are given, m. See fig. 7 and section (e), p. 27.
RHIN, RTIN	r-Coordinates corresponding to ZHIN and ZTIN, m. Leave these spaces blank if LROT = 0. If RADIN is given as input (LSFR = 1), RHIN and RTIN cannot be equal to each other.
SFIN	Array of values of stream function for input points from hub to shroud along line on which upstream flow conditions are given. SFIN is given when LSFR = 0. See fig. 7 and section (e), p. 27.
RADIN	Array of r-coordinates of input points along line from hub to shroud on which upstream flow conditions are given, m. RADIN is given when LSFR = 1. See fig. 7 and section (e), p. 27.
TIP	Array of absolute total temperatures $T_i^!$ at input points along line from hub to shroud on which upstream flow conditions are given, K. See fig. 7 and section (e), p. 27

PRIP Array of absolute total pressures  $p'_i$  at input points along line from hub to shroud on which upstream flow conditions are given,  $N/m^2$ . See fig. 7 and section (e), p. 27.

LAMIN Array of values of absolute whirl  $(rV_\theta)_i$  at input points along line from hub to shroud on which upstream flow conditions are given,  $m^2/sec$ . LAMIN is given when LAMVT = 0. See fig. 7 and section (e), p. 27.

VTHIN Array of values of absolute tangential velocity  $(V_\theta)_i$  at input points along line from hub to shroud on which upstream flow conditions are given,  $m/sec$ . VTHIN is given when LAMVT = 1. See fig. 7 and section (e), p. 27.

ZHOUT z-Coordinate of intersection with hub profile of line on which downstream flow conditions are given, m. Leave this entire card blank if LSFR = 0, LAMVT = 0, and MBI  $\neq$  0. See fig. 7 and section (e), p. 27.

ZTOUT z-Coordinate of intersection with shroud profile of line on which downstream flow conditions are given, m. See fig. 7 and section (e), p. 27.

RHOUT, RTOUT r-Coordinates corresponding to ZHOUT and ZTOUT, m. Leave these spaces blank if LROT = 0. If RADOUT is given as input (LSFR = 1), RHOUT and RTOUT cannot be equal to each other.

SFOUT Array of values of stream function for input points from hub to shroud along line on which downstream flow conditions are given. SFOUT is given when LSFR = 0. See fig. 7 and section (e), p. 27.

RADOUT Array of r-coordinates of input points along line from hub to shroud on which downstream flow conditions are given, m. RADOUT is given when LSFR=1. See fig. 7 and section (e), p. 27.

PROP Array of absolute total pressures  $p'_o$  at input points along line from hub to shroud on which downstream flow conditions are given,  $N/m^2$ . PROP is given when LTPL = 0. See fig. 7 and section (e), p. 27.

LOSOUT Array of fraction of absolute total pressure loss  $(p'_{o, id} - p'_o)/p'_{o, id}$  at input points along line from hub to shroud on which downstream flow conditions are given. LOSOUT is given when LTPL = 1. See fig. 7 and section (e), p. 27.

For the case without blades, omit input cards for the variables LAMOUT through BETATE, inclusive.

- LAMOUT            Array of values of absolute whirl  $(rV_{\theta})_0$  at input points along line from hub to shroud on which downstream flow conditions are given,  $m^2/sec$ . LAMOUT is given when LAMVT = 0. See fig. 7 and section (e), p. 27.
- VTHOUT            Array of values of absolute tangential velocity  $(V_{\theta})_0$  at input points along line from hub to shroud on which downstream flow conditions are given,  $m/sec$ . VTHOUT is given when LAMVT = 1. See fig. 7 and section (e), p. 27.
- ZBL                Two-dimensional array of z-coordinates of points describing mean blade surface, m. See figs. 6 and 10 and section (f), p. 28. This surface is described by a series (from 2 to 50) of blade sections from hub to shroud. The hub section is given first, followed by successive sections up to the shroud.
- RBL                Two-dimensional array of r-coordinates, corresponding to ZBL, of points describing mean blade surface, m. See fig. 6 and section (f), p. 28.
- THBL              Two-dimensional array of  $\theta$ -coordinates, corresponding to ZBL, of points describing mean blade surface, rad. See fig. 10 and section (f), p. 28. The tangential coordinate  $\theta$  is positive in direction of positive rotation (fig. 4). The origin of  $\theta$ -coordinates can be anywhere around the circumference. THBL is given only when LBLAD is 0 or 1.
- TNBL              Two-dimensional array of blade thicknesses normal to mean camber line, corresponding to ZBL, RBL coordinates, m. When there is little blade lean, small blade surface curvatures, and near-parallel suction and pressure blade surfaces, it is feasible to use the blade normal thicknesses for TNBL array (LBLAD=0). Otherwise it is recommended to give either the tangential thickness, TTBL (LBLAD = 1), or the suction and pressure blade surface coordinates, TH1BL and TH2BL (LBLAD = 2). See fig. 10(a) and section (f), p. 28.
- TTBL              Two-dimensional array of blade tangential (circumferential) thicknesses, corresponding to ZBL, RBL coordinates, rad. TTBL is the blade tangential thickness in meters, divided by

RBL. TTBL is given only when LBLAD = 1. See fig. 10(b) and section (f), p. 28.

TH1BL Two-dimensional array of upper blade surface coordinates (fig. 10(c)) corresponding to ZBL, RBL coordinates, rad. TH1BL is given only when LBLAD = 2. See fig. 10(c) and section (f), p. 28.

TH2BL Two-dimensional array of lower blade surface coordinates (fig. 10(c)) corresponding to ZBL, RBL coordinates, rad. TH2BL is given only when LBLAD = 2. See fig. 10(c) and section (f), p. 28.

BETALE Array of leading-edge, mean-camber-line tangency angle, deg. BETALE is given only when LETEAN = 1; omit this card if LETEAN = 0. See fig. 10(d) and section (f), p. 28.

BETATE Array of trailing-edge, mean-camber-line tangency angles, deg. BETATE is given only when LETEAN = 1; omit this card if LETEAN = 0. See fig. 10(d) and section (f), p. 28.

ZHST Array of z-coordinates of intersections of hub-shroud output station lines with hub profile, m. Omit this card if NOSTAT = 0. See fig. 9 and section (h), p. 29.

RHST Array of r-coordinates corresponding to ZHST array. Omit this card if NOSTAT = 0 or if LROT = 0. See fig. 9 and section (h), p. 29.

ZTST Array of z-coordinates of intersections of hub-shroud output station lines with shroud profile, m. Omit this card if NOSTAT = 0. See fig. 9 and section (h), p. 29.

RTST Array of r-coordinates corresponding to ZTST array. Omit this card if NOSTAT = 0 or if LROT = 0. See fig. 9 and section (h), p. 29.

FLFR Array of values of stream function designating streamlines along which output is to be printed. Omit this card if NSL = 0. See fig. 9 and section (h), p. 29. If no cards are given for FLFR array (i. e., NSL = 0), the program will automatically assign the following 11 values to FLFR: 0.0, 0.1, 0.2, ..., 0.9, 1.0.

PERCRD Array of streamwise fractional distances corresponding to the PERLOS array. Omit this card if NLOSS = 0. PERCRD should have 0. and 1. for the first and last values, respectively. When there are blades, PERCRD is the fractional distance between the leading and trailing edges. When there are no blades, PERCRD is the fractional distance between the upstream and downstream input stations.

PERLOS                    Array of fractional loss distribution in the streamwise direction within the blade, or between upstream and downstream input stations when there are no blades. Omit this card if NLOSS = 0. PERLOS should have increasing values from 0.1 to 1., although the final value need not reach 1.

The remaining seven integer variables, beginning with IMESH, are used to indicate what output is desired. The program reduces the input mass flow by REDFAC and solves the resulting problem iteratively with a stream-function analysis. The results of this analysis are then used with full mass flow to obtain a transonic analysis by velocity-gradient methods. Output can be obtained after each reduced-mass-flow iteration and also after the final transonic solution.

For all these variables except ISUPER, the integer given indicates the multiple of iterations at which the user wishes the output associated with the variables to be printed or plotted. A zero in any of these indicates that the output associated with that variable is to be omitted. A 1 will print or plot the output on every iteration. A 3, for example, would give the output on every third iteration. Any nonzero integer will cause output to be given on the first and last iterations and after the transonic solution, in addition to the output called for at other iterations. ITSON, however, does not give output on the first iteration. A large integer will obviously give only the first iteration and the final converged iteration. Care should be used not to call for more output than is really useful. The following list gives the output associated with each of these variables:

- IMESH                    Major output at every mesh point of the orthogonal mesh, that is, mesh point indices and coordinates, stream-function value, relative velocity components and magnitude, critical velocity ratio, and flow angles. This output is usually not requested, except for debugging purposes, since output called for by ISLINE or ISTATL is preferable in most cases.
- ISLINE                   Major output along streamlines (indicated by values in FLFR) at each point where streamlines are crossed by vertical mesh lines of the orthogonal mesh. Output includes z, r, and m streamline coordinates, relative velocity components and magnitude, critical velocity ratio, flow angles, and streamline curvature. Where the streamline passes within the blade region, an estimate of suction- and pressure-surface velocities is also printed.
- ISTATL                   Major output along station lines from hub to shroud, at locations specified by ZHST and ZTST arrays and at values of stream function specified by FLFR array. Output corresponds to that given for ISLINE with the addition that absolute velocity components, as well as density, pressure, and

temperature for static conditions and for absolute and relative stagnation conditions are printed. ISTATL should be zero if NOSTAT is zero.

- I PLOT      Plotting indicator requesting output to be plotted on microfilm. Any non-zero value in IPLOT will cause the input data and generated orthogonal mesh to be plotted. Also, at each iteration that is a multiple of IPLOT, streamlines will be plotted and meridional and surface velocities will be plotted for each streamline value. These will also be plotted after the final transonic solution.
- I SUPER     Integer (0 or 1) indicating which solution (subsonic or supersonic) of the velocity-gradient equation is desired. If ISUPER = 0, only the subsonic solution will be printed. If ISUPER = 1, both subsonic and supersonic solutions will be printed.
- I TSON      Integer indicating when information is desired for use in calculating input for the TSONIC program (ref. 3). If ITSON = 0, no information will be given for TSONIC. Otherwise, information will be listed with other output. Usually, the user only wants TSONIC data after subsonic convergence is reached. Using a high value for ITSON (i. e. , >20) will achieve this result.
- I DEBUG     Integer indicating whether additional debug output is desired. If IDEBUG=0, no extra output is printed. If IDEBUG > 0, blade geometry information on the alternate mesh and the coefficients of the finite-difference equations, as well as 21 arrays of debug output on the orthogonal mesh, are printed. Fifteen of these arrays change and are reprinted after each iteration of the reduced-mass-flow solution that is a multiple of IDEBUG.

#### Special Instructions for Preparing Input

It is unusual to have no errors in input to MERIDL the first time any new data set is run. Therefore, input should be checked thoroughly before it is submitted. Errors are commonly made for the following reasons: inconsistent units; improper sign on  $\omega$ ,  $V_\theta$ , or whirl; input for arrays not agreeing with the input bounds for those arrays; and upstream and downstream input not being of the form specified by LSFR, LTPL, and LAMVT. Also geometric input into the hub and shroud arrays and the blade-geometry arrays should be smooth enough that the hub, shroud, and blade sections will be fit well with cubic spline curves (see section (g), p. 29). These input geometric arrays are all plotted on microfilm by the program after spline fitting is completed; the microfilm

output will indicate whether or not the input was smooth. All output should be checked, especially that from a new input data set, to see if it is reasonable.

(a) Units of measurement. - The International System of Units (ref. 14) is used throughout this report. However, the program does not use any constants that depend on the system of units being used. Therefore, any consistent set of units may be used in preparing input for the program. For example, if force, length, temperature, and time are chosen independently, mass units are obtained from Force = Mass  $\times$  Acceleration. The gas constant R must then have the units of (Force  $\times$  Length)/(Mass  $\times$  Temperature). Density is mass per unit volume, and mass flow is mass per unit time. Output then gives velocity in the chosen units of length per unit time. Since any consistent set of units can be employed, the output is not labeled with any units.

(b) Damping factors FNEW and DNEW. - The input variables FNEW and DNEW are used as damping factors on the  $F_t$  and  $\partial(rV_\theta)/\partial t$  terms of equation (A1). During each iteration of the subsonic or finite-difference portion of the program, new values for  $F_t$  and  $\partial(rV_\theta)/\partial t$  are calculated. The calculated changes to these terms are often so large that, if the full change was accepted on each iteration, the solution would diverge. Using values of FNEW and DNEW less than 1.0 allows only a portion of these changes to be used. The value of FNEW or DNEW is the fraction of the predicted change in  $F_t$  or  $\partial(rV_\theta)/\partial t$  to be added to the previous values of these variables. Therefore, if  $F_t$  or  $\partial(rV_\theta)/\partial t$  does not converge, FNEW or DNEW should be reduced. However, this will reduce the rate of convergence so that caution should be used that FNEW and DNEW are not made too small. Because of the reduced rate of convergence, VELTOL is automatically reduced to obtain the same accuracy as when FNEW and DNEW are 1.0.

Limited experience has shown that for subsonic flows, where the gradients of flow variables are not large, converged solutions can be obtained with FNEW and DNEW equal to 1.0. For most practical flows, however, this is not the case and some damping is required. Values of FNEW and DNEW in the range of 0.5 are most commonly used, although at times values as low as 0.05 have been used. (Note that FNEW and DNEW do not have to be equal to each other.)

The user will have to gain experience with FNEW and DNEW before he can use them effectively to maximize rates of convergence. Maximum and minimum values and the maximum change for  $F_t$  and  $\partial(rV_\theta)/\partial t$  (DVTHDR) are printed with the output on each iteration. The maximum relative change in velocity at any point is also printed; it should gradually approach VELTOL for convergence. By observing these values, the user can learn the effects of changes in FNEW and DNEW for different runs of the program.

(c) Hub and shroud flow-channel geometry. - The hub and shroud flow-channel geometry is specified in the ZHUB, RHUB and ZTIP, RTIP arrays. Both of these curves must have the same z-origin (typically the blade leading edge at the hub). These two



arrays must extend far enough upstream and downstream to cover the upstream and downstream boundaries of the orthogonal mesh, as well as the upstream and downstream input stations where streamflow data are given. If they do not extend this far, they will be linearly extrapolated and an incorrect flow channel may result. Relatively few points are needed to describe these smooth surfaces (2 to 10 is a typical range for NHUB and NTIP) in order to have the program calculate smooth, accurate spline fits of these surfaces (fig. 6).

If the user knows the amount of the boundary-layer blockage along the hub and shroud profiles, he should revise the hub and shroud arrays to include this blockage effect. In this situation the output will represent a more realistic flow condition.

(d) Orthogonal mesh. - The number of orthogonal mesh lines is specified by MBI, MBO, MM, and MHT; and the positioning of the mesh is specified by ZOMIN, ZOMBI, ZOMBO, and ZOMOUT. When ANGROT is specified (LROT = 1), ROMIN, ROMBI, ROMBO, and ROMOUT must also be specified. The four z-coordinates, all located on the hub, must use the same z-origin as all other geometric input. The ZOMBI and ZOMBO locations are usually close to the leading and trailing edges of the blade at the hub, although they do not have to correspond to these locations (fig. 8). Mesh-size spacing in the horizontal direction is established by the relation between the four z-coordinates (ZOMIN, etc.) and the number of mesh spaces requested. For instance, MBO - MBI evenly spaced mesh spaces along the hub will be located in the distance given by ZOMBO - ZOMBI. Mesh spacing in the vertical direction is determined by locating MHT spaces in the hub-shroud distance. Usually, none of the vertical mesh lines follow the blade leading- or trailing-edge lines since the blade edges are not usually orthogonal to the hub or the shroud (fig. 8). So some vertical mesh lines will pass in or out of the blade region as they progress from hub to shroud. The suggested number of mesh lines between ZOMBI and ZOMBO that are required to cover the blade adequately is 15 to 30, depending on blade geometry.

(e) Upstream and downstream flow conditions. - Upstream flow conditions are given in the SFIN (or RADIN), TIP, PRIP, and LAMIN (or VTHIN) arrays, which are all of length NIN. Downstream conditions are given in the SFOUT (or RADOUT), PROP (or LOSOUT), and LAMOUT (or VTHOUT) arrays, which are all of length NOUT (fig. 7). Upstream and downstream flow conditions are used, along with the assumption of conservation of angular momentum along streamlines, to establish the flow field in the upstream and downstream portions of the solution region.

Ordinarily, the upstream and downstream flow conditions are given as a function of stream function (SFIN and SFOUT). In this case these input values apply at all points along streamlines upstream or downstream of the blade. If, in addition, the whirl is specified (LAMVT = 0) and there are blades ( $MBI \neq 0$ ), the ZHIN, ZTIN and ZHOUT, ZTOUT inputs are superfluous, so that these variables need not be specified.

However, in most cases, legitimate values must be supplied for ZHIN, ZTIN and ZHOUT, ZTOUT. In this case the upstream conditions are given on a straight line that passes through the two points given by ZHIN on the hub and ZTIN on the shroud. Downstream conditions are given on a straight line that passes through ZHOUT on the hub and ZTOUT on the shroud. These lines may lie anywhere in the regions from the blade edges upstream and downstream to the boundaries of the orthogonal mesh (figs. 7 and 8). If LROT is 1, values for RHIN, RTIN, RHOUT, and RTOUT must also be given as input.

The arrays of upstream and downstream input do not necessarily have to extend all the way from the hub to the shroud or lie on radial lines. They will be linearly extrapolated to the hub and the shroud, if necessary, by the program, should the user only give data in a portion of the flow channel.

(f) Mean blade surface and thickness coordinates. - The blade shape is described from hub to shroud by four arrays, all of which are two dimensional (figs. 6 and 10). Each of these arrays has NBLPL blade sections or planes, with NPPP points in each of these sections. When giving data for each of these four arrays, start each new section of data (NPPP points) at the beginning of a new card. There does not have to be any geometric relation between analogous points on adjacent blade sections. All the ZBL data for all the sections are given, followed by all the RBL data, etc. The origin for the z-coordinates of ZBL should be the same as that used for all other z-coordinate input arrays. Of the four arrays necessary to describe the blade shape, ZBL and RBL are always given. There are three options, controlled by LBLAD, for the other two arrays (see LBLAD definition in the input dictionary).

When LBLAD is 0 or 1, the THBL array must be given (figs. 10(a) and (b)). The THBL array is for input  $\theta$ -coordinates of the blade mean camber surface. Alternatively, the midchannel stream surface, obtained from a blade-to-blade solution (ref. 3), may be used for the THBL array. The program provides a solution on the midchannel stream surface. It obtains that stream surface by smoothly fairing the inlet and outlet flow angles onto the input blade surface at an appropriate distance back on the blades from the leading and trailing edges. This distance is a function of solidity (appendix F).

The TNBL array is given when LBLAD = 0 (fig. 10(a)). The TNBL array is for input blade thicknesses normal to the blade-section mean camber line and lies on a surface of revolution cutting through the blade (figs. 6 and 10). So, in general, the thicknesses lie on a curved line whose ends may be at different radii and may or may not be normal to the blade surfaces (fig. 10(a)). Because it is difficult to obtain proper blockage or proper TSONIC input, caution should be exercised when giving TNBL input. Also, when TNBL is given as input, the THBL coordinates must be for the blade mean camber surface and not the midchannel stream surface.

The TTBL array is used for input tangential (circumferential) blade thicknesses (when LBLAD = 1) and is given in radians (i. e.,  $t_\theta/r$ ) (fig. 10(b)). Thick blades,

blades with high curvature, or blades with significant lean should use TTBL input in preference to TNBL input.

The TH1BL and TH2BL arrays are used to give blade surface  $\theta$ -coordinates (when LBLAD = 2) (fig. 10(c)). This input is similar to that used in the TSONIC program (ref. 3).

To obtain a smooth solution near the leading and trailing edges, it is recommended to use nonzero values of leading-edge and trailing-edge thicknesses, as figure 10 indicates.

In addition to the four arrays necessary to describe the blade, there are two one-dimensional arrays (BETALE and BETATE) that are optional. These arrays specify the leading-edge and trailing-edge mean-camber-line tangency angle in degrees. The angles are measured on the input blade-section surfaces (fig. 10(d)). Use LETEAN = 1 when BETALE and BETATE are given, and LETEAN = 0 when they are not given.

The first blade section given at the hub or the last one at the blade tip does not necessarily have to conform to the hub or shroud profile. It can be given within the flow region, crossing the boundary, or completely outside the boundary (fig. 6). Extrapolation or interpolation will be used when necessary to obtain blade data where the blades meet the hub and shroud profiles.

The user should attempt to give smooth data for these four blade-shape arrays. The program makes use of spline fits of these curves to compute gradients that are used throughout the program. The mean-camber-line first and second derivatives, as well as microfilm plots of the blade sections, given as output will indicate whether input data for these arrays were acceptable.

(g) How to specify points for spline curves. - All the input arrays are fit with cubic spline curves for the purposes of interpolating, calculating derivatives, or any other required calculation. A cubic spline curve is a piecewise cubic polynomial that expresses mathematically the shape taken by an idealized spline passing through the given points. Reference 15 describes the method used for determining the equation of the spline curve. By this method, smooth curves can be specified accurately with a few points, usually not more than four or five. Curves with uneven places, dips, or highly variable curvatures require more points and are more difficult to fit properly. As a guide, enough points should be specified so that a physical spline passing through these points would accurately follow the curve. The minimum number of points to follow the curve should be used, since the closer the spline points are, the greater the effect of an inaccuracy in a coordinate.

(h) Requests for output data. - The seven variables IMESH, ISLINE, ISTATL, IPLOT, ISUPER, ITSON, and IDEBUG all request different portions of output from the program. The optional arrays ZHST, RHST, ZTST, RTST, and FLFR are also used in this regard. The user should be careful to request only the output needed. Usually,

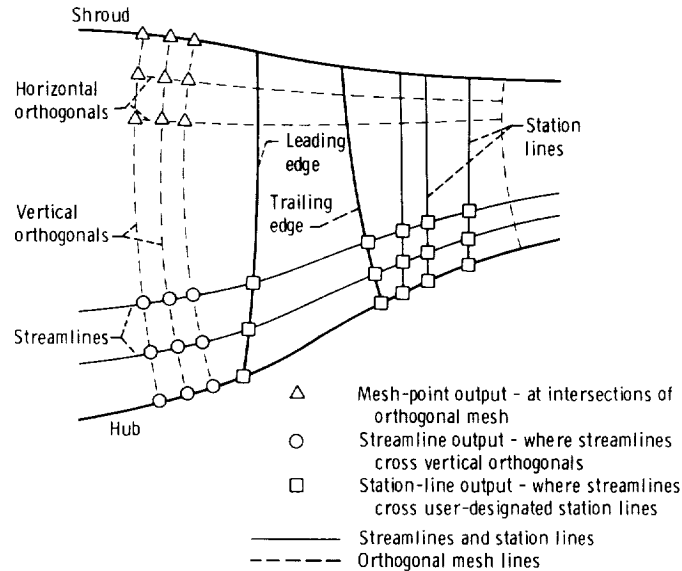


Figure 11. - Location of three major types of output.

only one of the three major types of output (at the mesh points (IMESH), along streamlines (ISLINE), or along hub-shroud stations (ISTATL)) is needed, since the ISLINE and ISTATL outputs are obtained from calculated mesh-point data by interpolation (fig. 11). Most likely, streamline output (ISLINE) or station-line output (ISTATL) would be chosen. The frequency at which output is requested is also significant; this is controlled by the values given to IMESH, ISLINE, and ISTATL.

ISTATL output should be requested only if NOSTAT is greater than zero (and the ZHST, RHST, ZTST, and RTST arrays are given). If LROT = 0, omit the RHST and RTST cards. Output will be given along straight lines from hub to shroud that connect corresponding points in these arrays. Through the values in these arrays, the user can control exactly the locations at which his output is given. These lines do not have to be radial. Output can be requested at several upstream and downstream locations, at the blade leading and trailing edges, and at several stations within the blade at percentages of chord from the leading to the trailing edge. To obtain output at the leading and trailing edges, the values in ZHST, RHST, ZTST, and RTST should correspond (within a tolerance of 1 percent of local chord) to the intersection points of the leading and trailing edges with the hub and shroud.

The array FLFR need be given only if the user wishes to specify the values of streamline along which he wishes output (when ISLINE or ISTATL are used). If the user does not specify otherwise (using FLFR), the program will automatically give output at 10-percent streamlines.

(i) Incompressible flow. - Incompressible flow cases can be executed on MERIDL by using special input for GAM and AR. Use  $GAM = 0.$  and set AR equal to the fluid density (RHO). In this case, TIP, PRIP, and PROP are not used by the program, but blank cards should be furnished with the input. No other special input is required for an incompressible case, except that REDFAC should be set to 1.0 to avoid the transonic solution, which would be redundant and less accurate.

(j) Straight infinite cascade. - The program is primarily designed for circular, stationary, or rotating blade rows; but the input can be adapted to apply to a straight infinite cascade as well. Since the radius for such a cascade would be infinite, an artificial convention must be adopted. The user should pick a large average radius for his cascade, in the neighborhood of  $r = 1000.$  Then, since the blade pitch P is known, the approximate number of blades to use can be calculated from  $NBL = (2\pi r)/P.$  This value must be rounded to an integer for use in the input. With this value of NBL and a large mean radius, all the r-coordinate arrays of input (RHUB, RTIP, RADIN, RADOUT, and RBL) can be established about the mean radius, and a value of MSFL can be calculated. Using this artificial input at large radius, the program will obtain a solution for a pitch that varies very slightly from hub to shroud and, therefore, simulates almost exactly a straight infinite cascade.

(k) Choosing a value for REDFAC. - If possible, REDFAC should be 1.0. However, if there is locally supersonic flow, REDFAC must be less than 1.0, usually between 0.5 and 0.95. For the best accuracy the largest possible value of REDFAC should be used (see the section NUMERICAL EXAMPLE, p. 70). When REDFAC is 1.0, the full mass flow will be used in the finite-difference solution for the stream function, and no transonic velocity-gradient calculation will be made.

(l) Choosing a value for ANGROT. - If the flow is close to axial (within about  $45^\circ$  from axial), ANGROT need not be given (use LROT = 0). If the flow deviates more than  $45^\circ$  from axial, use LROT = 1 and specify ANGROT in degrees so as to minimize the maximum slope of the hub or shroud from the rotated axis. For example, an impeller with axial inlet and radial discharge should have  $ANGROT = 45^\circ.$  A radial inflow turbine rotor with axial discharge should have  $ANGROT = -45^\circ.$

## OUTPUT

There are four different types of output generated by the MERIDL program:

- (1) Main output - controlled by the variables IMESH, ISLINE, ISTATL, and ISUPER
- (2) Debug output - controlled by IDEBUG
- (3) Information for the TSONIC program - controlled by ITSON
- (4) Plotted output - controlled by IPLOT

Most of this output is optional and is controlled by the final input card, as already described.

The output controlled by each of the variables IMESH, ISLINE, and ISTATL is essentially the same but is given at different locations for the convenience of the user. The IMESH output is given at the orthogonal mesh points along horizontal mesh lines, as indicated in figure 11. The ISLINE output is given along streamlines where the streamlines are intersected by the vertical orthogonal mesh lines (fig. 11). The ISTATL output is given from hub to shroud along station lines (fig. 11) where these lines are intersected by the streamlines. Also, additional ISTATL output is given beyond that given with IMESH or ISLINE output.

In the following sections, output is presented from the problem solved in the section NUMERICAL EXAMPLE (p. 70). Since the complete output would be lengthy, only the first few lines of each section of output are reproduced here. For debug output (IDEBUG  $\neq$  0), output labels are simply internal variable names, which are defined in the main dictionary of part II (ref. 6).

The following three sections discuss the different sections of printed output, the plotted output, and all possible error messages.

### Printed Output

Table I presents the printed output from the numerical example. Each section of this output has been numbered to correspond to the following description:

(1) The first output is a listing of the input data. Variable names are used as labels, and the output corresponds to the input form (fig. 5). This output is listed for every run, regardless of the values given to IMESH, etc.

(2) The second output gives information to assist the user in checking input blade geometry. This output is listed for every run. For each input blade section from hub to shroud the following is given: ZBL, RBL, THBL, and TTBL, all defined as in the input dictionary; blockage at each input point (tangential blade thickness TTBL divided by blade-to-blade pitch in radians); SZRBL, the meridional arc length of the input blade section; and DTHDSP and DTHDSP2, first and second derivatives of THBL against SZRBL along the input blade sections. The smoothness of DTHDSP and DTHDSP2 indicates where inaccurate data or errors may have occurred in input blade geometry.

(3) The third output corresponds to IDEBUG. It has four principal sections, as the printed output indicates. The first section gives blade geometry where the blade is intersected by the  $21 \times 21$  alternate mesh used for calculating gradients of the mean camber surface. The  $z$ ,  $r$ ,  $\theta$ , and tangential thickness coordinates are given, followed by the gradients of  $\theta$ , calculated by spline curves, along the two directions of the alter-

TABLE I. - SAMPLE OUTPUT

\*\*\*\*\*  
 \* MFIDL \*  
 \* PROGRAM INPUT \*  
 \*\*\*\*\*

DATA 12 - AXIAL COMPRESSOR ROTOR - INLET WHIRL - S.I. UNITS

GENERAL INPUT DATA		AR	NSFL	OMEGA	PRDFAC	VELTOL	FNEK	DNEW
GAM	1.400000	287.0530	42.82988	-826.5496	0.9999900	0.999999E-02	0.5000000	0.5000000
VELTOL HAS BEEN REDUCED BY THE MINIMUM OF PNEW OR DNEW TO =								
MHI	MBO	MH	MHT	NBL	MHUB	NTIP	MIN	MOUT
11	31	41	20	17	6	11	11	11
LSPR	LTPH	LAVT	LROT	LBLAD	LEFRAN			
1	0	1	0	0	0			
HUB AND SHROUD INPUT DATA								
ZOMIN	ZOMBI	ZOMRO	ZOMOUT	ROMIN	ROMBI	ROMRO	ROMOUT	
-0.4572000E-01	0.0000000	0.1219200	0.1676400	-0.0000000	-0.0000000	-0.0000000	-0.0000000	
ZHUB	ZHUB	ZHUB	ZHUB	ZHUB	ZHUB	ZHUB	ZHUB	
ARRAY	ARRAY	ARRAY	ARRAY	ARRAY	ARRAY	ARRAY	ARRAY	
-0.9140998E-01	-0.4063000E-01	0.1018000E-01	0.6099000E-01	0.1371900	0.2133900	0.1645920	0.2133900	
0.1178660	0.1430120	0.1554480	0.1612999	0.1640739	0.1640739	0.1640739	0.1640739	
ZTIP	ZTIP	ZTIP	ZTIP	ZTIP	ZTIP	ZTIP	ZTIP	
ARRAY	ARRAY	ARRAY	ARRAY	ARRAY	ARRAY	ARRAY	ARRAY	
-0.9140998E-01	-0.4063000E-01	0.1018000E-01	0.6099000E-01	0.1371900	0.2133900	0.1640739	0.2133900	
RTIP	RTIP	RTIP	RTIP	RTIP	RTIP	RTIP	RTIP	
ARRAY	ARRAY	ARRAY	ARRAY	ARRAY	ARRAY	ARRAY	ARRAY	
0.3246120	0.3159860	0.3111399	0.3083659	0.3073300	0.3073300	0.3073300	0.3073300	
UPSTREAM INPUT DATA								
ZHIN	ZTIM	RHIN	RTIN	ZHIN	ZTIM	RHIN	RTIN	
-0.1521000E-01	-0.1521000E-01	-0.0000000	-0.0000000	-0.1521000E-01	-0.1521000E-01	-0.0000000	-0.0000000	
RADIN	RADIN	RADIN	RADIN	RADIN	RADIN	RADIN	RADIN	
ARRAY	ARRAY	ARRAY	ARRAY	ARRAY	ARRAY	ARRAY	ARRAY	
0.1506630	0.1737660	0.1933350	0.2113180	0.2280509	0.2437789	0.2586840	0.2724570	
0.2863600	0.2992830	0.3131210	0.3131210	0.3131210	0.3131210	0.3131210	0.3131210	
TIP	TIP	TIP	TIP	TIP	TIP	TIP	TIP	
ARRAY	ARRAY	ARRAY	ARRAY	ARRAY	ARRAY	ARRAY	ARRAY	
288.1499	288.1499	288.1499	288.1499	288.1499	288.1499	288.1499	288.1499	
288.1499	288.1499	288.1499	288.1499	288.1499	288.1499	288.1499	288.1499	
PRIP	PRIP	PRIP	PRIP	PRIP	PRIP	PRIP	PRIP	
ARRAY	ARRAY	ARRAY	ARRAY	ARRAY	ARRAY	ARRAY	ARRAY	
101352.9	101352.9	101352.9	101352.9	101352.9	101352.9	101352.9	101352.9	
101352.9	101352.9	101352.9	101352.9	101352.9	101352.9	101352.9	101352.9	
VTHIN	VTHIN	VTHIN	VTHIN	VTHIN	VTHIN	VTHIN	VTHIN	
ARRAY	ARRAY	ARRAY	ARRAY	ARRAY	ARRAY	ARRAY	ARRAY	
-5.943600	-15.13637	-21.02814	-25.74644	-29.73323	-33.18661	-36.23462	-38.95343	
-41.40402	-43.60773	-45.79619	-47.98470	-50.27421	-53.56172	-56.85023	-60.13974	
DOWNSTREAM INPUT DATA								
ZHOUT	ZTOUT	RHOUT	RTOUT	ZHOUT	ZTOUT	RHOUT	RTOUT	
0.1371900	0.1371900	-0.0000000	-0.0000000	0.1371900	0.1371900	-0.0000000	-0.0000000	
RADOUT	RADOUT	RADOUT	RADOUT	RADOUT	RADOUT	RADOUT	RADOUT	
ARRAY	ARRAY	ARRAY	ARRAY	ARRAY	ARRAY	ARRAY	ARRAY	
0.1640739	0.1837029	0.1997350	0.2147930	0.2290270	0.2426510	0.2557270	0.2684070	
0.2806900	0.2927100	0.3073300	0.3229270	0.3385800	0.3543300	0.3700800	0.3858300	

TABLE I. - Continued.

PROP ARRAY	129221.6	129221.6	129221.6	129221.6	129221.6	129221.6	129221.6
129221.6	129221.6	129221.6	129221.6	129221.6	129221.6	129221.6	129221.6
WITHOUT ARRAY	-153.3876	-149.5227	-146.627	-144.3655	-142.9390	-141.8753	129221.6
-168.3715	-142.2349	-153.3876	-149.5227	-146.627	-144.3655	-142.9390	-141.8753
-141.1803		-146.4107					
BLADE BEAM CAMBER LINE AND THICKNESS INPUT DATA							
ZBL ARRAY							
-0.000000	0.1128000E-02	0.6307997E-02	0.1362000E-01	0.2229900E-01	0.3327000E-01	0.4442200E-01	0.5570000E-01
0.670497E-01	0.783998E-01	0.897686E-01	0.9467895E-01	0.1064500	0.1119450	0.1128179	0.1128179
0.1105000E-02	0.2325000E-02	0.7351998E-02	0.1453000E-01	0.2291500E-01	0.3363700E-01	0.4457900E-01	0.5564500E-01
0.6633398E-01	0.7824898E-01	0.8958799E-01	0.9464396E-01	0.1065339	0.1121410	0.1129839	0.1129839
0.2751000E-02	0.3683000E-02	0.9550998E-02	0.1551200E-01	0.2365900E-01	0.3410100E-01	0.4479400E-01	0.5569700E-01
0.6676799E-01	0.7796496E-01	0.8924998E-01	0.9429998E-01	0.1062260	0.1118820	0.1126910	0.1126910
0.4230998E-02	0.5091999E-02	0.9808998E-02	0.1655900E-01	0.2469000E-01	0.3462600E-01	0.4505100E-01	0.5571000E-01
0.6656694E-01	0.7758898E-01	0.8873695E-01	0.9772950E-01	0.1056179	0.1126890	0.1120450	0.1120450
0.6634396E-01	0.7714998E-01	0.8810699E-01	0.9670989E-01	0.1047810	0.1103949	0.1111290	0.1111290
0.6610399E-02	0.7925998E-02	0.1237000E-01	0.1673000E-01	0.2618700E-01	0.3577600E-01	0.4564000E-01	0.5574000E-01
0.8561999E-02	0.7665998E-01	0.8738899E-01	0.9608799E-01	0.1037700	0.1092940	0.1100060	0.1100060
0.6588998E-01	0.7614598E-01	0.8662599E-01	0.9513497E-01	0.1037700	0.1092940	0.1100060	0.1100060
0.9888998E-02	0.1057700E-01	0.1478900E-01	0.2080900E-01	0.2703500E-01	0.3635400E-01	0.4594400E-01	0.5574500E-01
0.6560898E-01	0.7562000E-01	0.8582898E-01	0.9412795E-01	0.1026630	0.1080820	0.1087660	0.1087660
0.1114200E-01	0.1180600E-01	0.1591600E-01	0.2176500E-01	0.3092989E-01	0.4047900E-01	0.5024300E-01	0.5974500E-01
0.6535598E-01	0.7508695E-01	0.8501697E-01	0.9309298E-01	0.1002520	0.1054140	0.1060440	0.1060440
0.1224500E-01	0.1289000E-01	0.1690400E-01	0.2264400E-01	0.3194800E-01	0.4179400E-01	0.5167800E-01	0.6138000E-01
0.6511199E-01	0.7458895E-01	0.8426094E-01	0.9213197E-01	0.9910995E-01	0.1304150	0.1347590	0.1347590
0.1320800E-01	0.1383900E-01	0.1775500E-01	0.2338700E-01	0.32994500E-01	0.4383500E-01	0.5469790E-01	0.6548500E-01
0.6487799E-01	0.7413095E-01	0.8375400E-01	0.9125996E-01	0.9807599E-01	0.1029960	0.1035950	0.1035950
RBL ARRAY							
0.1554829	0.1558880	0.1560680	0.1567520	0.1575500	0.1585660	0.1596000	0.1606400
0.1616960	0.1627490	0.1637959	0.1646280	0.1653480	0.1659840	0.1665340	0.1670000
0.1763860	0.1764500	0.1767650	0.1772160	0.1777419	0.1784449	0.1791019	0.1796000
0.1805050	0.1812150	0.1819270	0.1826960	0.1835950	0.1846450	0.1858000	0.1870130
0.1952600	0.1952960	0.1954850	0.1957960	0.1962770	0.1968800	0.1976000	0.1983350
0.1977420	0.1981760	0.1986110	0.1990640	0.1996210	0.1999400	0.1995220	0.1955220
0.2126070	0.2126229	0.2127129	0.2128410	0.2129910	0.2131830	0.2133800	0.2135800
0.2137680	0.2139969	0.2142079	0.2143780	0.2145280	0.2146650	0.2147500	0.2147500
0.2287440	0.2287450	0.2287560	0.2287720	0.2287900	0.2288139	0.2288380	0.2288620
0.2288880	0.2289140	0.2289400	0.2289610	0.2289790	0.2289930	0.2289940	0.2289940
0.2438920	0.2438830	0.2438360	0.2437580	0.2436709	0.2435500	0.2434450	0.2433420
0.2568730	0.2581960	0.2580950	0.2580800	0.2579709	0.2578760	0.2577810	0.2576969
0.2699780	0.2696460	0.2716640	0.2736880	0.2757120	0.2777610	0.2798389	0.2819470
0.2848260	0.2847990	0.2846319	0.2843879	0.2840660	0.2836730	0.2832340	0.2827630
0.2825969	0.2821960	0.2817880	0.2814560	0.2811610	0.2809490	0.2809229	0.2809229
0.2972890	0.2972590	0.2970700	0.2968020	0.2964880	0.2960849	0.2956720	0.2952590
0.2948140	0.2943700	0.2939169	0.2934489	0.2929220	0.2923970	0.2918750	0.2913580
0.3092760	0.3092450	0.3090520	0.3087760	0.3084550	0.3080820	0.3077180	0.3073740
0.3067400	0.3062860	0.3058230	0.3054460	0.3050690	0.3047000	0.3043400	0.3039800
TBL ARRAY							
-0.000000	0.3439000E-02	0.1837000E-01	0.3721100E-01	0.5575800E-01	0.7440495E-01	0.9278496E-01	0.1104600E-01
0.9982092E-01	0.9814894E-01	0.9150296E-01	0.8266997E-01	0.7242697E-01	0.6169996E-01	0.5221300E-01	0.4444600E-01
-0.1324000E-01	-0.1007400E-01	0.2391000E-01	0.4765999E-02	0.4341400E-01	0.4616696E-01	0.4087598E-01	0.3838997E-01
0.1016760	0.1058310	0.1058190	0.1028300	0.9806299E-01	0.9440000E-01	0.9268800E-01	0.9144000E-01
-0.2017100E-01	-0.5377997E-02	-0.5377997E-02	0.1400900E-01	0.3423500E-01	0.5455600E-01	0.7552099E-01	0.9476100E-01
0.1031300	0.1116959	0.1167409	0.1182390	0.1177030	0.1162080	0.1147000	0.1131000
-0.2977900E-01	-0.2271800E-01	-0.1235300E-01	0.7083999E-02	0.2772400E-01	0.5107300E-01	0.7164097E-01	0.8493147E-01
0.1041840	0.1160610	0.1249610	0.1299220	0.1326810	0.1338470	0.1338410	0.1338410
-0.3428200E-01	-0.3167000E-01	-0.2177000E-02	0.2177000E-02	0.2300000E-01	0.2470000E-01	0.2686799E-01	0.2982044E-01
0.1049179	0.1193440	0.1312590	0.1389620	0.1443550	0.1474730	0.1477979	0.1477979
-0.3726900E-01	-0.3478500E-01	-0.23053200E-01	-0.1322000E-02	0.1954200E-01	0.4494200E-01	0.6462097E-01	0.8466940E-01
0.1054070	0.1121820	0.11361240	0.11460260	0.11535520	0.11582710	0.1158430	0.1158430

REPRODUCIBILITY OF THE ORIGINAL PAGE IS POOR



-0.390400E-01	-0.3866200E-01	-0.246500E-01	-0.3667000E-02	C.1712600E-01	0.4171000E-01	0.5469995E-01	0.4603698E-01
0.1058609	0.1235920	0.1397310	0.1513450	0.1605450	0.1665620	0.1672900	0.1672900
-0.4000000E-01	-0.3771100E-01	-0.239300E-01	-0.5233999E-02	0.1541200E-01	0.4005000E-01	0.5335044E-01	0.48527696E-01
0.1057900	0.1298580	0.1424370	0.1534150	0.1659639	0.1730320	0.1738819	0.1738819
-0.4032700E-01	-0.3811200E-01	-0.246200E-01	-0.6183998E-02	0.1426300E-01	0.3884700E-01	0.5231700E-01	0.48464139E-01
0.1057900	0.1298580	0.1444400	0.1584980	0.1701240	0.1780390	0.1789860	0.1789860
-0.3594600E-01	-0.3779100E-01	-0.2457100E-01	-0.6430998E-02	0.1376200E-01	0.3817500E-01	0.5164400E-01	0.48414096E-01
0.1056409	0.1261190	0.1455480	0.1603220	0.1726760	0.1811700	0.1823840	0.1823840
-0.3926100E-01	-0.3695300E-01	-0.2399100E-01	-0.6168998E-02	0.1373400E-01	0.3789400E-01	0.5123500E-01	0.48373499E-01
0.1053700	0.1261200	0.1459620	0.1611680	0.1739780	0.1828400	0.1839000	0.1839000
TNEL ARRAY							
0.236200E-02	0.202400E-02	0.342900E-02	0.530999E-02	0.6706998E-02	0.8006997E-02	0.9110000E-02	0.9110000E-02
0.8862000E-02	0.8017998E-02	0.6571997E-02	0.4979998E-02	0.3294000E-02	0.1838000E-02	0.1613000E-02	0.1613000E-02
0.2173000E-02	0.2395000E-02	0.3490000E-02	0.4832000E-02	0.6093998E-02	0.7269997E-02	0.7971998E-02	0.8226000E-02
0.7985998E-02	0.7220998E-02	0.5925998E-02	0.4503998E-02	0.2976000E-02	0.1723000E-02	0.1530000E-02	0.1530000E-02
0.2035000E-02	0.2223000E-02	0.3234000E-02	0.4463997E-02	0.5617998E-02	0.6681997E-02	0.7323998E-02	0.7544998E-02
0.7317998E-02	0.6614998E-02	0.5434997E-02	0.4145997E-02	0.2765000E-02	0.1632000E-02	0.1470000E-02	0.1470000E-02
0.1933000E-02	0.2103000E-02	0.3036000E-02	0.4177998E-02	0.5245999E-02	0.6228000E-02	0.6817997E-02	0.7015999E-02
0.6799998E-02	0.6146997E-02	0.5157998E-02	0.3870000E-02	0.2600000E-02	0.1560000E-02	0.1417000E-02	0.1417000E-02
0.1855000E-02	0.2009000E-02	0.2985000E-02	0.3954998E-02	0.4956000E-02	0.5733997E-02	0.6422997E-02	0.6661997E-02
0.6396998E-02	0.5783997E-02	0.4764996E-02	0.3650000E-02	0.2472000E-02	0.1502000E-02	0.1373000E-02	0.1373000E-02
0.1798000E-02	0.1939000E-02	0.2769000E-02	0.3784000E-02	0.4731998E-02	0.5600998E-02	0.6118998E-02	0.6285998E-02
0.6086998E-02	0.5504999E-02	0.4539996E-02	0.3492000E-02	0.2373000E-02	0.1457000E-02	0.1338000E-02	0.1338000E-02
0.1755000E-02	0.1887000E-02	0.2683000E-02	0.3655000E-02	0.4562996E-02	0.5393997E-02	0.5888999E-02	0.6046999E-02
0.5854998E-02	0.5295998E-02	0.4371997E-02	0.3365000E-02	0.2298000E-02	0.1422000E-02	0.1311000E-02	0.1311000E-02
0.1724000E-02	0.1850000E-02	0.2622000E-02	0.3563000E-02	0.4441999E-02	0.5245999E-02	0.5723000E-02	0.5874999E-02
0.5686998E-02	0.5145997E-02	0.4249997E-02	0.3279000E-02	0.2243000E-02	0.1397000E-02	0.1292000E-02	0.1292000E-02
0.1705000E-02	0.1827000E-02	0.2616000E-02	0.3546000E-02	0.4361000E-02	0.5146999E-02	0.5612998E-02	0.5759999E-02
0.5576000E-02	0.5049997E-02	0.4169997E-02	0.3220000E-02	0.2207000E-02	0.1379000E-02	0.1277000E-02	0.1277000E-02
0.1694000E-02	0.1814000E-02	0.2559000E-02	0.3468000E-02	0.4315998E-02	0.5084998E-02	0.5548997E-02	0.5698997E-02
0.5512998E-02	0.4988998E-02	0.4123997E-02	0.3186000E-02	0.2186000E-02	0.1369000E-02	0.1269000E-02	0.1269000E-02
0.1692000E-02	0.1811000E-02	0.2552000E-02	0.3457000E-02	0.4300997E-02	0.5071998E-02	0.5530000E-02	0.5674999E-02
0.5492996E-02	0.4972000E-02	0.4109997E-02	0.3176000E-02	0.2180000E-02	0.1366000E-02	0.1267000E-02	0.1267000E-02

OUTPUT STATION LOCATION DATA

ZHST ARRAY	0.0000000	0.1128190	0.1371900
ZTST ARRAY	0.1320700E-01	0.1035950	0.1371900

OUTPUT STREAMLINE FLOW FRACTION DATA

FLEF ARRAY	0.9999996E-01	0.2000000	0.3000000
	0.9000000	1.0000000	0.4000000

DISTRIBUTION OF LOSS DATA

PERCRD ARRAY	0.9999996E-01	0.2000000	0.3000000
	0.9000000	1.0000000	0.4000000
PERLOS ARRAY	0.7999998E-01	0.1580000	0.2350000
	0.8220000	1.0000000	0.3140000

OUTPUT PRINT CONTROL DATA	ISUPER	ITSON	IDEBUG
IMESH	ISLINE	ISTAIL	IPLCOT
Z0	Z0	Z0	Z0
		5	20
		1	20
		20	20

TABLE I. - Continued.

\*\*\*\*\*  
 \*\* BLADE GEOMETRY ON INPUT BLADE SECTIONS \*\*\*\*\*  
 \*\*

** INPUT BLADE PLANE NUMBER 1 **	ZBL	RBL	TBRL	TTBRL	BLOCKAGE	SZBRL	DTHDSP	DTHDSP2
1	-0.000000	0.155429	-0.000000	0.1681922E-01	0.4550664E-01	0.000000	3.056142	-27.15805
2	0.1128000E-02	0.1555880	0.343000E-02	0.1862269E-01	0.5038672E-01	0.1132878E-02	3.009992	-54.31610
3	0.6307997E-02	0.1560680	0.1937000E-01	0.2667079E-01	0.7216138E-01	0.6335061E-02	2.731719	-52.66695
4	0.1369260E-01	0.1567520	0.3721100E-01	0.3610774E-01	0.9769928E-01	0.1375069E-01	2.353996	-49.20595
5	0.2229900E-01	0.1575500	0.5575800E-01	0.4451797E-01	0.1204493	0.2239459E-01	1.941688	-46.19423
6	0.3327000E-01	0.1585660	0.7440395E-01	0.5181282E-01	0.1401865	0.3342535E-01	1.449449	-43.15729
7	0.4422000E-01	0.1596000	0.8797896E-01	0.5586207E-01	0.1539686	0.4461236E-01	0.9776569	-41.09265
8	0.5570000E-01	0.1606449	0.9646699E-01	0.5481043E-01	0.1482970	0.5593867E-01	0.5203287	-39.86234
9	0.6704497E-01	0.1616960	0.9916894E-01	0.4935350E-01	0.1335375	0.7873599E-01	0.2368307E-01	-38.74096
10	0.7839996E-01	0.1627890	0.9150296E-01	0.4047038E-01	0.1094978	0.9009123E-01	-0.3663378	-38.44309
11	0.8970696E-01	0.1637959	0.8266997E-01	0.3076214E-01	0.8323109E-01	0.7332211E-01	-0.4094943	-38.82036
12	0.9867895E-01	0.1646280	0.7242697E-01	0.2025460E-01	0.5480194E-01	0.9910166E-01	-1.156135	-39.13141
13	0.1064500	0.1653480	0.7242697E-01	0.2025460E-01	0.5480194E-01	0.1069959	-1.472486	-41.94005
14	0.1119450	0.1658570	0.6369996E-01	0.1150574E-01	0.3113032E-01	0.1124244	-1.683536	-34.58765
15	0.1128179	0.1659380	0.6221300E-01	0.1010266E-01	0.2743395E-01	0.1133011	-1.706250	-17.27382

** INPUT BLADE PLANE NUMBER 2 **	ZBL	RBL	TBRL	TTBRL	BLOCKAGE	SZBRL	DTHDSP	DTHDSP2
1	0.1305000E-02	0.1763960	-0.1322400E-01	0.1403865E-01	0.3798332E-01	0.000000	3.009770	-22.78632
2	0.2325000E-02	0.1764500	-0.1007400E-01	0.1542856E-01	0.4174404E-01	0.1022002E-02	3.062778	-65.57265
3	0.7351998E-02	0.1767650	0.4765999E-02	0.2207329E-01	0.5972226E-01	0.6058857E-02	2.828061	-47.82714
4	0.1454000E-01	0.1772160	0.2391000E-01	0.2982339E-01	0.8069092E-01	0.1325101E-01	2.500511	-43.45807
5	0.2291500E-01	0.1777419	0.4414000E-01	0.3669515E-01	0.9928364E-01	0.2165249E-01	2.146020	-40.92976
6	0.3363700E-01	0.1784149	0.6416696E-01	0.4257690E-01	0.1151975	0.3239559E-01	1.723058	-37.81145
7	0.4457900E-01	0.1791019	0.8305998E-01	0.4573725E-01	0.1237482	0.4335914E-01	1.319632	-35.78258
8	0.5569500E-01	0.1798000	0.9333497E-01	0.4639658E-01	0.1250570	0.5449703E-01	0.9303874	-34.11293
9	0.6693399E-01	0.1805050	0.1016740	0.4446186E-01	0.1272975	0.6575811E-01	0.5523181	-33.03323
10	0.7824899E-01	0.1812150	0.1358310	0.3259172E-01	0.8818126E-01	0.7709333E-01	0.1820876	-32.27911
11	0.8958799E-01	0.1819270	0.1528190	0.2477230E-01	0.6702477E-01	0.8845663E-01	-0.1839717	-32.16052
12	0.9864396E-01	0.1824960	0.1628300	0.1640929E-01	0.4439750E-01	0.9753042E-01	-0.4743754	-31.84872
13	0.1065339	0.1829910	0.9806299E-01	0.9344000E-01	0.2577466E-01	0.1154359	-0.7343568	-33.92365
14	0.1123410	0.1833430	0.9266800E-01	0.9526079E-02	0.2577466E-01	0.1110539	-0.8046478	-26.69923
15	0.1129839	0.1833960	0.9266800E-01	0.9484562E-02	0.2296604E-01	0.1118985	-0.9215604	-13.34963

\*\*\*\*\*  
 \*\* BLADE GEOMETRY ON ALTERNATE MESH 21 HUB-TO-TIP \* 21 L.E.-TO-T.E. \*\*\*\*\*  
 \*\*

KN	LN	ZPC	REC	TBPC	TTPC	DTHDSP	DTHDTP
1	1	0.000000	0.1554839	-0.000000	0.1491922E-01	3.056144	-0.6693680
2	1	0.5440894E-02	0.1560681	0.1652801E-01	0.2568609E-01	2.767075	-0.6731678
3	1	0.1128179E-01	0.1565284	0.3116775E-01	0.3329170E-01	2.474467	-0.6586294
4	1	0.1692268E-01	0.1570513	0.4459159E-01	0.3955803E-01	2.196191	-0.6354768
5	1	0.2252635E-01	0.1575744	0.5627288E-01	0.4473736E-01	1.929420	-0.6094040

6	1	0.2820447E-01	0.1580968	0.5647074E-01	0.4888923E-01	1.572565	-0.5536102
7	1	0.3384537E-01	0.1586192	0.7523924E-01	0.5209988E-01	1.424541	-0.4947599
8	1	0.3948626E-01	0.1591422	0.8252414E-01	0.5445472E-01	1.183614	-0.4235023
9	1	0.4512715E-01	0.1596653	0.8866066E-01	0.5601572E-01	0.9485874	-0.3396449
10	1	0.5076805E-01	0.1601880	0.9338063E-01	0.5682332E-01	0.7183282	-0.2429024
11	1	0.5640894E-01	0.1607105	0.9680736E-01	0.5687022E-01	0.4921104	-0.1327316
12	1	0.6204984E-01	0.1612329	0.9896213E-01	0.5673670E-01	0.2690462	-0.8593488E-02

\*\*\*\*\*  
 \* CONSTANT QUANTITIES ON THE ORTHOGONAL MESH \*  
 \*\*\*\*\*

I	J	SOM	TOM	BTH	DTHDT	CPHI	SPHI
1	1	0.00000	0.00000	0.36960	0.00000	0.92985	0.36794
2	1	0.48944E-02	0.00000	0.36960	0.00000	0.93836	0.34567
3	1	0.97453E-02	0.00000	0.36960	0.00000	0.94649	0.32273
4	1	0.14557E-01	0.00000	0.36960	0.00000	0.95372	0.30070
5	1	0.19334E-01	0.00000	0.36960	0.00000	0.96009	0.27971
6	1	0.24082E-01	0.00000	0.36960	0.00000	0.96565	0.25986
7	1	0.28805E-01	0.00000	0.36960	0.00000	0.97046	0.24127
8	1	0.33506E-01	0.00000	0.36960	0.00000	0.97459	0.22400
9	1	0.38188E-01	0.00000	0.36960	0.00000	0.97810	0.20815
10	1	0.42855E-01	0.00000	0.36960	0.00000	0.98105	0.19376
11	1	0.47510E-01	0.00000	0.35236	-1.4053	0.98350	0.18090
12	1	0.53699E-01	0.00000	0.34292	-1.2858	0.98609	0.16619

4 { CALCULATED OVERRELAXATION FACTOR (ORF) = 1.838

5 { INITIAL CALCULATED LOSOUT ARRAY

JM	LOSOUT
1	0.014471
2	0.014175
3	0.014758
4	0.016312
5	0.017744
6	0.019191
7	0.021363
8	0.023636
9	0.026226
10	0.033048
11	0.049433

REPRODUCIBILITY OF THE ORIGINAL PAGE IS POOR

TABLE I. - Continued.

CALCULATED ILE AND ITE ARRAYS	
J	ITE
1	29
2	29
3	29
4	29
5	29
6	29
7	29
8	29
9	29
10	29
11	29
12	29
13	29
14	29
15	28
16	28
17	28
18	28
19	28
20	28
21	28

\*\*\*\*\*  
 \* ITERATION NO. 11 \*  
 \*\*\*\*\*

MAXIMUM CHANGE IN DVTHDT = 17.448  
 MAXIMUM VALUE OF DVTHDT = 47.003  
 MINIMUM VALUE OF DVTHDT = -233.46  
 MAXIMUM RELATIVE CHANGE IN VELOCITY = 0.3371E-02 AT I = 18, J = 19  
 AVERAGE RELATIVE CHANGE IN VELOCITY = 0.1367E-03  
 NUMBER OF UNCONVERGED MESH POINTS = 0  
 MAXIMUM CHANGE IN FT = 718.44  
 MAXIMUM VALUE OF FT = 42324.  
 MINIMUM VALUE OF FT = -0.11813E 06

AT I = 17, J = 18, WHERE DVTHDT = -90.681  
 AT I = 17, J = 14, WHERE FT = -28638.

***** CHANGING QUANTITIES ON THE ORTHOGONAL MESH *****											
I	J	MSUBS	MSBT	VTH	RHO	RHOAV	DELPHO	DLDU	PLOSS		
1	1	213.36	0.00000	-6.2756	0.99832	0.99832	0.00000	-16.992	0.00000		
2	1	210.56	0.00000	-6.1988	1.0039	1.0039	0.00000	-16.992	0.00000		
3	1	208.54	0.00000	-6.1292	1.0079	1.0079	0.00000	-16.992	0.00000		
4	1	206.85	0.00000	-6.0663	1.0112	1.0112	0.00000	-16.992	0.00000		
5	1	205.32	0.00000	-6.0092	1.0142	1.0142	0.00000	-16.992	0.00000		
6	1	203.84	0.00000	-5.9574	1.0170	1.0170	0.00000	-16.992	0.00000		
7	1	202.31	0.00000	-5.9104	1.0200	1.0200	0.00000	-16.992	0.00000		
8	1	200.60	0.00000	-5.8675	1.0232	1.0232	0.00000	-16.992	0.00000		
9	1	198.50	0.00000	-5.8285	1.0272	1.0272	0.00000	-16.992	0.00000		
10	1	195.55	0.00000	-5.7927	1.0328	1.0328	0.00000	-16.992	0.00000		
11	1	206.24	0.00000	-6.6136	1.0133	1.0125	-0.12678	0.00000	0.16553E-14		
12	1	213.69	0.00000	-22.322	1.0148	1.0103	-0.28948	0.00000	0.44545E-13		

I	J	DTHDS	FT	DPDM	XIOM	ZETOM	CAMP	SAMP
1	1	0.00000	0.00000	0.00000	0.59426E-04	62030.	1.0000	0.00000
2	1	0.00000	0.00000	0.00000	-0.33051E-04	62373.	1.0000	0.00000
3	1	0.00000	0.00000	0.00000	-0.64075E-05	62666.	1.0000	0.00000
4	1	0.00000	0.00000	0.00000	-0.29474E-04	63056.	1.0000	0.00000
5	1	0.00000	0.00000	0.00000	-0.16272E-04	63318.	1.0000	0.00000
6	1	0.00000	0.00000	0.00000	0.26315E-04	63514.	1.0000	0.00000
7	1	0.00000	0.00000	0.00000	0.98348E-05	63781.	1.0000	0.00000
8	1	0.00000	0.00000	0.00000	-0.26464E-04	63909.	1.0000	0.00000
9	1	0.00000	0.00000	0.00000	-0.17554E-04	63821.	1.0000	0.00000
10	1	0.00000	0.00000	0.00000	0.59366E-04	63591.	1.0000	0.00000
11	1	3.7990	-53471.	56.345	0.28864E-03	62757.	1.0000	0.00000
12	1	3.1931	-0.11624E 06	130.03	0.37755E-02	60841.	1.0000	0.00000

\*\*\*\*\*  
 \*\*\* STREAM FUNCTION, INTERIOR VELOCITIES, VELOCITY COMPONENTS, AND ANGLES \*\*\*  
 AT ALL MESH POINTS OF THE ORTHOGONAL MESH  
 \*\*\*\*\*

\*\*\*\*\*  
 \* REDUCED MASSFLOW \*  
 \*\*\*\*\*  
 \* ITERATION NO. 11 \*  
 \*\*\*\*\*

\*\* HORIZONTAL ORTHOGONAL MESH LINE NO. 1 \*\*

MESH-POINT COLB ROW	AXIAL COORD. (Z)	RADIAL COORD. (R)	STREAM FUNC. (U)	HERID. VEL. (WH)	REL. TANG. VEL. (WTH)	REL. VEL. (W)	CRIT. VEL. RATIO (W/WCR)	HERID. ANGLE (ALPHA)	REL. FLOW ANGLE (BETA)	MESH ANGLE (PHI)
1	1	-0.45720E-01	0.14107	213.36	110.33	240.20	0.765	21.59	27.34	21.59
2	1	-0.41148E-01	0.14282	210.56	111.85	238.43	0.759	20.22	27.98	20.22
3	1	-0.36576E-01	0.14444	208.54	113.26	237.31	0.756	18.83	28.51	18.83
4	1	-0.32004E-01	0.14594	206.85	114.56	236.46	0.753	17.50	28.98	17.50
5	1	-0.27432E-01	0.14733	205.32	115.76	235.71	0.750	16.24	29.41	16.24
6	1	-0.22860E-01	0.14861	203.84	116.87	234.97	0.748	15.06	29.83	15.06
7	1	-0.18288E-01	0.14979	202.31	117.90	234.16	0.745	13.96	30.23	13.96
8	1	-0.13716E-01	0.15088	200.60	118.85	233.16	0.742	12.94	30.64	12.94
9	1	-0.91400E-02	0.15190	198.50	119.72	231.81	0.737	12.01	31.09	12.01
10	1	-0.45720E-02	0.15283	195.55	120.53	229.71	0.730	11.17	31.65	11.17
11	1	-0.33528E-07	0.15370	206.24	120.43	238.83	0.759	10.42	30.28	10.42
12	1	0.60960E-02	0.15478	213.69	105.61	238.36	0.758	9.57	26.30	9.57

TABLE I. - Continued.

\*\*\*\*\*  
 \*\*\* STREAM FUNCTION, INTERIOR VELOCITIES, VELOCITY COMPONENTS, ANGLES, AND SURFACE VELOCITIES \*\*\*  
 ALONG STREAMLINES  
 \*\*\*\*\*

\*\*\*\*\*  
 \* REDUCED MASSFLOW \*  
 \*\*\*\*\*  
 \* ITERATION NO. 11 \*  
 \*\*\*\*\*

\*\* STREAMLINE NUMBER 1 -- STREAM FUNCTION = 0.0000 \*\*

AXIAL COORD. (Z)	RADIAL COORD. (R)	MERID. COORD. (H)	MERID. VEL. (W <sub>H</sub> )	REL.TANG. VEL. (W <sub>T</sub> )	REL.TANG. VEL. (W <sub>T</sub> )	REL. VEL. (W)	CRIT. VEL. RATIO (W/WCR)	MERID. ANGLE (ALPHA)	REL. FLOW ANGLE (BETA)	STREAM. CURV. (1./DIST)	SUCT. SUR. VEL. (WS)	PRESS. SUR. VEL. (WP)
-0.45720E-01	0.14107	0.00600	213.36	110.33	240.20	0.765	0.759	21.59	27.34	-4.795	0.00	0.00
-0.41148E-01	0.14282	0.48944E-02	210.56	111.85	236.43	0.759	0.759	20.22	27.98	-4.944	0.00	0.00
-0.36576E-01	0.14444	0.97453E-02	206.54	113.26	237.31	0.756	0.756	18.83	28.51	-4.918	0.00	0.00
-0.32004E-01	0.14594	0.14557E-01	206.85	114.56	236.46	0.753	0.753	17.50	28.98	-4.706	0.00	0.00
-0.27432E-01	0.14733	0.19334E-01	205.32	115.76	235.71	0.750	0.750	16.24	29.41	-4.466	0.00	0.00
-0.22860E-01	0.14861	0.24082E-01	203.84	116.87	234.97	0.748	0.748	15.06	29.83	-4.204	0.00	0.00
-0.18288E-01	0.14979	0.28805E-01	202.31	117.90	234.16	0.745	0.745	13.96	30.23	-3.921	0.00	0.00
-0.13716E-01	0.15088	0.33506E-01	200.60	118.85	233.16	0.742	0.742	12.94	30.64	-3.622	0.00	0.00
-0.91400E-02	0.15190	0.38188E-01	198.50	119.72	231.81	0.737	0.737	12.01	31.09	-3.307	0.00	0.00
-0.45720E-02	0.15283	0.42855E-01	195.55	120.53	229.71	0.730	0.730	11.17	31.65	-2.980	0.00	0.00
-0.33528E-07	0.15370	0.47510E-01	206.24	120.43	238.83	0.759	0.759	10.42	30.28	-2.642	267.00	210.66
0.60960E-02	0.15478	0.53699E-01	213.69	105.61	238.36	0.758	0.758	9.57	26.30	-2.191	303.37	173.34

\*\*\*\*\*  
 \*\*\* STREAM FUNCTION, INTERIOR VELOCITIES, VELOCITY COMPONENTS, ANGLES, AND SURFACE VELOCITIES \*\*\*  
 ALONG LINES FROM HUB TO SHROUD AT VARIOUS STATIONS THROUGH THE BLADE ROW  
 \*\*\*\*\*

\*\*\*\*\*  
 \* REDUCED MASSFLOW \*  
 \*\*\*\*\*  
 \* ITERATION NO. 11 \*  
 \*\*\*\*\*

\*\* HUB-SHROUD STATION NO. 1 \*\*

RADIAL COORD. (R)	AXIAL COORD. (Z)	MERID. COORD. (H)	STREAM FUNC. (U)	MERID. VEL. (W <sub>H</sub> )	REL.TANG. VEL. (W <sub>T</sub> )	REL. VEL. (W)	CRIT. VEL. RATIO (W/WCR)	MERID. ANGLE (ALPHA)	REL. FLOW ANGLE (BETA)	STREAM. CURV. (1./DIST)	SUCT. SUR. VEL. (WS)	PRESS. SUR. VEL. (WP)
0.15054	-0.15210E-01	0.31973E-01	0.0000	201.14	118.54	233.47	0.743	13.28	30.51	-3.719	0.00	0.00
0.17215	-0.15210E-01	0.39772E-01	0.1000	187.02	127.74	226.49	0.719	11.57	34.33	-2.408	0.00	0.00
0.19191	-0.15210E-01	0.46250E-01	0.2000	179.12	137.99	226.11	0.716	9.46	37.61	-1.961	0.00	0.00
0.21018	-0.15210E-01	0.51408E-01	0.3000	173.32	148.27	228.09	0.721	7.25	40.55	-1.557	0.00	0.00
0.22726	-0.15210E-01	0.55277E-01	0.4000	169.16	158.30	231.68	0.731	5.10	43.10	-1.154	0.00	0.00
0.24335	-0.15210E-01	0.57911E-01	0.5000	165.94	168.05	236.18	0.743	3.02	45.36	-0.8058	0.00	0.00
0.25862	-0.15210E-01	0.59386E-01	0.6000	163.55	177.55	241.39	0.758	1.10	47.35	-0.3965	0.00	0.00
0.27118	-0.15210E-01	0.59805E-01	0.7000	162.00	186.78	247.24	0.774	-0.68	49.06	0.3285E-01	0.00	0.00
0.28708	-0.15210E-01	0.59287E-01	0.8000	161.25	195.76	253.62	0.792	-2.36	50.52	0.3940	0.00	0.00
0.30040	-0.15210E-01	0.57969E-01	0.9000	161.11	204.51	260.35	0.811	-3.90	51.77	0.7758	0.00	0.00
0.31318	-0.15210E-01	0.55983E-01	1.0000	160.78	213.05	266.91	0.829	-5.29	52.96	1.163	0.00	0.00

RADIAL COORD. (R)	AXIAL COORD. (Z)	STATIC PRES. (P)	STATIC TEMP. (T)	STATIC DENS. (RH0)	ABS.TANG. VEL. (VTH)	ABS. VEL. (V)	ABS.TOT. PRES. (PP)	ABS.TOT. TEMP. (TP)	ABS.FLOW ANGLF (BETA)	REL.TOT. PRES. (RPP)	REL.TOT. TEMP. (RTP)
0.17215	-0.15210E-01	78637.50	268.00	1.0222015	-5.89	261.23	101353.1	288.15	-1.68	110203.9	295.13
0.19191	-0.15210E-01	81374.31	270.63	1.0474892	-14.54	187.59	101384.4	288.14	-4.45	111540.0	296.16
C.21018	-0.15210E-01	82791.31	271.97	1.0604858	-20.63	180.30	101389.9	288.15	-6.57	113220.5	297.41
C.22726	-0.15210E-01	83759.88	272.87	1.0693331	-25.45	175.18	101388.1	288.15	-8.35	115032.6	298.76
C.24335	-0.15210E-01	84402.13	273.47	1.0751829	-29.54	171.72	101347.7	288.15	-9.91	116954.8	300.18
C.25862	-0.15210E-01	84864.00	273.90	1.0793829	-33.09	169.21	101388.6	288.15	-11.28	118977.6	301.66
C.27318	-0.15210E-01	85173.69	274.18	1.0821843	-36.22	167.51	101388.6	288.15	-12.69	121036.8	303.18
C.28708	-0.15210E-01	85334.88	274.33	1.0836573	-39.61	166.63	101350.1	288.15	-13.54	123306.6	304.75
C.30040	-0.15210E-01	85355.63	274.35	1.0838851	-41.53	166.51	101349.9	288.15	-14.88	125598.8	306.36
C.31318	-0.15210E-01	85274.75	274.27	1.0831118	-43.78	166.96	101349.4	288.15	-15.20	127879.1	308.01
		85237.81	274.24	1.0827761	-45.81	167.18	101352.4	288.15	-15.90	130449.1	309.70

10

\*\*\* HUB-SHOUD STATION NO. 2 \*\*\*

\*\*\* LEADING EDGE \*\*\*

RADIAL COORD. (R)	AXIAL COORD. (Z)	MERID. COORD. (H)	STREAM FVNC. (U)	MERID. VEL. (WH)	REL.TANG. VEL. (WTH)	REL. VEL. (W)	CRIT.VEL. RATIO (H/WCR)	MERID. ANGLE (ALPHA)	REL.FLOW ANGLF (BETA)	STREAM. CURV. (1./DIST)	SUCT.SURF. VEL. (WS)	PRES.SUP. VEL. (RP)
0.15370	-0.99671E-04	0.47415E-01	0.0000	192.71	121.31	227.72	0.724	10.33	32.19	-2.651	266.12	211.10
C.17523	0.12246E-02	0.56494E-01	0.1000	186.92	130.60	228.03	0.724	10.02	34.94	-3.052	259.81	208.79
0.19458	0.26956E-02	0.64357E-01	0.2000	184.41	140.51	231.84	0.734	7.57	37.30	-2.276	249.74	217.55

\*\*\*\*\*  
 \*\*\* INCIDENCE AND DEVIATION ANGLES \*\*\*  
 \*\*\*\*\*

\*\*\*\*\*  
 \* REDUCED MASSFLOW \*  
 \*\*\*\*\*  
 \* ITERATION NO. 11 \*  
 \*\*\*\*\*

MESH LINE	INCIDENCE UNBLOCKED	BLADE ANGLE AT L.E.	DEVIATION UNBLOCKED	ELADE ANGLF AT T.E.
1	6.01	24.33	8.62	-17.82
2	5.84	25.46	8.21	-15.37
3	5.77	26.67	8.37	-12.69
4	5.84	27.95	8.29	-9.95
5	5.02	29.31	8.22	-7.22
6	4.94	30.70	8.14	-4.55
7	5.03	32.03	8.01	-1.90
8	5.03	33.33	7.85	0.72
9	4.84	34.60	7.70	3.31
10	4.15	35.87	7.25	5.97
11	4.07	37.06	7.03	8.41
12	4.19	38.16	6.85	10.88
13	4.18	39.23	6.70	13.25
14	4.14	40.27	6.53	15.56
15	4.16	41.24	6.31	17.82
16	4.08	42.15	6.13	20.04

11

TABLE I. - Continued.

17	*	3.53	4.76	43.02	*	6.03	6.44	22.18	*
18	*	3.48	4.64	43.85	*	5.95	6.36	24.16	*
19	*	3.60	4.72	44.64	*	5.91	6.33	25.93	*
20	*	3.56	4.64	45.38	*	5.99	6.42	27.51	*
21	*	3.72	4.78	46.08	*	6.06	6.50	29.01	*

\*\*\*\*\*  
 \*\*\* INPUT DATA FOR TSONIC PROGRAM \*\*\*  
 \*\*\*\*\*

\*\*\*\*\*  
 \* REDUCED MASSFLOW \*  
 \*\*\*\*\*  
 \* ITERATION NO. 11 \*  
 \*\*\*\*\*

\*\*\*\*\*  
 \* TSONIC INPUT -- STREAMLINE NUMBER 1 -- STREAM FUNCTION = 0.0000 \*  
 \*\*\*\*\*  
 \* NOTE -- THE ORIGIN FOR MERIDIONAL AND TANGENTIAL COORDINATES ON THIS BLADE SECTION IS THE TSONIC ORIGIN, \*  
 \* THAT IS, THE FARTHEST POINT UPSTREAM ON THE LEADING EDGE RADIUS. THE MERID COORDINATES, \*  
 \* WHICH HAVE A DIFFERENT ORIGIN, HAVE BEEN SHIFTED BY THE PROGRAM TO GIVE THESE TSONIC INPUTS. \*  
 \*\*\*\*\*

```

GAM      AP      TIP      KHOIP      OMEGA      ZMSEL
1.400000 287.0530 288.1499 1.225336 -826.5893 0.2519401E-01
REDFAC   VELTOL
0.0100

MBI  MBO  MN  MBSI  MEL  NSPL1  NSPL2  NRSP  NSL
          C      1      1
LRVB LOSS LWCR LIPS
          C      1      1
RVTHO
-0.885319 -27.62529      FSN1      FSN0      SSM1      SSM2
          STGR
( .113429) 0.5493018E-11

BLADE SURFACE 1 *****
          RI1      RI2      BET11      BET12      BET01      BET02
          0.1345579E-02 29.51558      0.2225510E-03 -24.85971
  
```

```

POINT      ZMSP1      THSP1      DERIVATIVE      2ND DERIVATIVE      CURVATURE      RADIUS
1      0.6832844E-03 0.7619105E-02 3.667833 -39.73868 -1.532855 0.1533291
2      0.6282075E-02 0.2745441E-01 3.257735 -75.43771 -7.766722 0.1547774
3      0.1246765E-01 0.4681924E-01 2.924503 -64.96450 -6.274663 0.1557658
4      0.1863208E-01 0.6364536E-01 2.534515 -60.34187 -7.258762 0.1566918
5      0.2878667E-01 0.7815182E-01 2.176773 -57.93557 -7.447711 0.1575291
6      0.3303245E-01 0.9045637E-01 1.830520 -54.84399 -7.496574 0.1582598
7      0.3707242E-01 0.1006725 1.560545 -52.07513 -7.554742 0.1589204
8      0.4320418E-01 0.1134891 1.311879 -51.27734 -7.584976 0.1596810
9      0.4914634E-01 0.1151712 1.089281 -51.86091 -7.613309 0.1604782
10     0.5584465E-01 0.1195372 0.8575802 -51.74482 -7.635735 0.1612143
11     0.6156113E-01 0.1219864 0.2422148 -52.00977 -7.6565873 0.1619275
12     0.6767231E-01 0.1244942 -0.7557977E-01 -52.33639 -7.6761804 0.1627284
13     0.7379318E-01 0.1270262 -1.44391774 -57.06964 -7.694474 0.1631177
  
```

11

12



POINT	7985368E-01	11174713	-1.7950766	-55.30274	-2.942095	0.1624475
1	0.39094E-01	0.111827	-1.101947	-57.20055	-5.939415	0.1627425
2	0.4905171E-01	0.130996	-1.404714	-61.18144	-6.776601	0.1629895
3	0.5941305E-01	0.146211E-01	-1.733702	-65.35134	-8.002785	0.1632318
4	0.7112499E-01	0.158062E-01	-2.241849	-71.27733	-9.966112	0.1634132
5	0.851119E-01	0.177215E-01	-3.050489	-80.07780	-13.066793	0.1635773
6	0.1122773	0.213507E-01	-4.73283	-92.15225	-18.571736	0.1636372

GUIDE SURFACE 2 *****	HI2	BEI2	R02	RETD2
0.1122773	0.112456795E-02	17.59296	1.022551E-13	-5.011790

POINT	43224	CHSP2	DERIVATIVE	2ND DERIVATIVE	CUMULATIVE	4ADMS
1	0.1751318E-02	-0.8342454E-02	2.150390	-17.33481	-23.55114	0.1539995
2	0.4294375E-02	0.7711594E-03	1.840957	-22.93116	-4.177734	0.1540776
3	0.1246768E-01	0.1221191E-01	1.768233	-24.57835	-3.116141	0.1557658
4	0.1964205E-01	0.2282376E-01	1.493841	-26.39260	-3.926357	0.1566818
5	0.2478662E-01	0.3197745E-01	1.433651	-27.57240	-5.771790	0.1575291
6	0.3793245E-01	0.4731172E-01	1.265273	-27.73224	-4.032450	0.1593398
7	0.4721418E-01	0.6493019E-01	1.193958	-28.36187	-4.154570	0.1592264
8	0.4321418E-01	0.8493019E-01	1.325045	-28.55653	-4.325274	0.15906810
9	0.4594505E-01	0.9579213E-01	1.745426	-28.81334	-4.336802	0.1602762
10	0.5545055E-01	0.6296518E-01	1.511826	-28.36704	-4.418390	0.1612975
11	0.6150113E-01	0.857170E-01	1.339802	-27.88400	-4.439569	0.1617286
12	0.6767218E-01	0.6770789E-01	0.646173E-01	-27.18724	-4.357494	0.1621107
13	0.7476118E-01	0.6552285E-01	0.646173E-01	-29.72775	-4.813407	0.1624475
14	0.7995399E-01	0.497313E-01	0.119743	-29.28985	-4.763169	0.1627425
15	0.8598843E-01	0.3723348E-01	0.2453417	-28.25743	-4.596360	0.1629995
16	0.9234715E-01	0.4486999E-01	0.4709101	-29.28455	-4.751243	0.1632218
17	0.2918463E-01	0.6193403E-01	0.4483397	-28.86264	-4.657833	0.1634132
18	0.1490446	0.3695545E-01	0.42933	-30.53641	-4.876252	0.1635773
19	0.1123867	0.5126883E-01	0.690713	-23.03818	-3.741952	0.1636372
20	0.1123532	0.4071325E-01	0.133665	-16.27215	-2.156423	0.1636248

STREAM CHANNEL DATA *****	ZMSP	BMSP	BESE	WOMCP	PLDSS	DRDY	DZBDM2
1	-0.4743718E-01	0.110747	0.2264049E-02	0.7692447	0.000000	-0.1953235E-02	-0.6331742E-01
2	-0.4251274E-01	0.1428218	0.2257929E-02	0.7551879	0.000000	-0.2416092E-02	-0.1266348
3	-0.3760140E-01	0.1840476	0.2265247E-02	0.7556252	0.000000	-0.4630912E-02	0.3521959E-01
4	-0.3285248E-01	0.1459424	0.2283078E-02	0.7527162	0.000000	-0.2444892E-02	0.4372240E-01
5	-0.2837276E-01	0.1473248	0.2221982E-02	0.7501658	0.000000	-0.2171904E-02	0.7307665E-01
6	-0.2332462E-01	0.1446078	0.2251258E-02	0.7476541	0.000000	-0.1771562E-02	0.9518682E-01
7	-0.1865231E-01	0.1447318	0.2250975E-02	0.7449186	0.000000	-0.1291098E-02	0.1081625
8	-0.1391346E-01	0.1539945	0.2250975E-02	0.7416027	0.000000	-0.4455238E-03	0.4517619
9	-0.1021961E-02	0.1518462	0.2250948E-02	0.7331638	0.000000	-0.2186689E-03	0.3192931E-01
10	-0.4551469E-02	0.1529335	0.2250948E-02	0.7333928	0.000000	0.4350536E-02	1.742567
11	0.1324194E-03	0.1537706	0.2233217E-02	0.7392594	0.1053488E-04	0.3204938E-02	-2.238713
12	0.6202370E-02	0.1547774	0.2227744E-02	0.7576115	0.6954638E-03	-0.2129276E-02	0.5151901

TABLE I. - Continued.

```

*****
*** STREAM FUNCTION, INTERIOR VELOCITIES, VELOCITY COMPONENTS, AND ANGLES ***
AT ALL MESH POINTS OF THE ORTHOGONAL MESH
*****
* PULL MASSFLOW *
*****
* TRANSOMIC SOLUTION *
*****
* BY VELOCITY GRADIENT APPROXIMATE METHOD *
*****
* ALL VELOCITIES SMALLER THAN CHOKING MASSFLOW SOLUTION *
*****

```

\*\* HORIZONTAL ORTHOGONAL MESH LINE NO. 1 \*\*

MESH-POINT COLM (I)	AXIAL COORD. (Z)	RADIAL COORD. (R)	STREAM FUNC. (U)	MERID. VEL. (WM)	REL.TANG. VEL. (WTH)	REL. VEL. (W)	CRIT.VEL. RATIO (W/WCR)	MERID. ANGLE (ALPHA)	REL.FLOW ANGLE (BETA)	MESH ANGLE (PHI)
1	-0.45720E-01	0.14107	0.0000	203.39	110.33	231.38	0.737	21.59	28.48	21.59
2	-0.41148E-01	0.14282	0.0000	207.53	111.85	235.75	0.751	20.22	28.32	20.22
3	-0.36576E-01	0.14444	0.0000	208.00	113.26	236.84	0.754	18.83	28.57	18.83
4	-0.32004E-01	0.14594	0.0000	205.85	114.56	235.59	0.750	17.50	29.10	17.50
5	-0.27432E-01	0.14733	0.0000	204.50	115.76	234.99	0.748	16.24	29.51	16.24
6	-0.22860E-01	0.14861	0.0000	202.92	116.88	234.17	0.745	15.06	29.94	15.06
7	-0.18288E-01	0.14979	0.0000	201.32	117.90	233.30	0.742	13.96	30.35	13.96
8	-0.13716E-01	0.15088	0.0000	199.74	118.85	232.43	0.739	12.94	30.75	12.94

13

```

*****
*** STREAM FUNCTION, INTERIOR VELOCITIES, VELOCITY COMPONENTS, ANGLES, AND SURFACE VELOCITIES ***
ALONG STREAMLINES
*****
* PULL MASSFLOW *
*****
* TRANSOMIC SOLUTION *
*****
* BY VELOCITY GRADIENT APPROXIMATE METHOD *
*****
* ALL VELOCITIES SMALLER THAN CHOKING MASSFLOW SOLUTION *
*****

```

\*\* SURFACELINE NUMBER 1 -- STREAM FUNCTION = 0.0000 \*\*

AXIAL COORD. (Z)	RADIAL COORD. (R)	MERID. VEL. (WM)	REL.TANG. VEL. (WTH)	REL. VEL. (W)	CRIT.VEL. RATIO (W/WCR)	MERID. ANGLE (ALPHA)	REL.FLOW ANGLE (BETA)	STREAM CURV. (1./DIST)	SUCT.SUR. VEL. (WS)	PRES.SUR. VEL. (WP)
-0.45720E-01	0.14107	203.39	110.33	231.38	0.737	21.59	28.48	-4.795	0.00	0.00
-0.41148E-01	0.14282	207.53	111.85	235.75	0.751	20.22	28.32	-4.904	0.00	0.00
-0.36576E-01	0.14444	208.00	113.26	236.84	0.754	18.83	28.57	-4.919	0.00	0.00
-0.32004E-01	0.14594	205.85	114.56	235.59	0.750	17.50	29.10	-4.706	0.00	0.00
-0.27432E-01	0.14733	204.50	115.76	234.99	0.748	16.24	29.51	-4.466	0.00	0.00
-0.22860E-01	0.14861	202.92	116.88	234.17	0.745	15.06	29.94	-4.204	0.00	0.00
-0.18288E-01	0.14979	201.32	117.90	233.30	0.742	13.96	30.35	-3.921	0.00	0.00
-0.13716E-01	0.15088	199.74	118.85	232.42	0.739	12.94	30.75	-3.622	0.00	0.00

13

\*\*\*\*\*  
 \*\*\* STREAM FUNCTION, INTERIOR VELOCITIES, VELOCITY COMPONENTS, ANGLES, AND SURFACE VELOCITIES \*\*\*  
 ALONG LINES FROM HUB TO SHROUD AT VARIOUS STATIONS THROUGH THE BLADE ROW  
 \*\*\*\*\*

\*\*\*\*\*  
 \* FULL MASSFLOW \*  
 \*\*\*\*\*  
 \* TRANSONIC SOLUTION \*  
 \* BY VELOCITY GRADIENT APPROXIMATE METHOD \*  
 \*\*\*\*\*  
 \* ALL VELOCITIES SMALLER THAN CHOKING MASSFLOW SOLUTION \*  
 \*\*\*\*\*

\*\* HUB-SHROUD STATION NO. 1 \*\*

RADIAL COORD. (R)	AXIAL COORD. (Z)	HUBID. COORD. (H)	STREAM FUNC. (U)	HUBID. VEL. (WR)	REL.TANG. VEL. (WTH)	REL. VEL. (W)	CRIT.VEL. RATIO (W/ACR)	MERID. ANGLE (ALPHA)	REL.FLOW ANGLE (BETA)	STREAM. CURV. (1./DIST)	SUCT.SUR. VEL. (WS)	PRES.SUR. VEL. (WP)
0.15054	-0.15210E-01	0.31973E-01	0.0000	200.24	118.54	232.70	0.740	13.28	30.62	-3.719	0.00	0.00
0.17215	-0.15210E-01	0.39754E-01	0.1000	186.98	127.75	226.45	0.719	11.57	34.34	-2.408	0.00	0.00
0.19191	-0.15210E-01	0.46298E-01	0.2000	179.08	137.99	226.08	0.716	9.46	37.62	-1.961	0.00	0.00
0.21018	-0.15210E-01	0.51469E-01	0.3000	173.38	148.27	228.13	0.721	7.25	40.54	-1.557	0.00	0.00
0.22725	-0.15210E-01	0.55337E-01	0.4000	169.14	158.29	231.66	0.731	5.11	43.10	-1.154	0.00	0.00
0.24334	-0.15210E-01	0.57957E-01	0.5000	165.91	168.04	236.15	0.743	3.02	45.37	-0.8061	0.00	0.00
0.25861	-0.15210E-01	0.59416E-01	0.6000	163.52	177.53	241.36	0.757	1.10	47.35	-0.3969	0.00	0.00
0.27316	-0.15210E-01	0.59820E-01	0.7000	161.97	186.77	247.22	0.774	-0.68	49.07	0.3246E-01	0.00	0.00
0.28707	-0.15210E-01	0.59253E-01	0.8000	161.16	195.55	253.56	0.792	-2.36	50.54	0.3937	0.00	0.00
0.30040	-0.15210E-01	0.57970E-01	0.9000	161.00	204.51	260.28	0.810	-3.90	51.79	0.7756	0.00	0.00
0.31318	-0.15210E-01	0.55983E-01	1.0000	161.45	213.05	267.32	0.830	-5.29	52.85	1.163	0.00	0.00

RADIAL COORD. (R)	AXIAL COORD. (Z)	STATIC PRES. (P)	STATIC TEMP. (T)	STATIC DENS. (RHO)	ABS.TOT. VEL. (V)	ABS.TOT. PRES. (PP)	ABS.TOT. TEMP. (TPP)	ABS.FLOW ANGLE (BETA)	REL.TOT. PRES. (PPP)	REL.TOT. TEMP. (TPP)
0.15054	-0.15210E-01	78822.50	268.18	1.0239182	200.33	101353.1	288.15	-1.68	11C203.9	295.13
0.17215	-0.15210E-01	81383.31	270.64	1.0475721	187.54	101344.4	288.14	-4.45	111560.0	296.16
0.19191	-0.15210E-01	82799.69	271.98	1.0605621	-20.63	101350.1	288.15	-6.57	113221.3	297.41
0.21018	-0.15210E-01	83748.63	272.86	1.0692301	-25.45	101348.1	288.15	-8.35	115033.1	298.76
0.22725	-0.15210E-01	84405.75	273.47	1.0752163	-29.54	101347.7	288.15	-9.91	116953.8	300.18
0.24334	-0.15210E-01	84869.63	273.90	1.0794334	-33.09	101348.1	288.15	-11.28	118974.6	301.65
0.25861	-0.15210E-01	85179.19	274.19	1.0822449	-36.22	101348.6	288.15	-12.49	121092.6	303.18
0.27316	-0.15210E-01	85339.69	274.33	1.0837002	-39.01	101350.1	288.15	-13.54	123302.9	304.75
0.28707	-0.15210E-01	85370.75	274.36	1.0839825	-41.53	101349.9	288.15	-14.45	125596.6	306.36
0.30040	-0.15210E-01	85294.38	274.29	1.0832901	-43.78	101349.4	288.15	-15.21	127978.3	308.01
0.31318	-0.15210E-01	85120.50	274.13	1.0817108	-45.81	101352.4	288.15	-15.84	130449.6	309.70

REPRODUCIBILITY OF THE ORIGINAL PAGE IS POOR

TABLE I. - Concluded.

```

*****
*** INCIDENCE AND DEVIATION ANGLES ***
*****

*****
* FULL MASSFLOW *
*****
* TRANSONIC SOLUTION *
* BY VELOCITY GRADIENT APPROXIMATE METHOD *
*****
* ALL VELOCITIES SMALLER THAN CHOKING MASSFLOW SOLUTION *
*****

* MESH *
* LINE *   BLOCKED   UNBLOCKED   BLADE ANGLE AT L.E. *   DEVIATION   UNBLOCKED   BLADE ANGLE AT T.E. *
* 1 *     5.65     7.58     24.33 *     8.58     8.27     -17.82 *
* 2 *     5.16     6.98     25.66 *     8.72     8.44     -15.37 *
* 3 *     5.35     7.03     26.67 *     8.55     8.39     -12.69 *
* 4 *     5.38     6.95     27.95 *     8.34     8.29     -9.95 *
* 5 *     4.75     6.25     29.31 *     8.16     8.19     -7.22 *
* 6 *     4.75     6.16     30.70 *     7.99     8.09     -4.55 *
* 7 *     4.69     6.02     32.03 *     7.79     7.95     -1.90 *
* 8 *     4.62     5.89     33.33 *     7.57     7.78     0.72 *

*****
*** INPUT DATA FOR TSONIC PROGRAM ***
*****

*****
* PULL MASSFLOW *
*****
* TRANSONIC SOLUTION *
* BY VELOCITY GRADIENT APPROXIMATE METHOD *
*****
* ALL VELOCITIES SMALLER THAN CHOKING MASSFLOW SOLUTION *
*****

*****
* STREAMLINE NUMBER 1 -- STREAM FUNCTION = 0.0000 *
* NOTE -- THE ORIGIN FOR MERIDIONAL AND TANGENTIAL COORDINATES ON THIS BLADE SECTION IS THE TSONIC ORIGIN, *
* THAT IS, THE FARTHEST POINT UPSTREAM ON THE LEADING EDGE RADIUS. THE MERID COORDINATES, *
* WHICH HAVE A DIFFERENT ORIGIN, HAVE BEEN SHIFTED BY THE PROGRAM TO GIVE THESE TSONIC INPUTS. *
*****

GAM      AR      TIP      SHOIP      OMEGA      ZMSPL
1.40000  287.351J  288.149J  1.225336  -626.549J  0.2619403E-01

```

REDFAC VELTOL  
 0.0100  
 MBI MBO MH MBB1 NBL NSPL1 NSPL2 MRSP NSL  
 17 20 20 41  
 LEVB LOSS LKCR LIPS  
 1 1  
 PWITHI RVTHO  
 -0.8853319 -27.62529  
 CHORD SAGR  
 0.1134290 0.5493019E-01

SSM1 SSM2  
 DELTA THSTAK  
 0.3445956E-02 0.4641660E-02

BLADE SURFACE 1 \*\*\*\*\*  
 RI1 RI2 RETI1 RETI2 RO1 RO2 BTO1 BTO2  
 0.1345579E-02 17.59296 0.9225516E-03 -23.85901

POINT	ZMSP1	THSP1	DERIVATIVE	2ND DERIVATIVE	CURVATURE	RADIUS
1	0.6822804E-03	0.7619105E-02	3.680743	-39.73868	-3.592805	0.1538091
2	0.6292075E-02	0.2745481E-01	3.357705	-75.43071	-7.766721	0.1547776
3	0.1246765E-01	0.681934E-01	2.324503	-64.86450	-7.274664	0.1557658
4	0.1863208E-01	0.6364536E-01	2.539515	-60.74187	-7.254760	0.1566818
5	0.2478667E-01	0.7815182E-01	2.176771	-57.83557	-7.467710	0.1575291
6	0.3093245E-01	0.9045637E-01	1.830520	-54.84399	-7.495579	0.1583098
7	0.3707042E-01	0.1006725	1.500545	-52.67513	-7.554742	0.1590264
8	0.4320141E-01	0.1088911	1.181879	-51.27734	-7.654977	0.1596810
9	0.4932638E-01	0.1151112	0.8692411	-50.18091	-7.833899	0.1602762
10	0.5544605E-01	0.1195378	0.5575802	-51.04842	-8.065035	0.1609143
11	0.6156113E-01	0.1219864	0.2422148	-52.09736	-8.365876	0.1612875
12	0.6767231E-01	0.1224942	-0.7597476E-01	-52.03639	-8.418918	0.1617286
13	0.7378018E-01	0.1210282	-0.4091774	-57.06960	-9.214760	0.1621107
14	0.7988536E-01	0.1174713	-0.7552766	-56.30908	-8.982695	0.1624475
15	0.8598840E-01	0.1118070	-1.101946	-57.29655	-8.939615	0.1627425
16	0.920871E-01	0.1039996	-1.460180	-60.13184	-9.076601	0.1629995
17	0.9818965E-01	0.9396631E-01	-1.830702	-61.35194	-8.862785	0.1632218
18	0.1042886	0.8158600E-01	-2.241249	-73.27733	-9.968112	0.1634132
19	0.1103867	0.6671721E-01	-2.608809	-47.27090	-6.066792	0.1635773
20	0.1128799	0.6008580E-01	-2.702830	-28.15025	-3.571738	0.1636372

BLADE SURFACE 2 \*\*\*\*\*  
 RI2 RETI2 RO2 BTO2  
 0.1345579E-02 17.59296 0.9225516E-03 -9.601790

POINT	ZMSP2	THSP2	DERIVATIVE	2ND DERIVATIVE	CURVATURE	RADIUS
1	0.1751314E-02	-0.8345854E-02	2.058990	-17.39491	-2.005116	0.1539995
2	0.6292075E-02	0.7711546E-03	1.944957	-32.83116	-4.177735	0.1547776
3	0.1246765E-01	0.1221196E-01	1.769233	-24.07835	-3.116141	0.1557658
4	0.1863208E-01	0.2262998E-01	1.605810	-28.94260	-3.926357	0.1566818

nate mesh. This first section of debug output is given only once. The second section of debug output lists orthogonal mesh quantities that are held constant. These quantities are also listed only once. The third and fourth sections of debug output list the coefficients of the matrix equation that is solved for the stream function and the orthogonal mesh quantities that change with each iteration. These two sections are listed following an iteration of the solution, as called for by the value of IDEBUG. The output giving the changing orthogonal mesh quantities contains two different sets of variables.

(4) The fourth output indicates the calculated value of overrelaxation factor ORF to be used in the successive overrelaxation solution of the finite-difference equations. This matrix equation for the stream function  $u$  is solved iteratively (this is referred to as the "inner iteration") during each of the "outer iterations" of the reduced-mass-flow solution. The ORF output is given automatically on each run of the program.

(5) The fifth output lists the calculated LOSOUT array at the points along the line where input downstream flow conditions are given. This array is printed if PROP is given as input.

(6) The sixth output lists the ILE and ITE arrays. For the  $J^{\text{th}}$  horizontal mesh line from the hub, ILE(J) and ITE(J) are the vertical mesh line numbers of the mesh points that are within the blades and closest to the leading and trailing edges.

(7) The seventh output gives convergence information about DVTHDT, FT, and the relative velocity. Convergence is determined by the maximum relative change in velocity. When the maximum change becomes less than the input value of VELTOL (reduced by the minimum of FNEW or DNEW), the stream-function (either reduced or full mass flow) solution is considered converged. Also given are the indices where the maximum change occurred, the average relative change in velocity, and the number of unconverged points.

If there is a convergence problem, the behavior of DVTHDT and FT are of interest. Therefore, the maximum and minimum values and the maximum change in DVTHDT ( $\partial(rV_\theta)/\partial t$ ) and FT( $F_\theta$ ) are printed for each iteration. The input variables DNEW and FNEW are used to control the fraction of the calculated changes of these variables to be used for the next following iteration. If the maximum change in either DVTHDT or FT is increasing with each iteration, it is suggested that either DNEW or FNEW be decreased.

(8) The eighth output corresponds to IMESH for one of the iterations of the stream-function solution. The output is given along each horizontal mesh line at each mesh point. The output given at each mesh point includes the following: z- and r-coordinates of the point, stream function  $u$ , meridional velocity  $W_m$ , relative tangential velocity  $W_\theta$ , relative velocity  $W$ , critical velocity ratio  $W/W_{cr}$ , meridional flow angle  $\alpha$ , relative flow angle  $\beta$ , and mesh angle  $\varphi$ .

(9) The ninth output corresponds to ISLINE for one of the iterations of the stream-function solution. This output is given along each streamline, corresponding to a given stream-function value. The points along the streamline correspond to where it is intersected by the vertical mesh lines. The origin for the m-coordinate is located where each streamline begins at the upstream boundary of the orthogonal mesh. The output given at each streamline point includes the following: z-, r-, and m-coordinates of the point; meridional velocity  $W_m$ ; relative tangential velocity  $W_\theta$ ; relative velocity  $W$ ; critical velocity ratio  $W/W_{cr}$ ; meridional flow angle  $\alpha$ ; relative flow angle  $\beta$ ; streamline curvature  $1/r_c$ ; and within the blade-to-blade passage, the estimated suction-surface and pressure-surface velocities.

(10) The 10th output corresponds to ISTATL for one of the iterations of the reduced-mass-flow solution. Instead of output being given along horizontal mesh lines (IMESH) or streamlines (ISLINE), it is now given in the other direction, along lines from hub to shroud. This output is given along each of the station lines specified by the input ZHST, ZTST arrays. Output is given at each point where these station lines are crossed by the streamlines (the values in the FLFR array). The output given at each point is identical to the output given for ISLINE, with the addition of the stream function  $u$ . The second row of output includes the following additional variables: a repeat of z- and

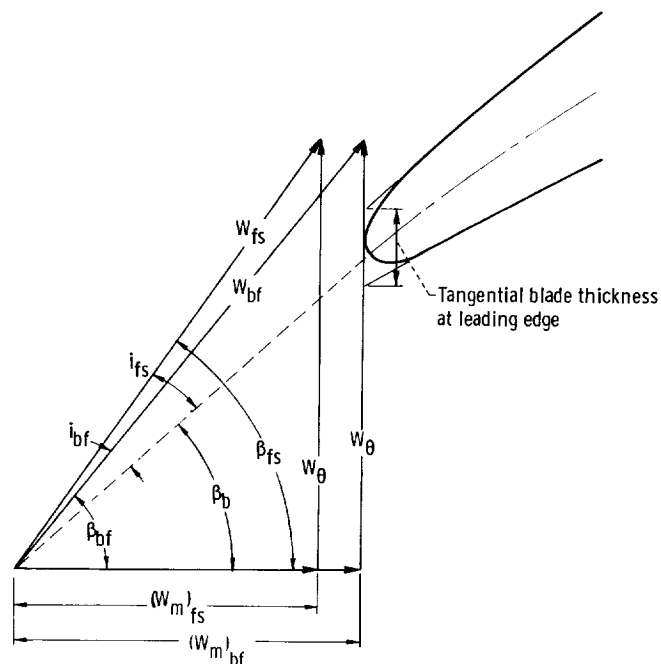


Figure 12. - Definition of incidence angles.

r-coordinates of the point, static pressure  $p$ , static temperature  $T$ , static density  $\rho$ , absolute tangential velocity  $V_\theta$ , absolute velocity  $V$ , absolute total pressure  $p'$ , absolute total temperature  $T'$ , absolute flow angle  $\beta_{abs}$ , relative total pressure  $p''$ , and relative total temperature  $T''$ .

(11) The 11th output consists of blocked and unblocked incidence and deviation angles and blade angles at the blade leading and trailing edges where each of the horizontal mesh lines intersects the blade. The blocked incidence  $i_{bf}$  or deviation is based on the velocity diagram within the blade (subscript  $bf$  in fig. 12); the unblocked incidence  $i_{fs}$  is based on the free-stream velocity diagrams (subscript  $fs$  in fig. 12). This output is printed after each iteration in which output is given for either IMESH, ISLINE, or ISTATL. These angles are defined as shown in figure 12.

(12) The 12th output corresponds to ITSON. It is a listing of the information required to prepare input for the TSONIC blade-to-blade analysis program of reference 3. (The TSONIC program is being updated and will be reported in the future. The definitions of all the input variables for TSONIC will be given in the updated version of TSONIC.) The TSONIC program was run for both the hub and tip blade sections of the compressor blade used in the numerical example of this report. The input numbers shown in the input form in figure 13 are those computed for use with the TSONIC run at the hub.

The information printed by MERIDL can in some cases serve as input for TSONIC without revision. In other cases, some of the input may need revision. The information from spline fits (derivative, second derivative, and curvature) of the THSP-against-ZMSP arrays for each blade surface is printed alongside these arrays. The user may wish to make small changes in the BETI and BETO tangency angles, which serve as end conditions for these spline fits, in order to smooth the resultant first and second derivatives.

The final five arrays of stream-channel data - ZMRSP, RMSP, BESP, WOWCR, and PLOSS - can in general be used as they are printed, unless the user wishes to reduce the number of points (NRSP) in them. The BESP array is calculated to correspond to the given mass flow ZMSFL. Any value could be used for ZMSFL if BESP is chosen accordingly. The value of ZMSFL calculated by MERIDL is 1 percent of the mass flow between any two blades. The BESP array is sometimes bumpy and may also have to be smoothed before it can be used as input to TSONIC. The derivatives of BESP against ZMRSP are printed and will indicate if smoothing is necessary. The WOWCR array is only needed as TSONIC input if REDFAC < 1.0 is used for TSONIC. The printed PLOSS array (NLOSS > 1) can be used for TSONIC rather than a single value for PLOSS if a nonlinear loss distribution through the blade is used in MERIDL.

(13) The 13th output is analogous to outputs 8, 9, 10, 11, and 12 for the variables IMESH, ISLINE, ISTATL, and ITSON but is given after the transonic velocity-gradient



1	5	6	10	11	15	16	20	21	25	26	30	31	35	36	40	41	45	46	50	51	60	61	70	71	80
TITLE																									
DATA12 - AXIAL COMPRESSOR ROTOR - HUB - STREAMLINE NO. 1 - U = 0.00																									
GAM		AR		TIP		RHOIP		OMEGA		ZMSFL															
1.4		287.053		288.15		1.22534		-826.55		0.025194															
REDFAC		VELTOL																							
1.0		0.001																							
MBI	MBO	MM	MBBI	NBL	NSPL1	NSLP2	NRSP	NSL																	
10	50	60	20	17	20	20	14	0																	
LRVB	LOSS	LWCR	LIPS																						
0	1	0	0																						
RVTHI		RVTHO		FSMI		FSMO		SSM1		SSM2															
-0.88533		-27.6253																							
CHORD		STGR																							
0.113429		0.054930																							
RI1		BETI1		RO1		BETO1																			
0.001346		29.516		0.0009226		-23.859																			
ZMSP1 ARRAY																									
0.00068		0.00629		0.01247		0.01863		0.02479		0.03093		0.03707		0.04320											
0.04933		0.05545		0.06156		0.06767		0.07378		0.07989		0.08599		0.09209											
0.09819		0.10429		0.11039		0.11288																			
THSP1 ARRAY																									
0.00762		0.02745		0.04682		0.06365		0.07815		0.09046		0.10067		0.10889											
0.11517		0.11954		0.12199		0.12249		0.12103		0.11747		0.11181		0.10400											
0.09397		0.08159		0.06672		0.06009																			
RI2		BETI2		RO2		BETO2																			
0.001346		17.593		0.0009226		-9.602																			
ZMSP2 ARRAY																									
0.00175		0.00629		0.01247		0.01863		0.02479		0.03093		0.03707		0.04320											
0.04933		0.05545		0.06156		0.06767		0.07378		0.07989		0.08599		0.09209											
0.09819		0.10429		0.11039		0.11235																			
THSP2 ARRAY																									
-0.00835		0.00077		0.01221		0.02263		0.03198		0.04027		0.04751		0.05369											
0.05879		0.06283		0.06581		0.06775		0.06866		0.06847		0.06720		0.06487											
0.06145		0.05695		0.05137		0.04937																			
ZMRSP ARRAY																									
-0.04741		-0.03285		-0.01860		-0.00455		0.00629		0.02479		0.04320		0.06156											
0.07989		0.09819		0.11648		0.13173		0.14544		0.15916															
RMSP ARRAY																									
0.14107		0.14594		0.14979		0.15283		0.15478		0.15753		0.15968		0.16130											
0.16245		0.16322		0.16372		0.16399		0.16417		0.16431															
BESP ARRAY																									
0.002268		0.002233		0.002205		0.002208		0.002228		0.002199		0.002163		0.002110											
0.002049		0.001989		0.001926		0.001902		0.001892		0.001885															
PLOSS ARRAY																									
0.00		0.00		0.00		0.00		0.00065		0.00249		0.00432		0.00634											
0.00851		0.01119		0.01447		0.01447		0.01447		0.01447															
IMESH	ISLINE	IBSURF	IPL0T	IDEBUG																					
5	5	1	1	0																					

Figure 13. - TSONIC input form. (Data shown are for the numerical example at the hub.)

solution. Two solutions can be obtained by the velocity-gradient method: the larger or "supersonic" and the smaller or "subsonic." The input variable ISUPER controls which of these is obtained. The solution listed here is the smaller (i.e., the subsonic solution). If REDFAC = 1.0, no velocity-gradient solution will be obtained or printed because the final iteration of the stream-function solution is the correct solution to the problem.

### Plotted Output

Since the printed output from a MERIDL run can be quite large, microfilm plots are made to enable the user to quickly check the quality of both his input and output data. The coding that generates these plots uses NASA Lewis in-house plot routines and would have to be recoded for operation on another system. The principal sections of input data plotted are the upstream and downstream distributions of flow properties; the input blade sections; and the hub, shroud, and blade leading- and trailing-edge geometry. The frequency at which output data are plotted is controlled by the variable IPLOT. The plotted output data begin with the generated orthogonal mesh. Then for each iteration of the solution (indicated by IPLOT) and for the transonic solutions, streamlines are plotted, as well as midchannel and blade surface velocities along each streamline from hub to shroud. The user should carefully check the plots of his input data to ensure that the program's spline fits of these data are smooth.

Selected examples of some of the microfilm plots generated by the numerical example are presented in figure 14. The description of these plots is as follows:

(1) Figures 14(a) to (e) present the input upstream and downstream flow conditions. These quantities  $(T'_1, p'_1, \lambda \text{ or } (V_\theta)_1, p'_0 \text{ or total pressure loss, } (rV_\theta)_0 \text{ or } (V_\theta)_0)$  are plotted against either stream function or radius, whichever was used as input.

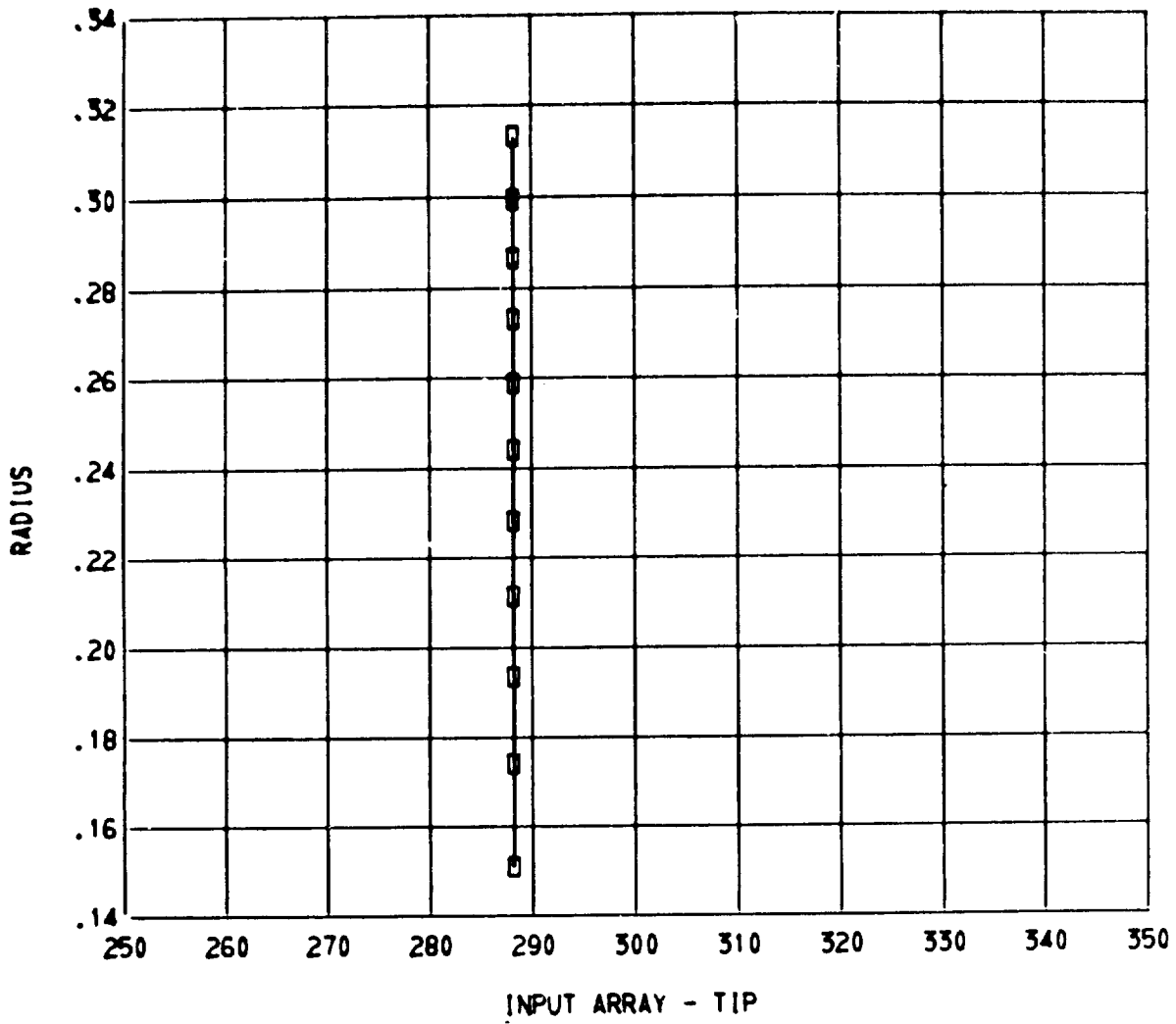
(2) Figure 14(f) shows the optional input of total-pressure-loss distribution against fraction of chord.

(3) Figures 14(g) and (h) indicate hub and shroud blade sections plotted from input data supplied by the user. All blade sections given as input are plotted.

(4) Figure 14(i) shows the hub and shroud channel geometry and the blade leading and trailing edges.

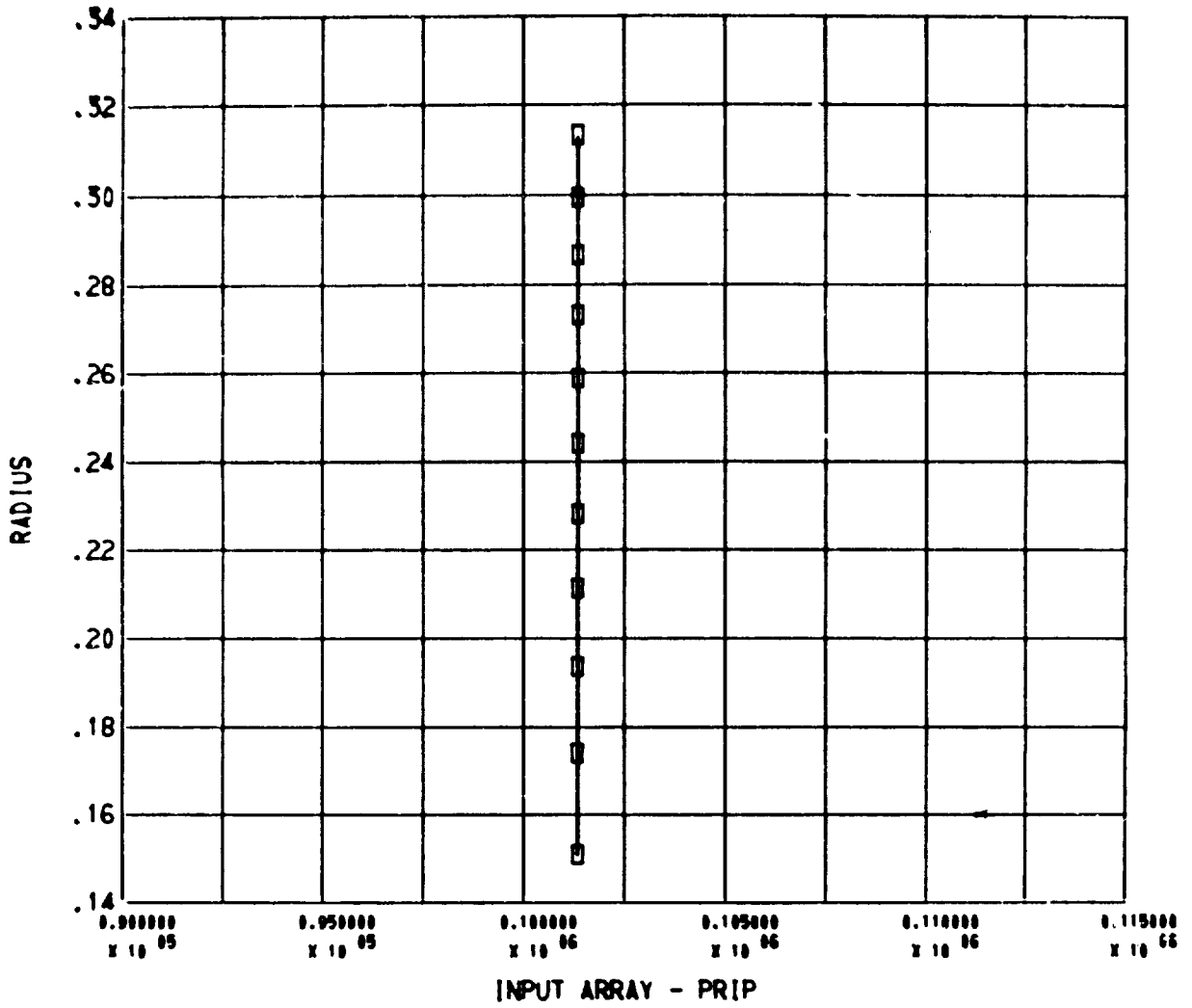
(5) Figure 14(j) shows the generated orthogonal mesh.

(6) Figure 14(k) shows the streamline pattern for the final iteration of the reduced-mass-flow solution.



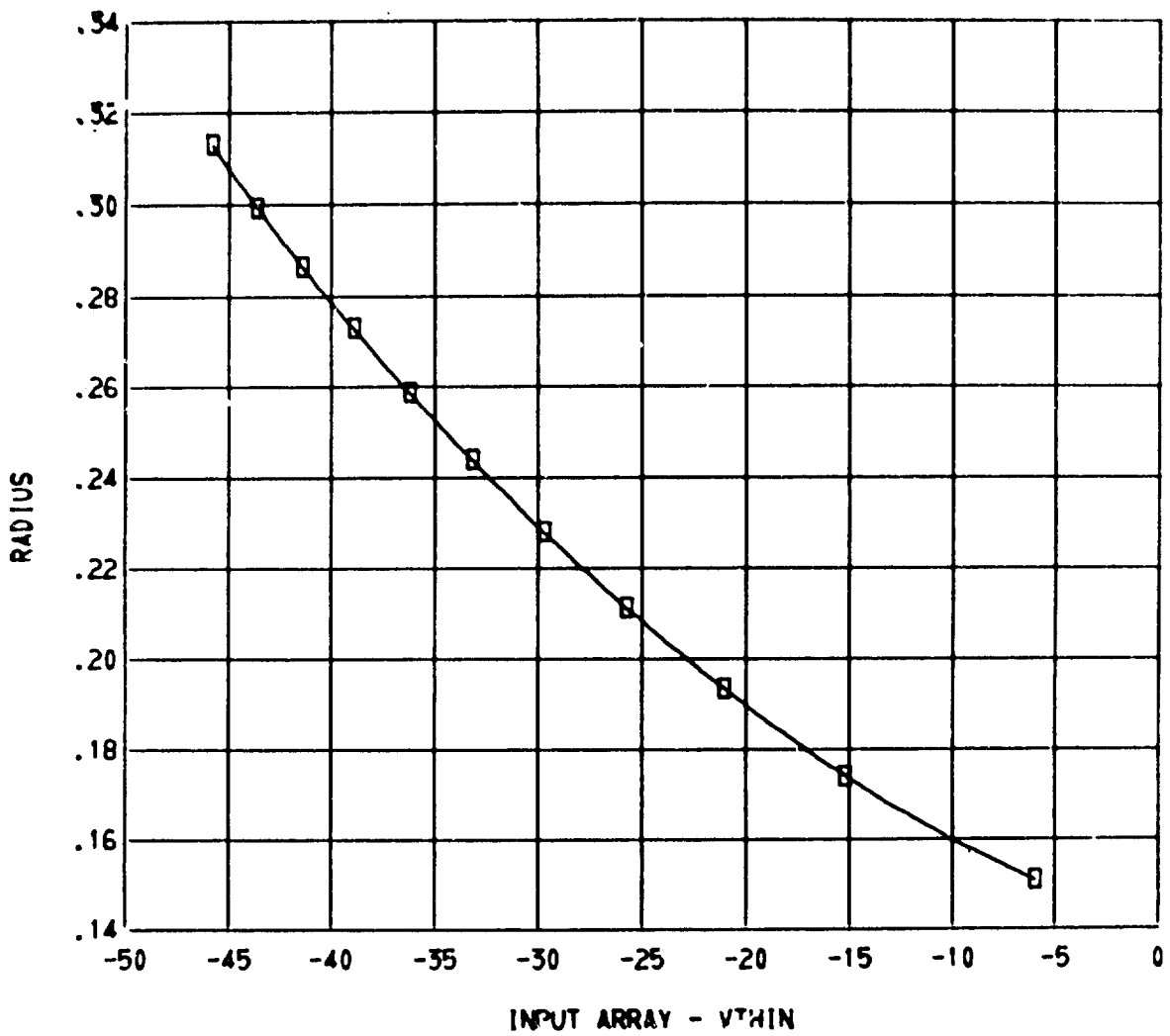
(a) Inlet absolute total temperature.

Figure 14. - Microfilm plots of input and output.



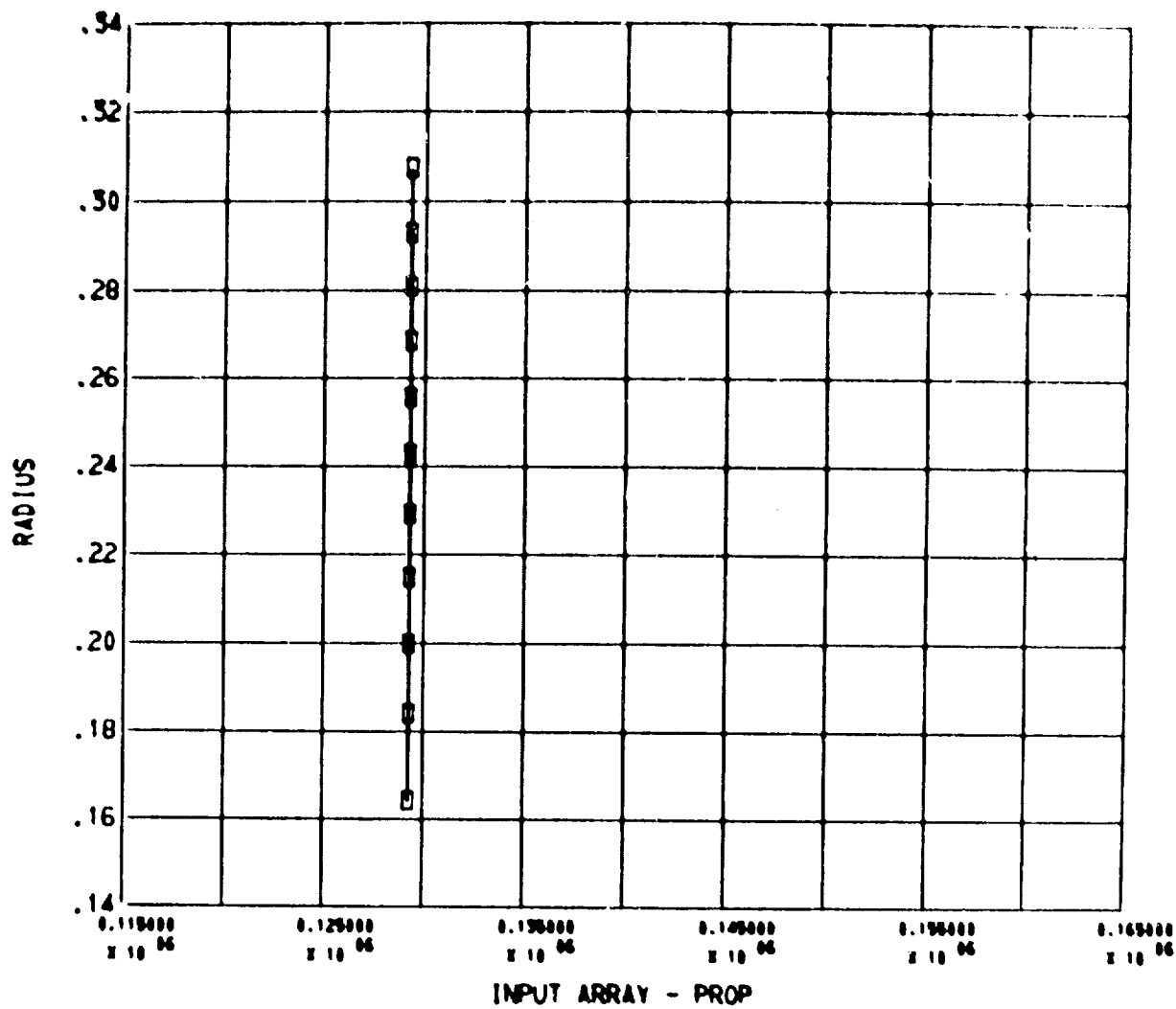
(b) Inlet absolute total pressure.

Figure 14. - Continued.



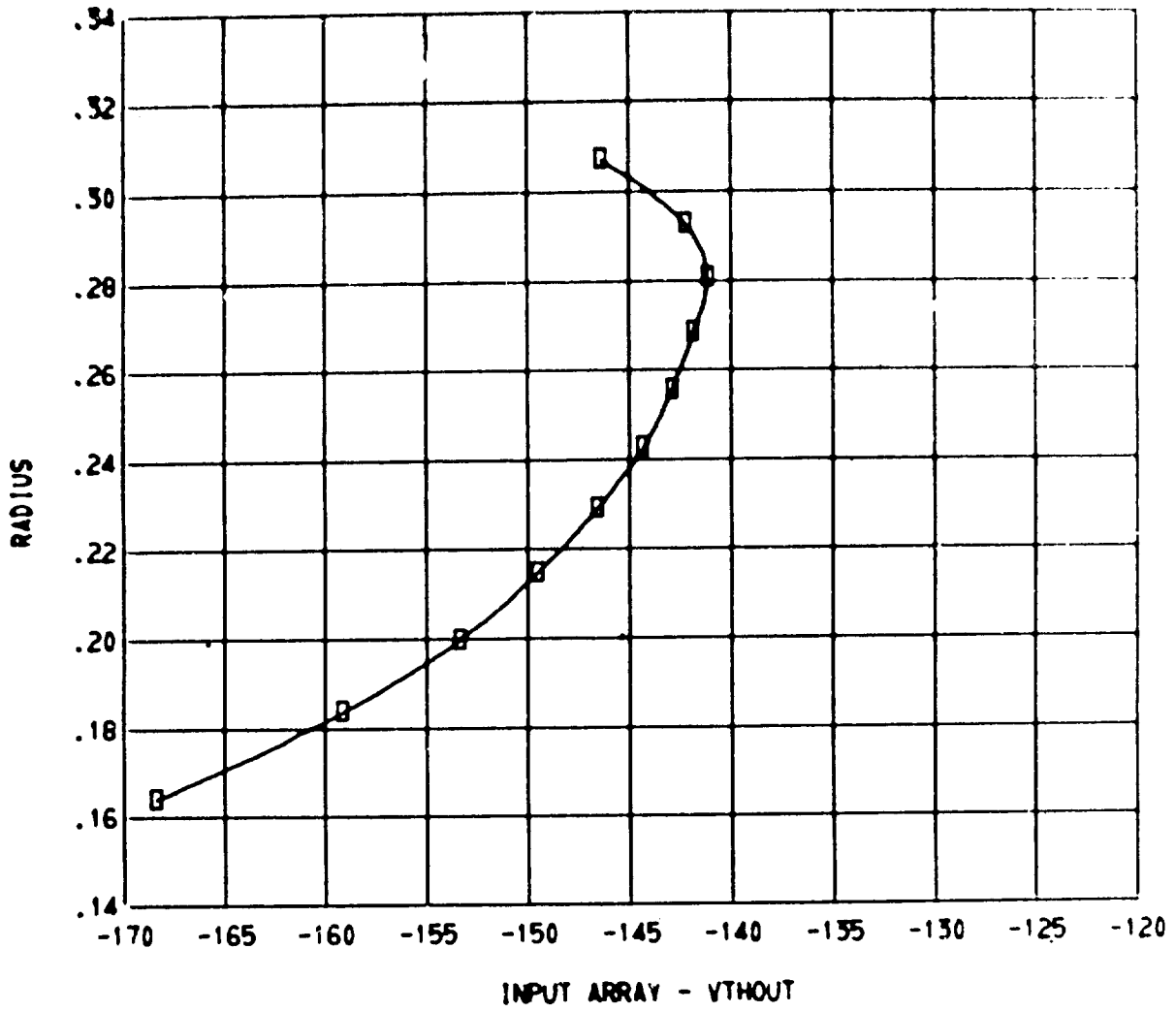
(c) Inlet absolute tangential velocity.

Figure 14. - Continued.



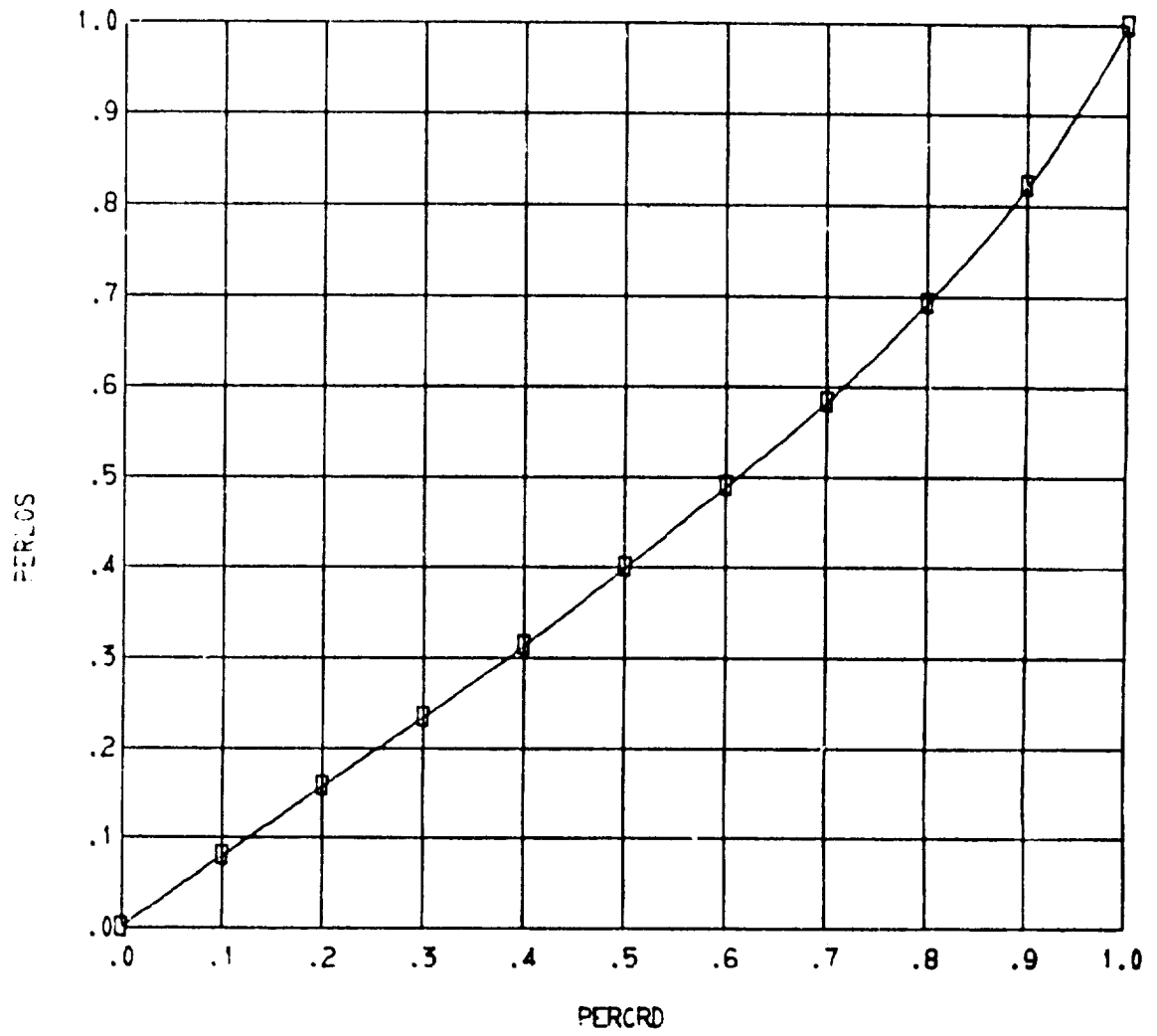
(d) Outlet absolute total pressure.

Figure 14. - Continued.



(e) Outlet absolute tangential velocity.

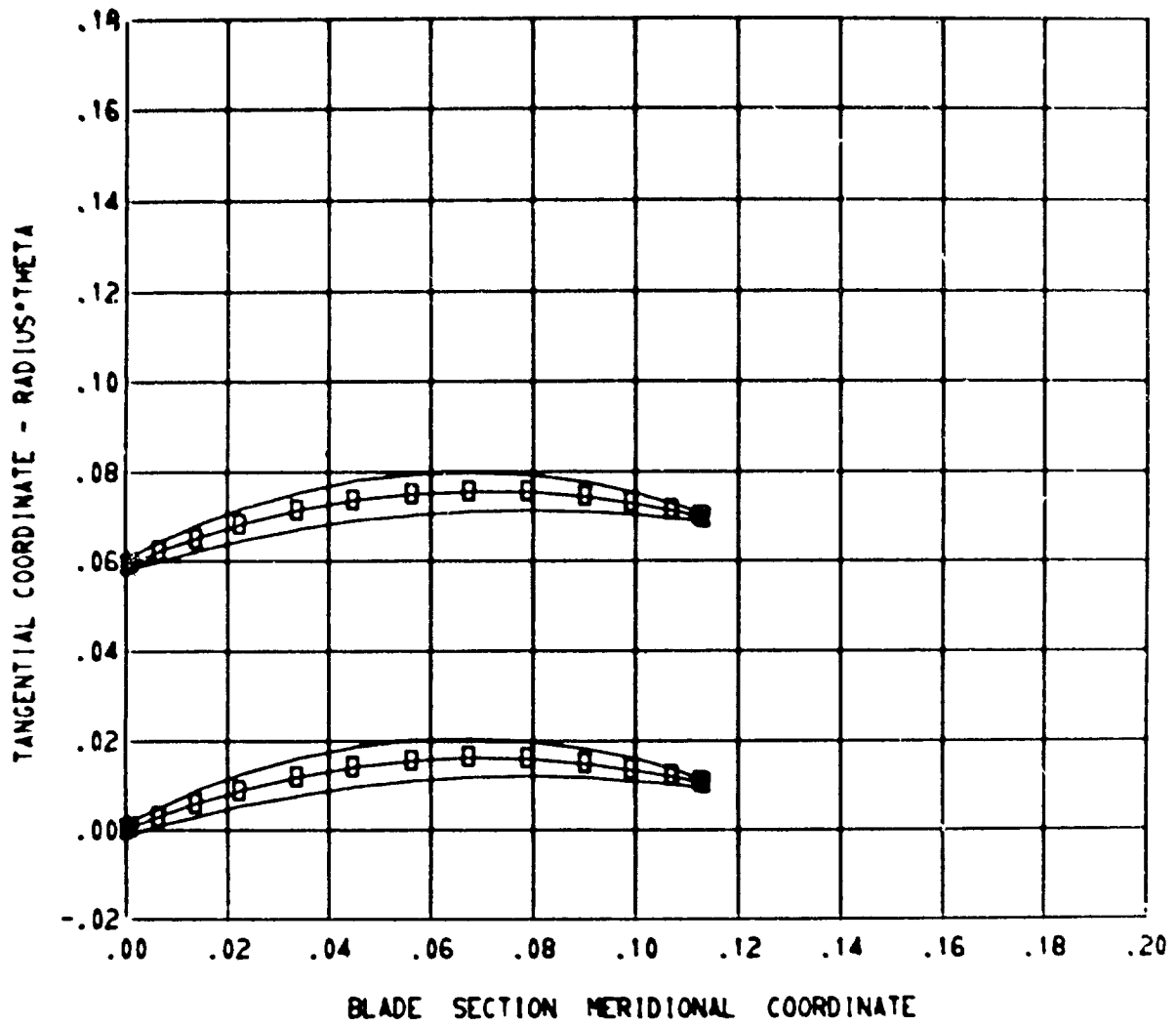
Figure 14. - Continued.



(f) Pressure loss distribution.

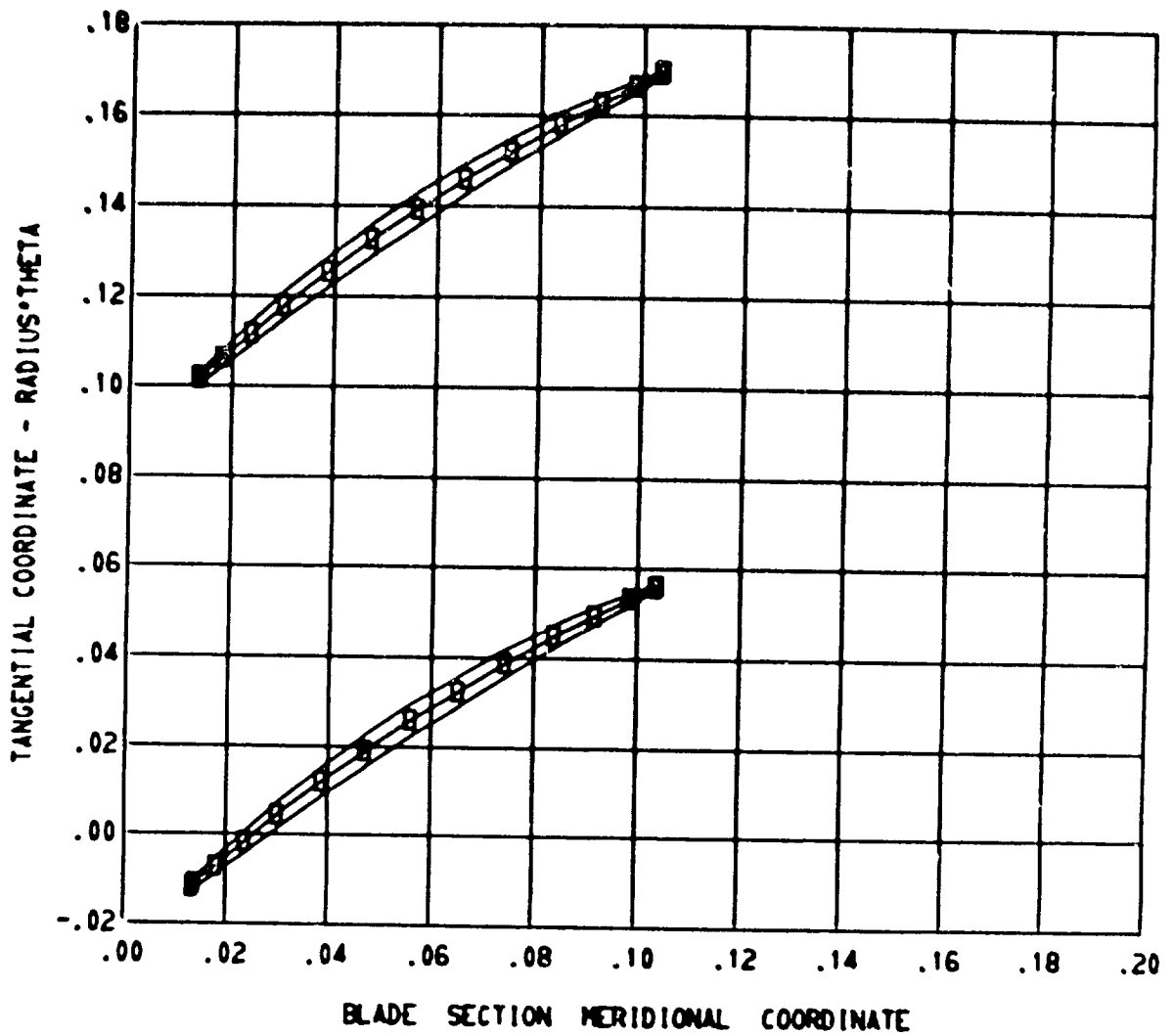
Figure 14. - Continued.





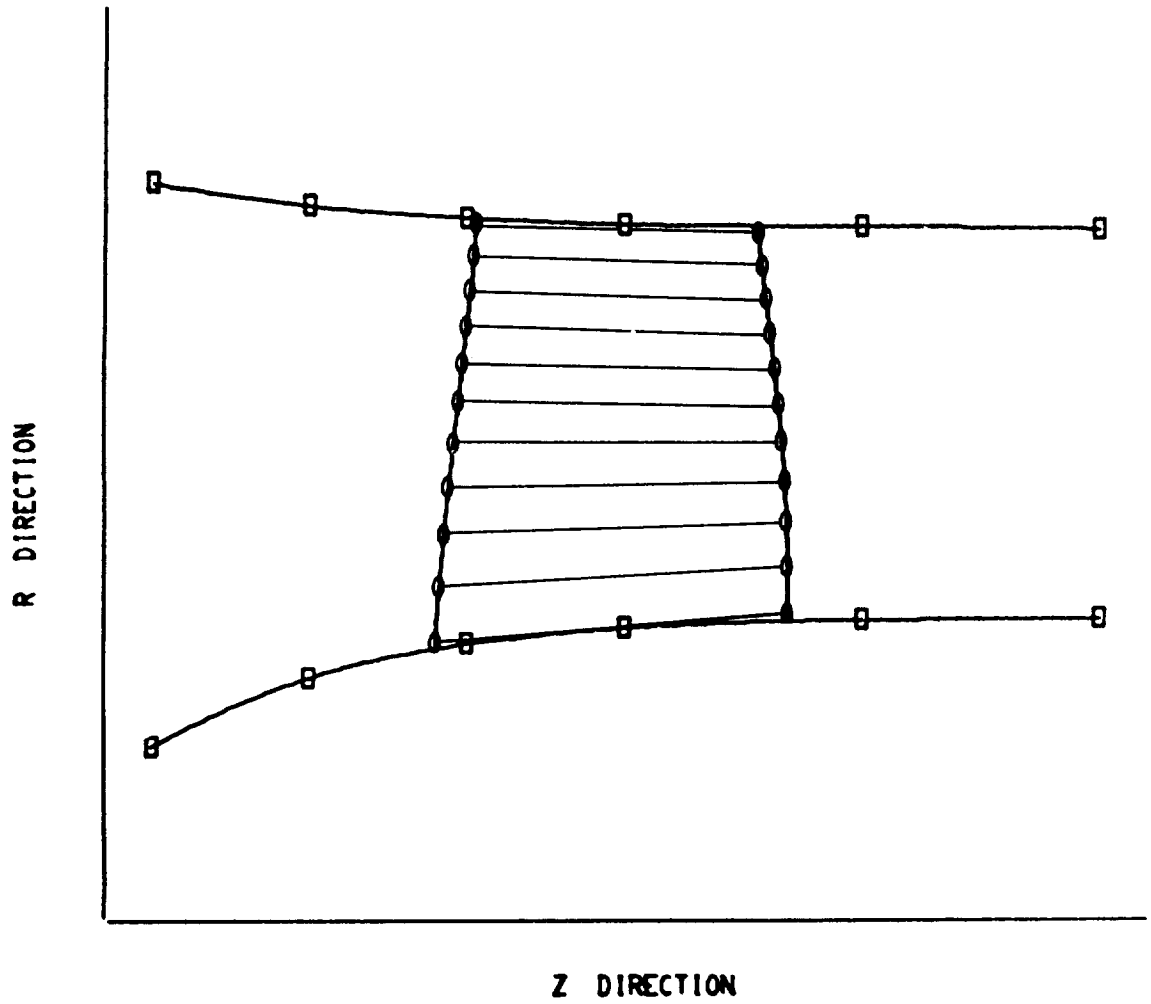
(g) Input blade sections from ZBL, RBL, THBL, and TNBL - blade section 1.

Figure 14. - Continued.



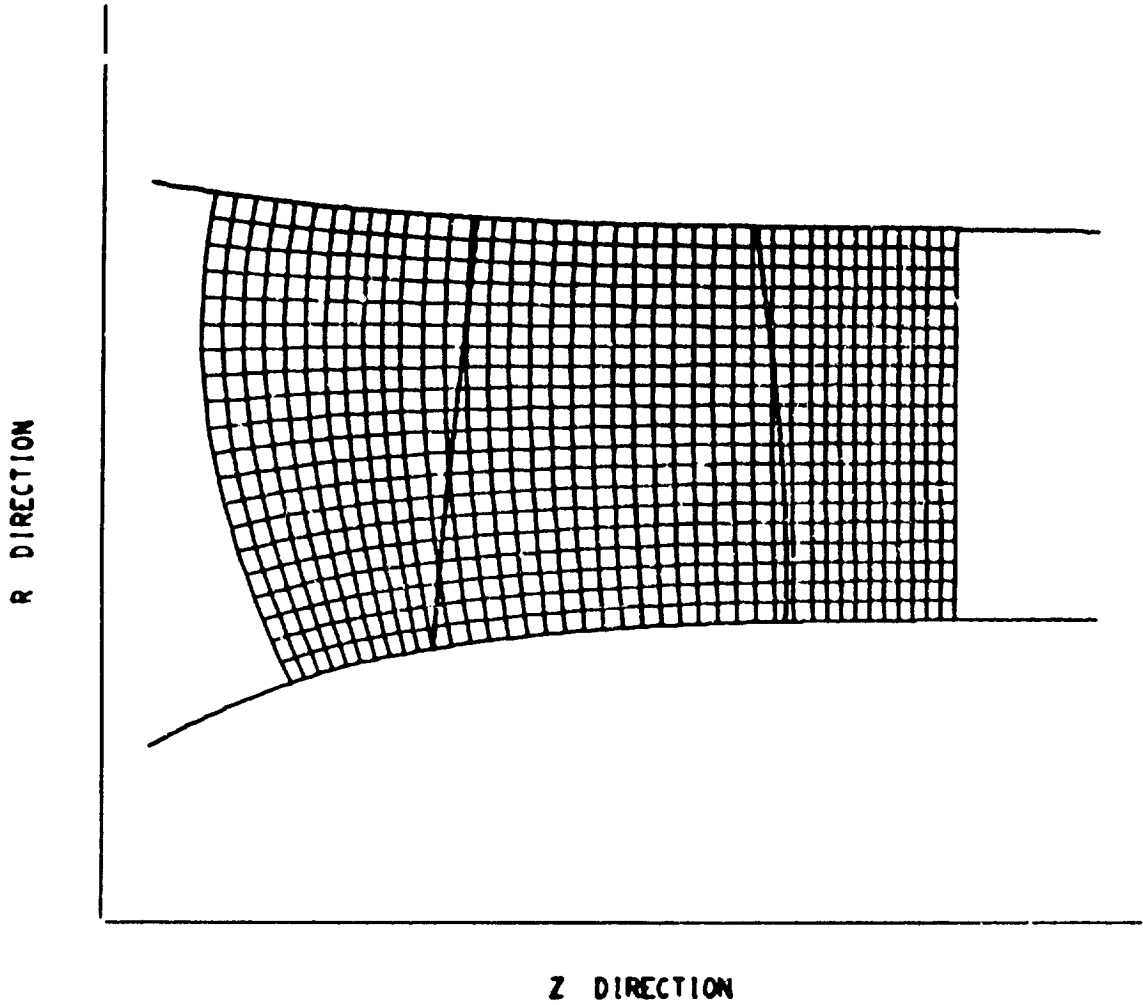
(h) Input blade sections from ZBL, RBL, THBL, and TNBL - blade section 11.

Figure 14. - Continued.



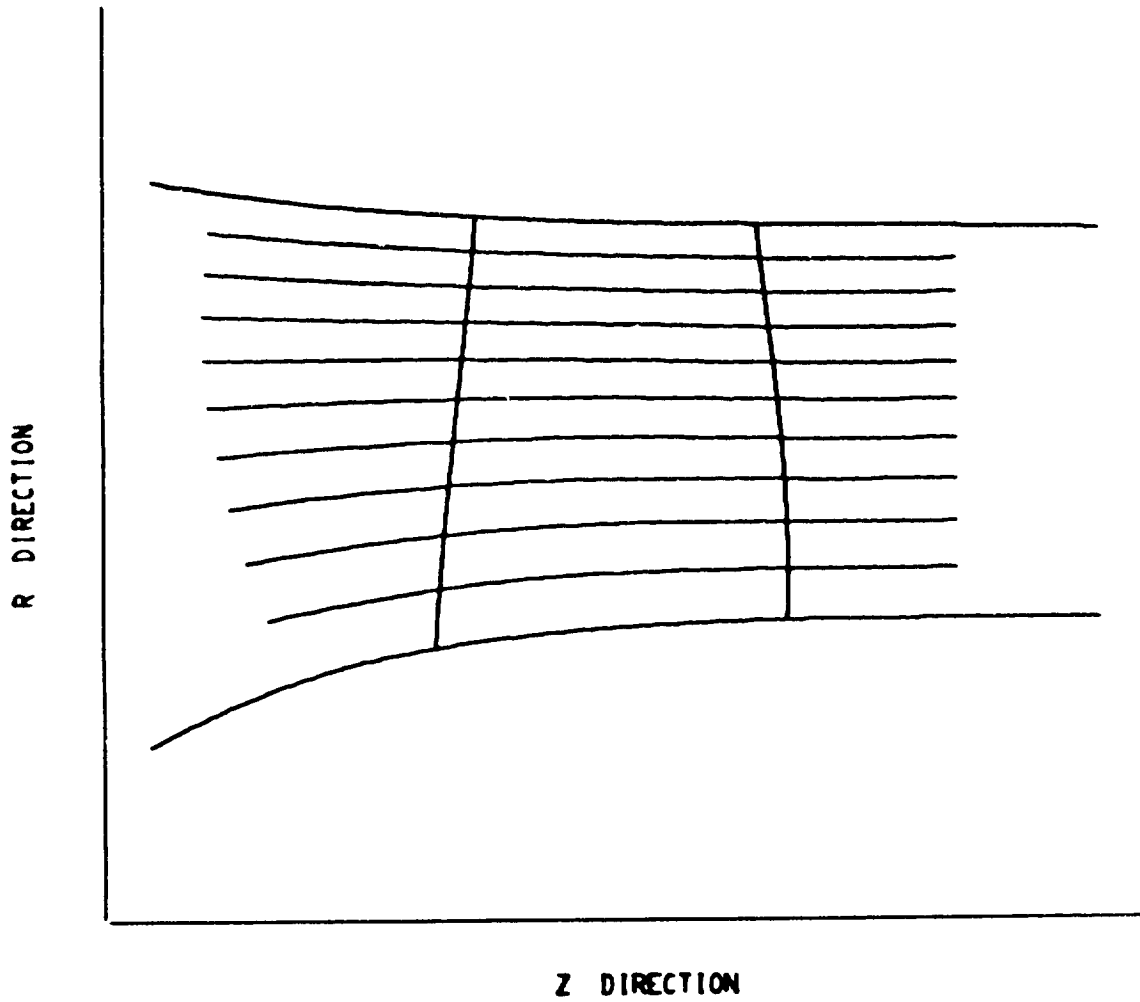
(i) Hub, shroud, and blade boundaries in meridional plane.

Figure 14. - Continued.



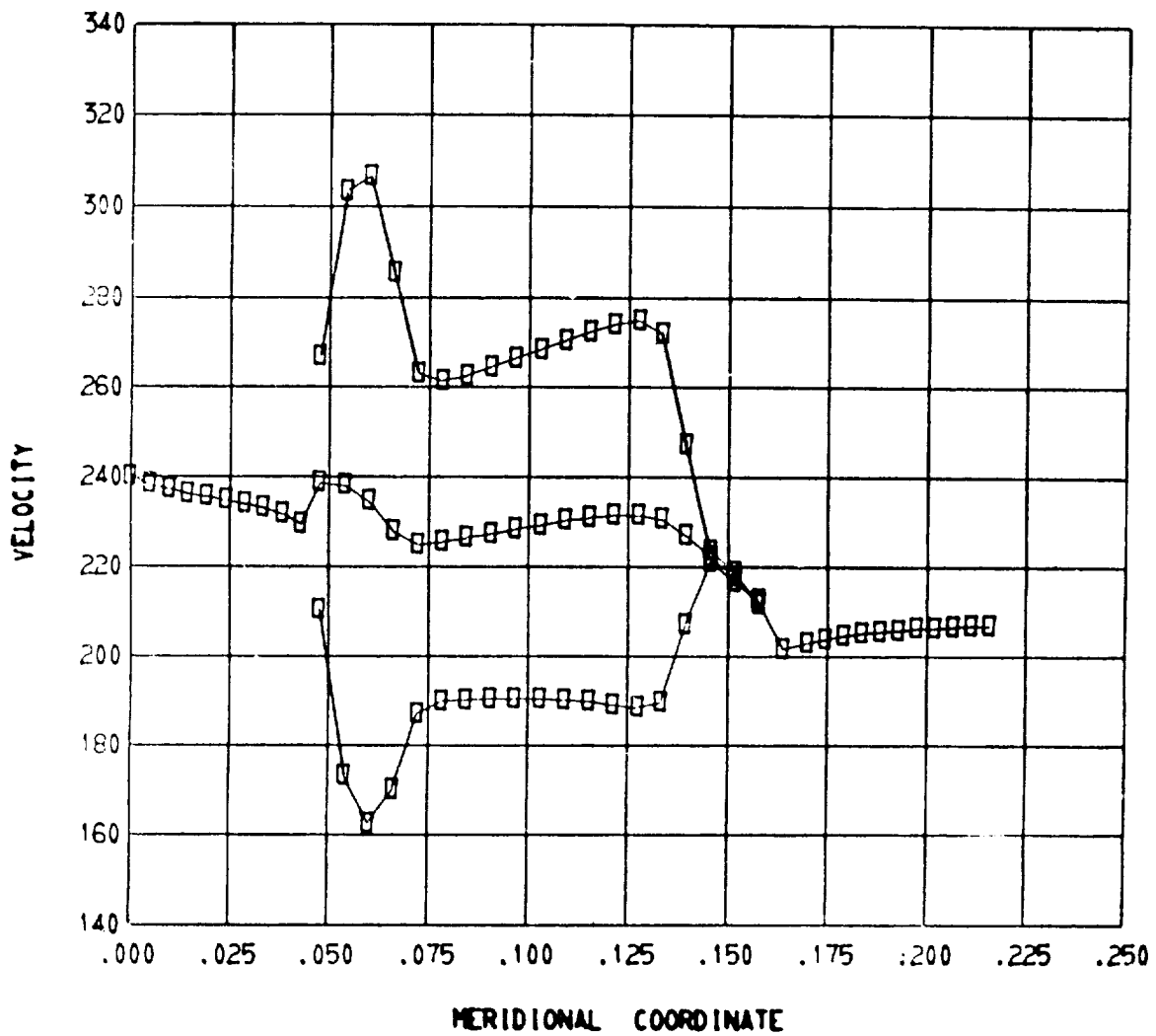
(j) Orthogonal mesh in meridional plane.

Figure 14. - Continued.



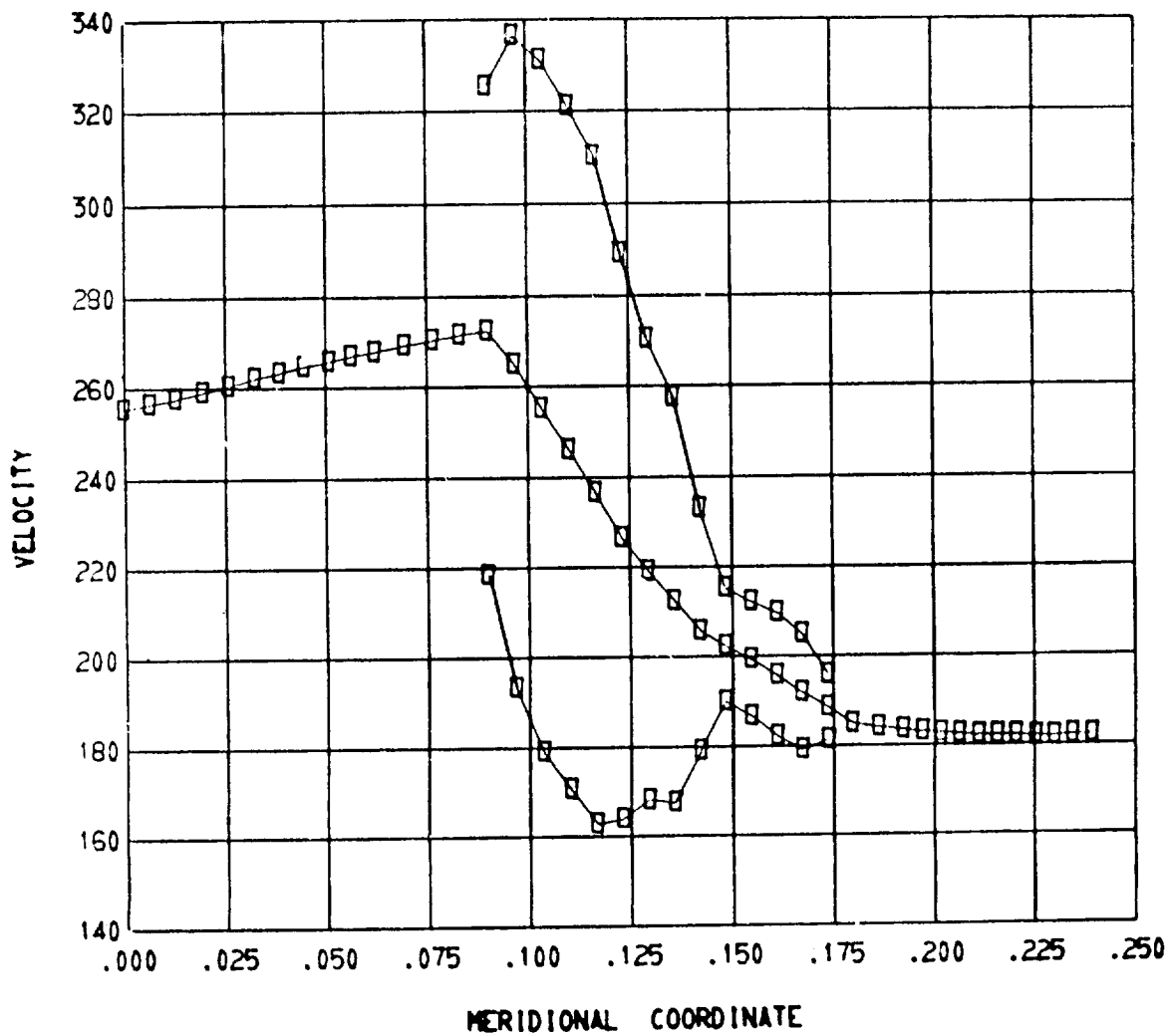
(k) Streamline plot in meridional plane.

Figure 14. - Continued.



(1) Meridional and blade surface relative velocities - streamline 1. Normalized stream function, 0.

Figure 14. - Continued.



(m) Meridional and blade surface relative velocities - streamline 11. Normalized stream function, 1.0.

Figure 14. - Concluded.

(7) Figures 14(l) and (m) show meridional velocities and blade surface velocities for the hub and shroud blade sections for the same iteration. A similar plot is made along each of the streamlines from hub to shroud.

Streamline and velocity plots similar to figures 14(k), (l), and (m) are made after each iteration (indicated by IPLOT) of the finite-difference, stream-function solution and also after the velocity-gradient solution.

### Error Messages

A number of error messages have been incorporated into the program. These error messages are listed here, followed by suggestions for finding and correcting the cause of the error:

```
MM, MHT, NHUB, NTIP, NIN, NOUT, NBLPL, NPPP, NOSTAT, NSL, NLOSS, LSFH, LTPL, LAMVT, LROT, LBLAD, OR LETEAM  
IS TCC LARGE OR TOO SMALL
```

The input dictionary gives the maximum and minimum values for all these input variables.

```
WHEN UPSTREAM AND DOWNSTREAM INPUT DATA ARE GIVEN AS A FUNCTION OF RADIUS,  
THERE MUST BE A CHANGE IN VALUE BETWEEN RHIN AND RTIN AND ALSO BETWEEN RHOUT AND RTOUT  
AND A CORRESPONDING CHANGE IN THE RADIN AND RADOUT ARRAYS
```

RHIN must differ from RTIN (and RHOUT from RTOUT) so that there will be a variation in the RADIN (and RADOUT) arrays, which are used to identify points along the hub-shroud lines at the upstream and downstream input stations.

```
LININT CANNOT FIND INTERPOLATED VALUE  
I =      1 J =      2
```

This message should occur only with erroneous geometry input.

```
INPUT PROP VALUES ARE LARGER THAN IDEAL TOTAL PRESSURE, RESULTING IN NEGATIVE LOSS
```

This message is for information only; the program will continue normally.

```
PROGRAM STOPPED IN NEWRHO DUE TO EXCESSIVE STREAM FUNCTION GRADIENT
```

This is usually caused by having supersonic flow in some region of the reduced-mass-flow solution. Try a smaller value for REDFAC.



THE UPSTREAM INPUT WHIRL OR TANGENTIAL VELOCITY IS TOO LARGE

This message is printed by subroutine NEWRHO or TVELCY if the upstream whirl gives a tangential velocity so large as to result in a negative relative stagnation temperature. The upstream whirl or tangential velocity given as input should be corrected.

BEWARE. THERE ARE 1 VERTICAL ORTHOGONAL MESH LINES WHICH ARE CHOKED.  
LOCATIONS OF THESE LINES ARE GIVEN ABOVE AT THE BEGINNING OF THE TRANSONIC OUTPUT.  
OUTPUT ON ANY STATION LINES LOCATED NEAR THESE CHOKED ORTHOGONAL LINES MAY BE IN ERROR.

When this message is printed, the user should be extremely cautious in using station line output after the transonic velocity solution. However, there may be little problem if the choking mass flow is close to the full mass flow or if the station line is not near one of the choked orthogonals.

A VELOCITY GRADIENT SOLUTION CANNOT BE OBTAINED FOR VERTICAL ORTHOGONAL MESH LINE I = 1  
ANY SUBSEQUENT OUTPUT FOR THAT MESH LINE MAY BE IN ERROR

If the approximate transonic solution for any particular vertical mesh line cannot be found for some reason, this message will be printed. Some of the following error messages will be printed to help determine the problem. The program will proceed to the next vertical mesh line.

CONTIN COULD NOT FIND A SOLUTION IN 100 ITERATIONS.

This message is printed when the transonic flow solution for some vertical mesh line cannot be obtained by subroutine CONTIN in 100 iterations. Possible causes for this error message could be unusual or impossible upstream or downstream input quantities (TIP, PRIP, LAMIN, VTHIN, PROP, LOSOUT, LAMOUT, or VTHOUT arrays).

ITERATION PROCEDURE HAD TO BE RESTARTED TO AVOID NEGATIVE TEMPERATURE OR VELOCITY  
MAGNITUDE LESS THAN TANGENTIAL VELOCITY, OR AFTER ADJUSTMENT OF STAGNATION TEMPERATURE,  
STAGNATION DENSITY, OR WHIRL.  
RESTART OF ITERATION PROCEDURE (LOOP TO STATEMENT 90) WAS ABORTED AFTER 1000 OR MORE  
TOTAL ITERATIONS (LOOP TO STATEMENT 150).

This message is printed when the transonic velocity-gradient solution cannot be found by subroutine TVELCY in 1000 iterations for some vertical mesh line. Possible causes are high input whirl, impossible upstream or downstream flow condition, and complex or erroneous blade or wall geometry.

```
THE MAXIMUM MASSFLOW FOR WHICH A SOLUTION COULD BE OBTAINED WAS 0.120000E-02
THE MINIMUM MASSFLOW FOR WHICH A SOLUTION COULD BE OBTAINED WAS 0.101000E-02
THE MAXIMUM VALUE OF W AT THE HUB FOR WHICH A SOLUTION COULD BE OBTAINED WAS 101.1000
THE MINIMUM VALUE OF W AT THE HUB FOR WHICH A SOLUTION COULD BE OBTAINED WAS 99.79999
```

This information is printed whenever the transonic, velocity-gradient solution cannot be found for some vertical mesh line. This information has debug value if there is no apparent reason for difficulty.

```
THE ITERATION PROCEDURE WAS RESTARTED 380 TIMES
WHUB WAS INCREASED 112 TIMES
WHUB WAS DECREASED 56 TIMES
BOUNDARY VALUES (TIPBDY, RHOIP, LAMBDA) WERE ADJUSTED 34 TIMES
```

This information is printed whenever the transonic solution cannot be found after re-starting the iteration procedure. This information has debug value if there is no apparent reason for difficulty.

```
MSFL EXCEEDS CHOKING MASS FLOW FOR VERTICAL ORTHOGONAL MESH LINE I = 1
CHOKING MASS FLOW = 0.950000E-03
```

This message is printed if the choking mass flow calculated by subroutine TVELCY is less than the input mass flow MSFL. The following message will be printed after all vertical lines have been checked:

```
CHOKING MASSFLOW IS 0.96000 OF THE INPUT MASSFLOW
INPUT MASSFLOW = 0.15000E-02
MINIMUM CHOKING MASSFLOW = 0.14400E-02
```

If the previous message was printed for any vertical mesh line, this message will be printed at the end to give the minimum choking mass flow, which is the choking mass flow for the blade row estimated by MERIDL. Use of the CHANEL program (ref. 13) is recommended to obtain a more accurate estimate of the choking mass flow.

```
SUPERSONIC CORRECTION - LEADING EDGE FOR J = 2
```

For the full-mass-flow solution when REDFAC < 1, the blockage correction at the leading edge requires calculating the density by an iterative procedure. Since the iterative procedure depends on whether the flow is subsonic or supersonic, the program first checks the subsonic procedure; if this fails, it is usually because the flow is supersonic. If the supersonic solution is found, the preceding message is printed for information only.

SUPERSONIC CORRECTION - TRAILING EDGE FOR J = 2

This is the same as the previous message but at the trailing edge.

NO DENSITY CORRECTION - LEADING EDGE FOR J = 2

If after the subsonic procedure fails the supersonic procedure is tried and also fails, that procedure is aborted and the density within the blade is taken to be the free-stream density. This problem would probably occur because of numerical problems associated with near-sonic flows, high blockage, and complex or erroneous wall or blade geometry. The program will continue after this message, although output near the leading edge may be poor.

NO DENSITY CORRECTION - TRAILING EDGE FOR J = 2

This is the same as the previous message but at the trailing edge.

INRSCT HAS FAILED TO CONVERGE IN 20 ITERATIONS  
TOLERANCE = 0.101000E-05  
DISTANCE BETWEEN LAST TWO INTERSECTION POINTS = 0.678900E-05

Subroutine INRSCT finds the intersection coordinates of input station lines, mesh lines, and streamlines with the blade leading or trailing edge by an iterative method. If the tolerance cannot be met after 20 iterations, the message is printed. If the distance between the last two intersection points is only slightly larger than the tolerance, a satisfactory solution will be obtained, with some loss of accuracy. If the distance is excessive, there is probably some error in the geometry input.

SPLINE ERROR -- ONE OF THREE POSSIBLE CAUSES  
1. ADJACENT X POINTS ARE DUPLICATES OF EACH OTHER.  
2. SOME X POINTS ARE OUT OF SEQUENCE.  
3. SOME X POINTS ARE UNDEFINED.

NUMBER OF POINTS = 3

X ARRAY	Y ARRAY
0.00000	10.000
0.00000	12.000
1.0000	15.000

The spline points for a spline curve must be distinct and given in sequence. If not, the spline fit subroutine (either SPLINE, SPLINT, SPLISL, or SPINSL) will print this message, and the program will terminate. Since spline curves are used so extensively in

the program, it is difficult to state the possible cause. However, the printout of the spline points should assist in pinpointing the cause of the error.

```
SPLINE ERROR -- NUMBER OF SPLINE POINTS GIVEN IS LESS THAN TWO
```

```
NUMBER OF POINTS = -3
```

```
X  ARRAY      Y  ARRAY  
0.00000      10.000
```

At least two points must be given to determine a spline curve. If not, the spline fit sub-routine (SPLINE, SPLINT, SPLISL, or SPINSL) will print this message, and the program will terminate. The one printed spline point may give a clue as to the error.

### NUMERICAL EXAMPLE

An example of an axial-flow compressor rotor is used to illustrate the use of the program and to show the type of results that can be obtained. Flow is analyzed on the midchannel stream surface of an axial-flow rotor designed with the computer program of reference 11. The design pressure ratio is 1.275, the inlet hub-tip radius ratio, 0.5; the aspect ratio, 1.5; the tip solidity, 1.0; and the tip relative Mach number at the inlet, 0.9. Although tip relative Mach number is near sonic, there are no locally supersonic regions on the midchannel stream surface.

The printed output from this example is given in table I. The input for this example is item 1 in that table. The number of mesh points used was 861: 41 in the axial direction, and 21 in the radial direction.

This rotor was run twice, with reduction factors (REDFAC) of 0.99999 and 0.70. This was done in order to test the effect of reduction factor and also the accuracy of the velocity-gradient method in comparison with the finite-difference method. Since both cases have REDFAC < 1.0, both the subsonic (finite difference) and the transonic (velocity gradient) solutions will be obtained in each of them. (If REDFAC = 1.0, only the finite-difference solution is obtained.)

The first case (REDFAC = 0.99999) permits a comparison to be made between the approximate velocity-gradient method (used to obtain transonic solutions) and the more exact finite-difference, stream-function solution (used for subsonic solutions). Since the reduction factor is 0.99999 (<1.0), both solutions will be obtained, but the answers should be very close if the methods compare well.

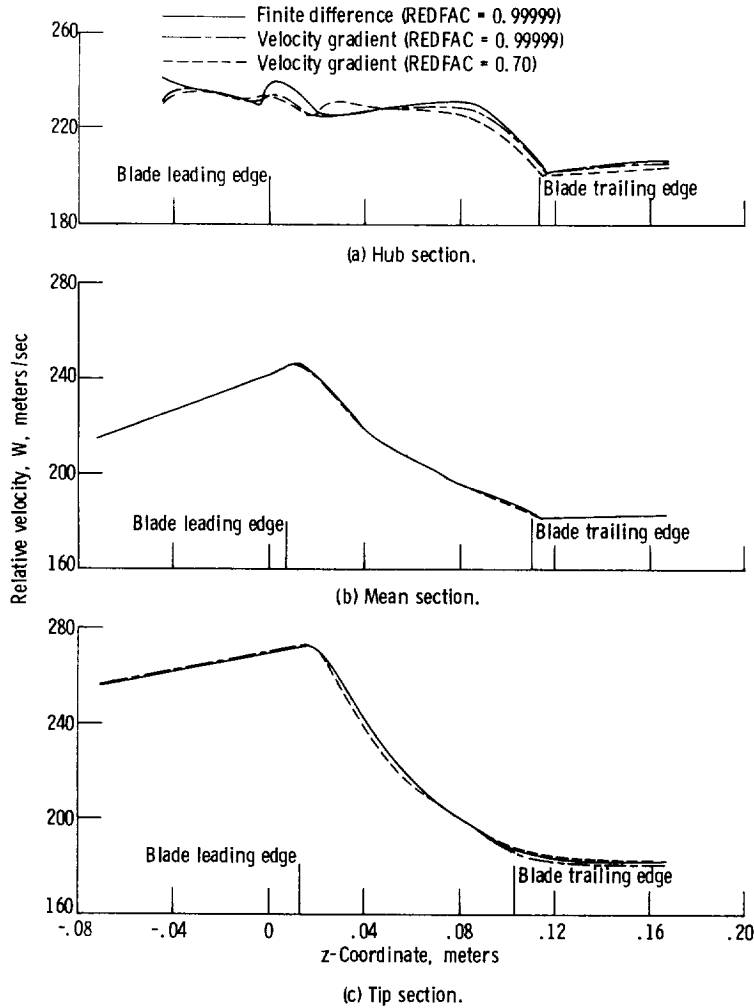


Figure 15. - Midchannel velocities for axial-flow compressor example.

The second case (REDFAC = 0.70) permits a comparison of reduction-factor effect. Since the finite-difference solution is now obtained at only 70 percent of the mass flow and rotational speed (appendix E), the results for the full-mass-flow, velocity-gradient solution will be less accurate than when a higher reduction factor is used.

Figure 15 shows midchannel flow surface velocities for both reduction factors and both types of solution (the finite difference and the velocity gradient). Results are presented for three values of stream function (0.0, 0.5, and 1.0) at hub, mean, and tip. On all parts of this figure, the solid line represents velocities from the final finite-difference iteration of the REDFAC = 0.99999 solution. This solution is mathematically most accurate. The results presented here show a much better comparison of velocity-

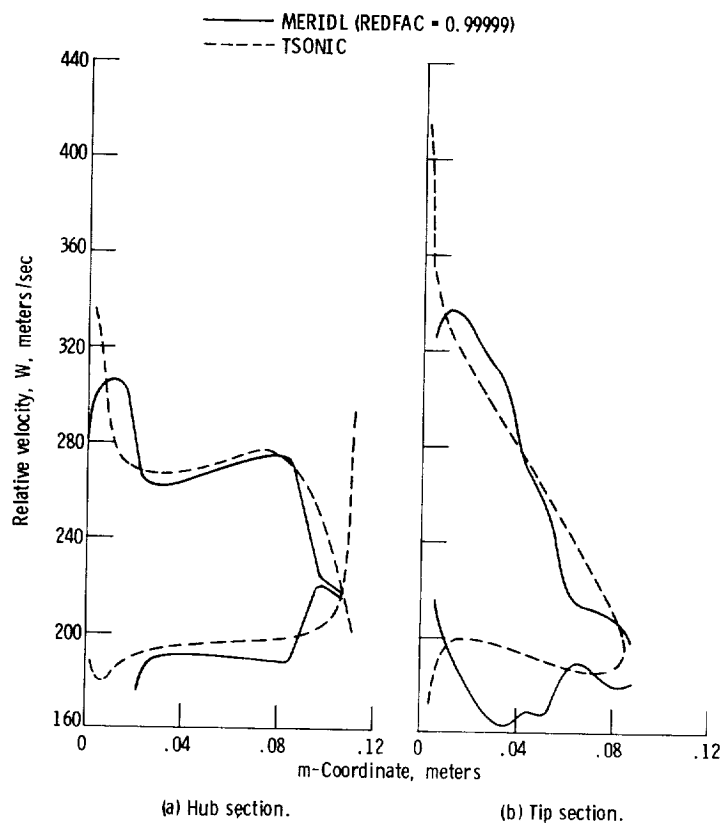


Figure 16. - Blade surface velocities for axial-flow compressor example.

gradient to finite-difference results than that presented previously for the MERIDL program in reference 4. The two different velocity-gradient solutions are likewise now in much better agreement.

Figure 16 shows a comparison of blade surface velocities estimated from the MERIDL program (appendix G) and calculated from the TSONIC program (ref. 3). The TSONIC velocities are more accurate for the design blade shape.

Lewis Research Center,  
 National Aeronautics and Space Administration,  
 Cleveland, Ohio, July 28, 1976,  
 505-04.

## APPENDIX A

### GOVERNING EQUATIONS

The cylindrical coordinate system is shown in figure 4. However, the solution is obtained on an orthogonal mesh, as illustrated in figure 3. The variables  $s$  and  $t$  are used to denote distance along the streamwise and normal orthogonals, respectively.

For subsonic solution, the stream function is used. In appendix B we obtain the stream-function differential equation derived from the assumptions given in the section METHOD OF ANALYSIS:

$$\begin{aligned} \frac{\partial^2 u}{\partial s^2} + \frac{\partial^2 u}{\partial t^2} - \frac{\partial u}{\partial s} \left( \frac{\sin \varphi}{r} + \frac{1}{B} \frac{\partial B}{\partial s} + \frac{1}{\rho} \frac{\partial \rho}{\partial s} - \frac{\partial \varphi}{\partial t} \right) - \frac{\partial u}{\partial t} \left( \frac{\cos \varphi}{r} + \frac{1}{B} \frac{\partial B}{\partial t} + \frac{1}{\rho} \frac{\partial \rho}{\partial t} + \frac{\partial \varphi}{\partial s} \right) \\ + \frac{rB\rho}{wW_s} \left[ \frac{W_\theta}{r} \frac{\partial(rV_\theta)}{\partial t} + \xi W^2 + \zeta + F_t \right] = 0 \end{aligned} \quad (A1)$$

where

$$\xi = \frac{1}{2} \left( \frac{R}{C_p p''} \frac{\partial p''}{\partial t} - \frac{1}{T''} \frac{\partial T''}{\partial t} \right) \quad (A2)$$

$$\zeta = \omega^2 r \cos \varphi - \frac{RT''}{p''} \frac{\partial p''}{\partial t} \quad (A3)$$

$$F_t = \frac{\partial \theta}{\partial t} \frac{1}{\rho} \frac{\partial p}{\partial \theta} \quad (A4)$$

Equations (A1) to (A4) are derived from the hub-shroud momentum equation in appendix B. Note that all the partials in equations (A1) to (A4) are on the stream surface except for  $\partial p / \partial \theta$  in equation (A4), which is at constant  $z$  and  $r$ .

The derivatives of the stream function satisfy the equations

$$\frac{\partial u}{\partial s} = - \frac{rB\rho W_t}{w} \quad (A5)$$

$$\frac{\partial u}{\partial t} = \frac{rB\rho W_s}{w} \quad (A6)$$

For the final transonic solution the velocity-gradient method is used. The stream-line curvatures and flow angles needed for the velocity-gradient equation are obtained first from a reduced-flow, subsonic-stream-function solution.

The velocity-gradient equation is

$$dW = \left( aW + b + \frac{c}{W} + d \cos \beta \right) dt + \frac{e}{W} + Wf \quad (A7)$$

The coefficients, a, b, c, and d, are given by different expressions in the blade region, in the upstream region, and in the downstream region. These coefficients are given as follows:

Blade-region coefficients:

$$\left. \begin{aligned} a &= \frac{\cos^2 \beta \cos(\alpha - \varphi)}{r_c} - \frac{\sin^2 \beta \cos \varphi}{r} + \sin \alpha \sin \beta \cos \beta \frac{\partial \theta}{\partial t} \\ b &= \cos \beta \frac{dW}{dm} \sin(\alpha - \varphi) - 2\omega \sin \beta \cos \varphi + r \cos \beta \left( \frac{dW}{dm} \frac{\partial \theta}{\partial t} + 2\omega \sin \alpha \right) \frac{\partial \theta}{\partial t} \\ c &= 0 \\ d &= 0 \end{aligned} \right\} (A8)$$

Upstream-region coefficients:



$$\left. \begin{aligned}
a &= \frac{\cos(\alpha - \varphi)}{r_c} \\
b &= 0 \\
c &= - \left( \frac{\lambda - \omega r^2}{r^2} \right) \left[ \frac{\lambda - \omega r^2}{r_c} \cos(\alpha - \varphi) + \frac{\lambda + \omega r^2}{r} \cos \varphi \right] \\
d &= \frac{dW_m}{dm} \sin(\alpha - \varphi)
\end{aligned} \right\} \quad (A9)$$

Downstream-region coefficients:

$$\left. \begin{aligned}
a &= \frac{\cos(\alpha - \varphi)}{r_c} \\
b &= 0 \\
c &= - \left[ \frac{(rV_\theta)_o - \omega r^2}{r^2} \right] \left[ \frac{(rV_\theta)_o - \omega r^2}{r_c} \cos(\alpha - \varphi) + \frac{(rV_\theta)_o + \omega r^2}{r} \cos \varphi \right] \\
d &= \frac{dW_m}{dm} \sin(\alpha - \varphi)
\end{aligned} \right\} \quad (A10)$$

Finally, in all three regions, we have

$$\left. \begin{aligned}
e &= C_p T'_i - \omega d\lambda - C_p dT'' + \frac{RT''}{p''} dp'' \\
f &= \frac{dT''}{2T''} - \frac{R dp''}{2C_p p''}
\end{aligned} \right\} \quad (A11)$$

Equations (A7) to (A11) are derived in appendix C. Equation (A7) is solved as an initial-value problem, where the initial value of  $W$  is specified at the hub for any given  $t$ -line running from hub to tip. By finding several solutions for varying values of  $W$  at the hub, a solution satisfying continuity will be found; that is, the solution will satisfy

$$\int_0^{t_{\text{tip}}} \rho W r B \cos(\alpha - \varphi) \cos \beta \, dt = w \quad (\text{A12})$$

When equation (A7) has been solved, subject to satisfying equation (A12), for every hub-to-tip mesh line in the region, the entire velocity distribution is obtained.

The solution obtained by either the finite-difference or velocity-gradient method is for the midchannel surface between the blades. Of greater interest are the blade surface velocities. These can be estimated since the blade loading depends on the rate of change of whirl. By assuming a linear variation of velocity between blade surfaces, velocities can be calculated. In appendix G the following equation for calculating blade surface velocities is derived:

$$\left. \begin{aligned} W_l &= W_{\text{mid}} - \frac{B}{2} \cos \beta \frac{d(rV_\theta)}{dm} \\ W_{\text{tr}} &= W_{\text{mid}} + \frac{B}{2} \cos \beta \frac{d(rV_\theta)}{dm} \end{aligned} \right\} \quad (\text{A13})$$

## APPENDIX B

### DERIVATION OF STREAM-FUNCTION EQUATION

Wu derives the following radial- and axial-momentum equations (eq. (96), ref. 1) on a meridional stream surface:

$$\left. \begin{aligned} -\frac{W_\theta}{r} \frac{\partial(rV_\theta)}{\partial r} + W_z \left( \frac{\partial W_r}{\partial z} - \frac{\partial W_z}{\partial r} \right) &= -\frac{\partial I}{\partial r} + T \frac{\partial s}{\partial r} + F_r \\ -W_r \left( \frac{\partial W_r}{\partial z} - \frac{\partial W_z}{\partial r} \right) - \frac{W_\theta}{r} \frac{\partial(rV_\theta)}{\partial z} &= -\frac{\partial I}{\partial z} + T \frac{\partial s}{\partial z} + F_z \end{aligned} \right\} \quad (\text{B1})$$

The partial derivatives here all refer to the rate of change on the midchannel stream surface. Wu used a bold derivative symbol to indicate this, but it is not necessary here since we consider the equation only on the stream surface. The first equation of (B1) is the radial momentum equation and the second is the axial momentum equation.

Our flow solution is obtained by using finite-difference methods on an orthogonal mesh. The orthogonal mesh distances are  $s$  in the throughflow direction and  $t$  in the hub-tip direction. Figure 3 illustrates the  $s$  and  $t$  distances and also shows the angle  $\varphi$  between the  $s$ -direction and the axial direction. We want the momentum equation in the  $t$ -direction. This  $t$ -momentum equation will be used to derive the desired stream-function equation. The  $t$ -momentum equation is obtained by adding the  $t$ -components of the radial and the axial momentum; that is, by multiplying the first equation of (B1) by  $\cos \varphi$  and subtracting the second equation of (B1) multiplied by  $\sin \varphi$ . Also, the chain rule for a partial derivative is

$$\frac{\partial}{\partial t} = \cos \varphi \frac{\partial}{\partial r} - \sin \varphi \frac{\partial}{\partial z}$$

Therefore, the momentum equation in the  $t$ -direction can be written

$$-\frac{W_\theta}{r} \frac{\partial(rV_\theta)}{\partial t} + (W_z \cos \varphi + W_r \sin \varphi) \left( \frac{\partial W_r}{\partial z} - \frac{\partial W_z}{\partial r} \right) = -\frac{\partial I}{\partial t} + T \frac{\partial s}{\partial t} + F_t \quad (\text{B2})$$

where  $F_t$  is the t-component of the vector  $F$ , which is given by equation (97) of reference 1 as

$$F_t = - \frac{n_t}{n_\theta r \rho} \frac{\partial p}{\partial \theta} \quad (\text{B3})$$

Here  $n_t$  and  $n_\theta$  are the t- and  $\theta$ -components of the unit normal to the stream surface. Note that  $\partial p / \partial \theta$  is in the blade-to-blade direction at constant  $r$  and  $z$  and not on the stream surface as the other partials are. In the t-direction, the stream surface has an angle to the meridional plane. The tangent of this angle is  $r(\partial \theta / \partial t)$ . Hence, the components of the normal to the stream surface must satisfy

$$\frac{n_\theta}{n_t} = - \frac{1}{r \left( \frac{\partial \theta}{\partial t} \right)} \quad (\text{B4})$$

We can substitute this into equation (B3) to get

$$F_t = \frac{\partial \theta}{\partial t} \frac{1}{\rho} \frac{\partial p}{\partial \theta} \quad (\text{B5})$$

It is desired to express the t-momentum equation (B2) entirely in s- and t-components and their derivatives. First, we will use

$$W_s = W_z \cos \varphi + W_r \sin \varphi \quad (\text{B6})$$

This leaves only

$$\frac{\partial W_r}{\partial z} - \frac{\partial W_z}{\partial r}$$

in equation (B2) to be expressed in s- and t-components. For this we use

$$\left. \begin{aligned} W_r &= W_t \cos \varphi + W_s \sin \varphi \\ W_z &= W_s \cos \varphi - W_t \sin \varphi \end{aligned} \right\} \quad (\text{B7})$$

and the chain rule (noting that  $\partial s/\partial r = \sin \varphi$ , etc.)

$$\left. \begin{aligned} \frac{\partial}{\partial r} &= \sin \varphi \frac{\partial}{\partial s} + \cos \varphi \frac{\partial}{\partial t} \\ \frac{\partial}{\partial z} &= \cos \varphi \frac{\partial}{\partial s} - \sin \varphi \frac{\partial}{\partial t} \end{aligned} \right\} \quad (B8)$$

By using equations (B7) and (B8) we can express, after combining and simplifying,

$$\frac{\partial W_r}{\partial z} - \frac{\partial W_z}{\partial r} = \frac{\partial W_t}{\partial s} - \frac{\partial W_s}{\partial t} + W_s \frac{\partial \varphi}{\partial s} + W_t \frac{\partial \varphi}{\partial t} \quad (B9)$$

The desired  $t$ -momentum equation in  $s$  and  $t$  could now be given by substituting equations (B6) and (B9) into equation (B2).

It is desired to obtain the stream-function equation expressing the velocity components as partials of a stream function. This will reduce the number of unknowns in the momentum equation from two ( $W_s$  and  $W_t$ ) to one (the stream function). But it changes the equation to a second-order partial differential equation. A normalized stream function  $u$  will be used. That is,  $u$  is zero at the hub and 1 at the shroud. The value of the stream function  $u$  can be obtained by integrating along a vertical mesh line.

$$u = \frac{1}{w} \int_0^t \rho W_s r B dt$$

By differentiating this expression,

$$\frac{\partial u}{\partial t} = \frac{r B \rho}{w} W_s$$

Similarly, the stream function  $u$  can be obtained by integrating along a vertical mesh line to any given mesh point  $s_1, t_1$  and then integrating along a horizontal mesh line:

$$u = \frac{1}{w} \int_0^{t_1} \rho W_s r B dt - \frac{1}{w} \int_{s_1}^s \rho W_t r B ds$$

We can differentiate this expression with respect to  $s$  to obtain

$$\frac{\partial u}{\partial s} = - \frac{rB\rho}{w} W_t$$

Hence, the derivatives of the normalized stream function in the s- and t-directions are related to the velocity components by

$$\left. \begin{aligned} \frac{\partial u}{\partial s} &= - \frac{rB\rho}{w} W_t \\ \frac{\partial u}{\partial t} &= \frac{rB\rho}{w} W_s \end{aligned} \right\} \quad (B10)$$

The quantity  $B$  is the stream-surface thickness corresponding to the overall mass flow  $w$ . However, the variation in local stream sheet thickness is not known, so that the overall blade-to-blade spacing is used, and  $w$  is the mass flow through one blade channel.  $B$  is a function of  $z$  and  $r$ , so that we can use

$$B(z, r) = \theta_{tr}(z, r) - \theta_l(z, r) \quad (B11)$$

where  $\theta_{tr}$  and  $\theta_l$  are the  $\theta$ -coordinates of the trailing and leading blade surfaces, respectively.

By solving equation (B10) for  $W_t$  and  $W_s$  and differentiating, we obtain

$$\left. \begin{aligned} \frac{\partial W_t}{\partial s} &= - \frac{w}{rB\rho} \left[ \frac{\partial^2 u}{\partial s^2} - \frac{\partial u}{\partial s} \left( \frac{\sin \varphi}{r} + \frac{1}{B} \frac{\partial B}{\partial s} + \frac{1}{\rho} \frac{\partial \rho}{\partial s} \right) \right] \\ \frac{\partial W_s}{\partial t} &= \frac{w}{rB\rho} \left[ \frac{\partial^2 u}{\partial t^2} - \frac{\partial u}{\partial t} \left( \frac{\cos \varphi}{r} + \frac{1}{B} \frac{\partial B}{\partial t} + \frac{1}{\rho} \frac{\partial \rho}{\partial t} \right) \right] \end{aligned} \right\} \quad (B12)$$

Equations (B10) and (B12) are now substituted into equation (B9) to eliminate  $W_s$  and  $W_t$  in favor of the stream function  $u$ :

$$\frac{\partial W}{\partial z} \frac{\partial W}{\partial r} - \frac{\partial W}{\partial r} \frac{\partial W}{\partial z} = \frac{w}{rB\rho} \left[ -\frac{\partial^2 u}{\partial s^2} - \frac{\partial^2 u}{\partial t^2} + \frac{\partial u}{\partial s} \left( \frac{\sin \varphi}{r} + \frac{1}{B} \frac{\partial B}{\partial s} + \frac{1}{\rho} \frac{\partial \rho}{\partial s} - \frac{\partial \varphi}{\partial t} \right) + \frac{\partial u}{\partial t} \left( \frac{\cos \varphi}{r} + \frac{1}{B} \frac{\partial B}{\partial t} + \frac{1}{\rho} \frac{\partial \rho}{\partial t} + \frac{\partial \varphi}{\partial s} \right) \right] \quad (\text{B13})$$

Now substitute equations (B6) and (B13) into equation (B2) and rearrange to obtain

$$\frac{\partial^2 u}{\partial s^2} + \frac{\partial^2 u}{\partial t^2} - \frac{\partial u}{\partial s} \left( \frac{\sin \varphi}{r} + \frac{1}{B} \frac{\partial B}{\partial s} + \frac{1}{\rho} \frac{\partial \rho}{\partial s} - \frac{\partial \varphi}{\partial t} \right) - \frac{\partial u}{\partial t} \left( \frac{\cos \varphi}{r} + \frac{1}{B} \frac{\partial B}{\partial t} + \frac{1}{\rho} \frac{\partial \rho}{\partial t} + \frac{\partial \varphi}{\partial s} \right) + \frac{rB\rho}{wW_s} \left[ \frac{W_\theta}{r} \frac{\partial(rV_\theta)}{\partial t} - \frac{\partial I}{\partial t} + T \frac{\partial s}{\partial t} + F_t \right] = 0 \quad (\text{B14})$$

The entropy change  $dS$  can be calculated from

$$dS = C_p \frac{dT}{T} - \frac{R dp}{p}$$

Since the entropy of a particle at actual flow velocity is the same as the entropy of that particle at stagnation conditions (either absolute or relative), we can also use

$$dS = C_p \frac{dT''}{T''} - \frac{R dp''}{p''} \quad (\text{B15})$$

This takes less calculation than using static values.

The static temperature  $T$  is calculated from  $T = T'' - W^2/2C_p$ . Using this with equation (B15), since  $I = C_p T_i' - \omega\lambda$ , yields

$$-\frac{\partial I}{\partial t} + T \frac{\partial s}{\partial t} = -\frac{\partial(C_p T_i' - \omega\lambda - C_p T'')}{\partial t} - \frac{RT''}{p''} \frac{\partial p''}{\partial t} + \frac{W^2}{2} \left( \frac{R}{C_p p''} \frac{\partial p''}{\partial t} - \frac{1}{T''} \frac{\partial T''}{\partial t} \right)$$

But

$$T_i' - T'' = \frac{2\omega\lambda - (\omega r)^2}{2C_p}$$

and

$$\frac{\partial r}{\partial t} = \cos \varphi$$

so that

$$-\frac{\partial I}{\partial t} + T \frac{\partial s}{\partial t} = \omega^2 r \cos \varphi - \frac{RT''}{p''} \frac{\partial p''}{\partial t} + \frac{W^2}{2} \left( \frac{R}{C_p p''} \frac{\partial p''}{\partial t} - \frac{1}{T''} \frac{\partial T''}{\partial t} \right) \quad (\text{B16})$$

Now, substitute equation (B16) into equation (B14) to obtain

$$\begin{aligned} \frac{\partial^2 u}{\partial s^2} + \frac{\partial^2 u}{\partial t^2} - \frac{\partial u}{\partial s} \left( \frac{\sin \varphi}{r} + \frac{1}{B} \frac{\partial B}{\partial s} + \frac{1}{\rho} \frac{\partial \rho}{\partial s} - \frac{\partial \varphi}{\partial t} \right) - \frac{\partial u}{\partial t} \left( \frac{\cos \varphi}{r} + \frac{1}{B} \frac{\partial B}{\partial t} + \frac{1}{\rho} \frac{\partial \rho}{\partial t} + \frac{\partial \varphi}{\partial s} \right) \\ + \frac{rB\rho}{wW_s} \left[ \frac{W_\theta}{r} \frac{\partial(rV_\theta)}{\partial t} + \xi W^2 + \zeta + F_t \right] = 0 \end{aligned} \quad (\text{B17})$$

where

$$\xi = \frac{1}{2} \left( \frac{R}{C_p p''} \frac{\partial p''}{\partial t} - \frac{1}{T''} \frac{\partial T''}{\partial t} \right) \quad (\text{B18})$$

$$\zeta = \omega^2 r \cos \varphi - \frac{RT''}{p''} \frac{\partial p''}{\partial t} \quad (\text{B19})$$

and  $F_t$  is given by equation (B5).

In the program,  $\sin \varphi$  and  $\cos \varphi$  are stored, so that it is more convenient to calculate the partials of  $\varphi$  in equation (B17) by



$$\left. \begin{aligned} \frac{\partial \varphi}{\partial s} &= \frac{1}{\cos \varphi} \frac{\partial(\sin \varphi)}{\partial s} = -\frac{1}{\sin \varphi} \frac{\partial(\cos \varphi)}{\partial s} \\ \frac{\partial \varphi}{\partial t} &= \frac{1}{\cos \varphi} \frac{\partial(\sin \varphi)}{\partial t} = -\frac{1}{\sin \varphi} \frac{\partial(\cos \varphi)}{\partial t} \end{aligned} \right\} \quad (\text{B20})$$

Either the middle term or the right term is used, depending on whether  $\cos \varphi$  or  $\sin \varphi$  is near zero.

In equation (B17),  $F_t$  and  $\partial(rV_\theta)/\partial t$  must be calculated differently outside the blade and within the blade. Within the blade,  $\partial(rV_\theta)/\partial t$  is calculated by a finite-difference approximation using the previous iteration. For the first iteration, the partials are assumed to be zero. Outside the blade, the partials are calculated from the input whirl distribution. From the input, the whirl is specified (or can be estimated) as a function of the stream function  $u$ . Hence, upstream of the blade,

$$\frac{\partial(rV_\theta)}{\partial t} = \frac{\partial \lambda}{\partial t} = \frac{d\lambda}{du} \frac{\partial u}{\partial t} = \frac{d\lambda}{du} \frac{rB\rho W_s}{w} \quad (\text{B21})$$

Similarly, downstream of the blade,

$$\frac{\partial(rV_\theta)}{\partial t} = \frac{d(rV_\theta)_o}{du} \frac{rB\rho W_s}{w} \quad (\text{B22})$$

The  $F_t$  is caused by the hub-shroud pressure gradient induced by the blade lean. We can calculate  $F_t$  from equation (B5). The blade-to-blade pressure gradient  $\partial p/\partial \theta$  can be calculated from the blade loading by assuming constant entropy blade to blade, so that

$$dp = \rho C_p dT \quad (\text{B23})$$

Using the fact that  $T = T'' - W^2/2C_p$ , we get

$$\frac{\partial p}{\partial \theta} = -\rho W \frac{\partial W}{\partial \theta} \quad (\text{B24})$$

since  $T''$  is constant from blade to blade.

Now, substitute this in equation (B5) to get

$$F_t = -\frac{\partial \theta}{\partial t} W \frac{\partial W}{\partial \theta} \quad (\text{B25})$$

The blade-to-blade velocity gradient is calculated from  $d(rV_\theta)/dm$ , as explained in appendix G, by using equation (G2). Outside the blade, there is no blade-to-blade pressure gradient. Hence,

$$F_t = 0 \quad (\text{B26})$$

outside the blade.

## APPENDIX C

### DERIVATION OF VELOCITY-GRADIENT EQUATION

The general velocity-gradient equation is an expression for the value of the directional derivative of the relative velocity. The velocity-gradient equation is derived from Newton's three-dimensional force equation. In this program the velocity-gradient equation is used to determine the approximate velocity distribution when there is locally supersonic velocity on the meridional midchannel stream surface.

The general velocity-gradient equation can be written

$$\frac{dW}{dq} = a \frac{dr}{dq} + b \frac{dz}{dq} + c \frac{d\theta}{dq} + \frac{1}{W} \left( C_p \frac{dT_i'}{dq} - \omega \frac{d\lambda}{dq} - T \frac{dS}{dq} \right) \quad (C1)$$

where

$$\left. \begin{aligned} a &= \frac{W \cos \alpha \cos^2 \beta}{r_c} - \frac{W \sin^2 \beta}{r} + \sin \alpha \cos \beta \frac{dW_m}{dm} - 2\omega \sin \beta \\ b &= - \frac{W \cos^2 \beta \sin \alpha}{r_c} + \cos \alpha \cos \beta \frac{dW_m}{dm} \\ c &= W \sin \alpha \sin \beta \cos \beta + r \cos \beta \left( \frac{dW_\theta}{dm} + 2\omega \sin \alpha \right) \end{aligned} \right\} \quad (C2)$$

Equation (C1) is the same as equations (B13) and (B14) of reference 2 but with the additional term  $T(dS/dq)$ , to allow for variation in entropy. The entropy variation is known from the input specification of relative total-pressure-loss distribution. Entropy variation along streamlines for adiabatic flow is possible only with viscous forces. However, these forces are primarily in the streamwise direction so that it is reasonable and consistent to neglect viscous forces along the hub-shroud mesh lines.

Outside the blade row,  $c = 0$ . This follows from the fact that  $d(rV_\theta)/dm = 0$  in this region. Using this identity and the relation  $W_\theta = V_\theta - \omega r$ , we can derive the expression

$$\frac{dW_\theta}{dm} = - \frac{W_\theta + 2\omega r}{r} \sin \alpha$$

When this is substituted into the expression for  $c$ , we find that  $c = 0$ .

The general velocity-gradient equations (C1) and (C2) will be applied along vertical mesh lines in the  $t$ -direction, so that  $q = t$ . (See appendix B and fig. 3 for a description of the orthogonal mesh.) Then

$$\left. \begin{aligned} \frac{dr}{dq} &= \cos \varphi \\ \frac{dz}{dq} &= - \sin \varphi \end{aligned} \right\} \quad (C3)$$

Note that, by using equation (C3),

$$\left. \begin{aligned} \sin(\alpha - \varphi) &= \sin \alpha \frac{dr}{dq} + \cos \alpha \frac{dz}{dq} \\ \cos(\alpha - \varphi) &= \cos \alpha \frac{dr}{dq} - \sin \alpha \frac{dz}{dq} \end{aligned} \right\} \quad (C4)$$

Using equations (C3) and (C4) in equations (C1) and (C2), we can get

$$\begin{aligned} \frac{dW}{dt} &= \frac{W \cos^2 \beta \cos(\alpha - \varphi)}{r_c} + \cos \beta \frac{dW_m}{dm} \sin(\alpha - \varphi) - \left( \frac{W \sin^2 \beta}{r} + 2\omega \sin \beta \right) \\ &\quad \times \cos \varphi + c \frac{d\theta}{dt} + \frac{1}{W} \left( C_p \frac{dT'_i}{dt} - \omega \frac{d\lambda}{dt} - T \frac{dS}{dt} \right) \end{aligned} \quad (C5)$$

We can express  $T \, dS$  in terms of the relative velocity  $W$  and relative stagnation conditions. We use

$$T = T'' - \frac{W^2}{2C_p} \quad (C6)$$

By using equations (B15) and (C6), we get

$$T dS = C_p dT'' - \frac{RT''}{p''} dp'' + \frac{W^2}{C_p} \left( \frac{R dp''}{2p''} - C_p \frac{dT''}{2T''} \right) \quad (C7)$$

Now we can write the velocity-gradient equation (C5) as

$$dW = (aW + b)dt + \frac{e}{W} + Wf \quad (C8)$$

where

$$\left. \begin{aligned} a &= \frac{\cos^2 \beta \cos(\alpha - \varphi)}{r_c} - \frac{\sin^2 \beta \cos \varphi}{r} + \sin \alpha \sin \beta \cos \beta \frac{d\theta}{dt} \\ b &= \cos \beta \frac{dW_\theta}{dm} \sin(\alpha - \varphi) - 2\omega \sin \beta \cos \varphi + r \cos \beta \left( \frac{dW_\theta}{dm} + 2\omega \sin \alpha \right) \frac{d\theta}{dt} \\ e &= C_p dT_i' - \omega d\lambda - C_p dT'' + \frac{RT''}{p''} dp'' \\ f &= \frac{dT''}{2T''} - \frac{R dp''}{2C_p p''} \end{aligned} \right\} (C9)$$

Equations (C8) and (C9) can be used directly within the blade row. However, outside the blade row, the angle  $\beta$  is not known directly so that we desire to eliminate  $\beta$  in favor of  $\lambda$ ,  $r$ , and  $W$ . This can easily be done since

$$W_\theta = \frac{\lambda}{r} - \omega r$$

and

$$\sin \beta = \frac{W_\theta}{W}$$

Then  $\cos \beta$  is obtained from

$$\cos^2 \beta = 1 - \sin^2 \beta$$

Also,  $c = 0$  in equation (C2) outside the blade as was shown previously. With these substitutions, equation (C5) becomes

$$dW = \left( aW + \frac{c}{W} + d \cos \beta \right) dt + \frac{e}{W} + Wf \quad (C10)$$

where

$$\left. \begin{aligned} a &= \frac{\cos(\alpha - \varphi)}{r_c} \\ c &= - \left( \frac{\lambda - \omega r^2}{r^2} \right) \left[ \frac{\lambda - \omega r^2}{r_c} \cos(\alpha - \varphi) + \frac{\lambda + \omega r^2}{r} \cos \varphi \right] \\ d &= \frac{dW}{dm} \sin(\alpha - \varphi) \\ e &= C_p dT'_i - \omega d\lambda - C_p dT'' + \frac{RT''}{p''} dp'' \\ f &= \frac{dT''}{2T''} - \frac{R dp''}{2C_p p''} \\ \cos \beta &= \sqrt{1 - \left( \frac{\lambda - \omega r^2}{rW} \right)^2} \end{aligned} \right\} \quad (C11)$$

Downstream of the blade, outlet whirl should be used. Hence, in equation (C11),  $(rV_\theta)_o$  is used instead of  $\lambda$ . Equations (A7) to (A11) are obtained directly from equations (C8) to (C11).

## APPENDIX D

### LOSS CORRECTIONS

An approximate loss correction is made by reducing the relative ideal stagnation pressure. This loss in stagnation pressure is specified by the input at the downstream input station by specifying either the loss fraction or the stagnation pressure. These quantities may vary from hub to tip. If the outlet stagnation pressure is given as input, the fractional loss of stagnation pressure is calculated. So, in all cases, the fractional loss of stagnation pressure at the outlet input station is known from hub to tip.

For the case where the downstream stagnation pressure is given as input, the fractional loss of stagnation pressure is calculated. First, the outlet total temperature  $T'_o$  is calculated from the change in whirl along a streamline,

$$T'_o = T'_i + \frac{\omega \left[ \left( rV_{\theta} \right)_o - \lambda \right]}{C_p} \quad (D1)$$

Then the ratio of actual to ideal stagnation pressure is calculated from

$$\frac{p'_o}{\left( p'_o \right)_{\text{ideal}}} = \frac{p'_o}{p'_i} \left( \frac{T'_i}{T'_o} \right)^{\gamma / (\gamma - 1)} \quad (D2)$$

Within the blade, the loss is distributed linearly or as specified by the input, from zero at the leading edge to the fraction given or calculated at the blade trailing edge. The loss fraction is the same whether it is expressed in terms of relative or absolute stagnation pressures. That is,

$$\frac{p''}{p''_{\text{ideal}}} = \frac{p'}{p'_{\text{ideal}}} \quad (D3)$$

When this ratio is known, the density can be calculated as a function of the velocity  $W$ , as follows:



$$\rho = \rho_i^! \left( \frac{T}{T_i^!} \right)^{1/(\gamma-1)} \frac{p''}{p_{\text{ideal}}''} \quad (\text{D4})$$

where

$$T = T_i^! - \frac{W^2 + 2\omega\lambda - (\omega r)^2}{2C_p} \quad (\text{D5})$$

Equation (D4) applies the loss correction by calculating the density from the ideal density. Equation (D4) is derived as equation (B6) in reference 13. Equation (D5) is equation (3) of reference 2. The value of  $p''/p_{\text{ideal}}''$  varies at each point of the region and is recalculated with each iteration. The value of  $\rho$  is used in checking continuity by means of equation (A12).

## APPENDIX E

### DEFINING REDUCED-MASS-FLOW PROBLEM

When the midchannel stream surface has locally supersonic flow, the solution cannot be obtained directly by solving the stream-function equation (eq. (A1)). However, an approximate solution can be obtained by getting a reduced-flow solution and extending this to the full-flow solution by the velocity-gradient method. This full-flow solution depends strongly on the reduced-flow solution, so it is important to establish the conditions that will give the most suitable stream-function solution. With a reduced mass flow, if both the inlet and outlet whirl and the rotational speed are reduced in the same ratio as the mass flow, a similar flow will result. That is, the reduced-flow streamlines will have approximately the same angles and curvatures as the full-flow streamlines throughout the flow field.

Another consideration is the boundary conditions at the upstream and downstream boundaries. Again, the flow distribution will be similar to the reduced mass flow if the mass flow, inlet and outlet whirl, and rotational speed are all reduced by the same ratio.

In summary, then, for the reduced-mass-flow solution, the mass flow, inlet and outlet whirl, and rotational speed are all reduced in the same ratio. This reduction factor is specified in the input by REDFAC, as explained in the section INPUT.

## APPENDIX F

### INCIDENCE AND DEVIATION CORRECTIONS

The solution region is divided into three subregions: upstream, within the blade, and downstream. These three regions should match each other; that is, there should be no difference in the tangential momentum of a particle on either side of the lines at the leading and trailing edges. If there were zero incidence and deviation angles, this condition would be satisfied automatically by using the actual blade shape in the blade region. Since there are almost always nonzero incidence and deviation angles, the mean flow will not follow the blade surface near the leading and trailing edges. Because of this, an empirical correction is made to the blade shape near the leading and trailing edges.

The blade-shape correction is made for a distance from the leading or trailing edge. This distance varies between  $1/6$  and  $1/2$  of the blade chord, depending on solidity. The solidity is defined to be the ratio of the true blade chord along a streamline to the blade-to-blade distance. When there is a change in radius, the solidity differs at the leading and trailing edges. For calculation purposes in the program the true blade chord along an  $s$ -coordinate line is used instead of that along a streamline. For a solidity of 2 or more, the distance is  $1/6$  of the chord; and for a solidity of  $1/2$  or less, the distance is  $1/2$  of the blade chord. The distance varies linearly with solidity between these limits. The correction is made to the flow angle so that tangential momentum is continuous at the blade leading or trailing edge, and then the angle correction is linearly decreased over the prescribed distance within the blade. This correction must be made to the flow angle  $\beta$ . However, the blade shape in the stream-function equation is expressed by the partial derivatives,  $\partial\theta/\partial s$  and  $\partial\theta/\partial t$ . Therefore, with the corrected  $\beta$ , the appropriate correction is made to  $\partial\theta/\partial s$ . It is assumed that the  $s$ -coordinate is close to a streamline. Therefore, only  $\partial\theta/\partial s$  is changed, and  $\partial\theta/\partial t$  is not changed.

The free-stream flow angle is not known in advance at the blade leading edge. Therefore, an iterative procedure is used to make the blade-shape correction. On the first iteration, no blade-shape correction is made. After the first iteration, an approximate solution is obtained, and the flow angle  $\beta$  is calculated throughout the region. From the requirement of continuous tangential momentum,

$$(W_{\theta})_{fs} = (W_{\theta})_{bf}$$

From continuity,

$$\left(\rho W_m\right)_{fs} \frac{2\pi}{NBL} = \left(\rho W_m B\right)_{bf}$$

where NBL is the number of blades. Hence, since  $\tan\beta = W_\theta/W_m$ ,

$$\tan \beta_{bf} = \tan \beta_{fs} \frac{B \times NBL}{2\pi} \frac{\rho_{bf}}{\rho_{fs}} \quad (F1)$$

Equation (F1) is used to calculate  $\beta_{bf}$ . The difference  $\beta_{bf} - \beta_b$  (see fig. 12) is then varied linearly within the blade for the specified distance. We can express  $\beta$  in terms of the partials of  $\theta$  by

$$\tan \beta_{bf} = r \frac{d\theta}{dm} = r \left[ \left(\frac{\partial\theta}{\partial s}\right)_{bf} \cos(\alpha - \varphi) + \frac{\partial\theta}{\partial t} \sin(\alpha - \varphi) \right]$$

When this is solved for  $(\partial\theta/\partial s)_{bf}$ , we obtain

$$\left(\frac{\partial\theta}{\partial s}\right)_{bf} = \frac{\frac{\tan \beta_{bf}}{r} - \frac{\partial\theta}{\partial t} \sin(\alpha - \varphi)}{\cos(\alpha - \varphi)} \quad (F2)$$

Equation (F2) is used to calculate  $(\partial\theta/\partial s)_{bf}$  from the linearly varying  $\beta$  at each mesh point. The calculations for these blade-shape corrections are done by subroutine INDEV for each iteration. When REDFAC is less than 1, the final transonic calculation uses the same method to correct  $\beta$  within the blade (subroutine LINDV), but  $\partial\theta/\partial s$  is not needed.



## APPENDIX G

### BLADE SURFACE VELOCITIES AND BLADE-TO-BLADE AVERAGE DENSITIES

The blade surface velocities can be calculated once a meridional midsurface solution is obtained. The blade-to-blade velocity gradient  $\partial W/\partial \theta$  depends on  $dW_\theta/dm$ . To obtain the desired relation, we use the velocity-gradient equations (C1) and (C2). In this case,  $q = \theta$  and  $dr/d\theta = dz/d\theta = 0$ . Also, it is assumed that  $T_1$ ,  $\lambda$ , and the entropy  $S$  are constant in the blade-to-blade direction. With this, equations (C1) and (C2) become

$$\frac{\partial W}{\partial \theta} = W \sin \alpha \sin \beta \cos \beta + r \cos \beta \left( \frac{dW_\theta}{dm} + 2\omega \sin \alpha \right) \quad (G1)$$

Using the fact that  $V_\theta = W_\theta + \omega r$  and  $W_\theta = W \sin \beta$ , we can rewrite equation (G1) as

$$\frac{\partial W}{\partial \theta} = \cos \beta \frac{d(rV_\theta)}{dm} \quad (G2)$$

Since only a midchannel solution is obtained, we assume that  $\cos \beta$  and  $d(rV_\theta)/dm$  are constant from blade to blade. This means that  $W$  varies linearly from blade to blade. (This may be in considerable error near the leading or trailing edge.) With this assumption, then

$$W_{\text{mid}} = \frac{W_l + W_{\text{tr}}}{2} \quad (G3)$$

Integrating (G2) from blade to blade (from  $\theta = \theta_l$  to  $\theta = \theta_{\text{tr}}$ ) and using (G3), we obtain

$$\left. \begin{aligned} W_{\text{tr}} &= W_{\text{mid}} + \frac{B \cos \beta}{2} \frac{d(rV_\theta)}{dm} \\ W_l &= W_{\text{mid}} - \frac{B \cos \beta}{2} \frac{d(rV_\theta)}{dm} \end{aligned} \right\} \quad (G4)$$

Note that equation (G4) is very close to that developed by Stanitz (eqs. (16) and (17), ref. 16).

Equation (G4) is used in subroutine BLDVEL to obtain blade surface velocities from the midchannel meridional solution.

It is desirable to consider the blade-to-blade variation in density to satisfy continuity for the blade passage. Equation (G4) gives information we need to do this. Since the midchannel solution is considered to be representative of all meridional-plane stream surfaces, we can consider the solution to be based on average blade-to-blade conditions. This means that in equation (B10) average blade-to-blade velocity and density should be used. Equation (B10) becomes

$$\left. \begin{aligned} \frac{\partial u}{\partial s} &= -\frac{rB}{w} \left( \rho W_t \right)_{av} \\ \frac{\partial u}{\partial t} &= \frac{rB}{w} \left( \rho W_s \right)_{av} \end{aligned} \right\} \quad (G5)$$

If we use Simpson's rule to calculate the average value, we obtain

$$\left( \rho W_s \right)_{av} = \frac{\rho_l W_{s,l} + 4\rho_{mid} W_{s,mid} + \rho_{tr} W_{s,tr}}{6} \quad (G6)$$

The velocity component  $W_s$  can be expressed in terms of the velocity and flow angles by

$$W_s = W \cos \beta \cos(\alpha - \varphi) \quad (G7)$$

This relation holds also on the blade surfaces, since the flow angles are assumed to be constant in the blade-to-blade ( $\theta$ ) direction, so that

$$\left. \begin{aligned} W_{s,l} &= W_l \cos \beta \cos(\alpha - \varphi) \\ W_{s,tr} &= W_{tr} \cos \beta \cos(\alpha - \varphi) \end{aligned} \right\} \quad (G8)$$

By using equations (G3), (G4), and (G8) in equation (G6), we can express  $\left( \rho W_s \right)_{av}$  as

$$\left( \rho W_s \right)_{av} = \rho_{av} W_s + \frac{\rho_l - \rho_{tr}}{12} \cos \beta \cos(\alpha - \varphi) (W_l - W_{tr}) \quad (G9)$$

where the subscript mid is omitted from  $W_s$ , and

$$\rho_{av} = \frac{\rho_l + 4\rho_{mid} + \rho_{tr}}{6}$$

When a solution of equation (A1) is obtained, all quantities in equation (G9) can be estimated from the previous iteration, except for  $W_s$ . So we solve for  $W_s$  in equation (G9) and use equation (G5) to obtain

$$W_s = \frac{w \frac{\partial u}{\partial t}}{rB\rho_{av}} - \frac{(\rho_l - \rho_{tr}) \cos \beta \cos(\alpha - \varphi) (W_l - W_{tr})}{12\rho_{av}} \quad (G10)$$

This is the equation used in subroutine NEWRHO to calculate  $W_s$  from  $\partial u/\partial t$ . On the first iteration,  $\rho_{av} = \rho_{ideal}$  is used, and the second term is omitted. After this, the values of  $\rho_{mid}$ ,  $\rho_{tr}$ ,  $\rho_l$ ,  $W_l$ ,  $W_{tr}$ ,  $\cos \beta$ , and  $\cos(\alpha - \varphi)$  from the previous iteration are used.

In a parallel manner, we can derive the equation for  $W_t$ :

$$W_t = -\frac{w \frac{\partial u}{\partial s}}{rB\rho_{av}} - \frac{(\rho_l - \rho_{tr}) \cos \beta \sin(\alpha - \varphi) (W_l - W_{tr})}{12\rho_{av}} \quad (G11)$$

## APPENDIX H

### SYMBOLS

a	coefficient in velocity-gradient equations (A7) and (C1)
B	tangential space between blades, rad
b	coefficient in velocity-gradient equations (A7) and (C1)
$C_p$	specific heat at constant pressure, J/(kg)(K)
c	coefficient in velocity-gradient equations (A7) and (C1)
d	coefficient in velocity-gradient equation (A7)
e	coefficient in velocity-gradient equation (A7)
F	vector normal to midchannel stream surface and proportional to tangential pressure gradient, N/kg
f	coefficient in velocity-gradient equation (A7)
I	rothalpy, $C_p T_i^2 - \omega \lambda$ , meters <sup>2</sup> /sec <sup>2</sup>
i	incidence angle, rad
m	meridional streamline distance, meters
n	unit vector normal to midchannel stream surface
p	pressure, N/meter <sup>2</sup>
q	distance along an arbitrary space curve, meters
R	gas constant, J/(kg)(K)
r	radius from axis of rotation, meters
$r_c$	radius of curvature of meridional streamline, meters
S	entropy, J/(kg)(K)
s	distance along orthogonal mesh lines in throughflow direction, meters
T	temperature, K
t	distance along orthogonal mesh lines in direction across flow
u	normalized stream function
V	absolute fluid velocity, meters/sec
W	fluid velocity relative to blade, meters/sec



w	mass flow, kg/sec
z	axial coordinate, meters
$\alpha$	angle between meridional streamline and axis of rotation, rad; see fig. 4
$\beta$	angle between relative velocity vector and meridional plane, rad; see fig. 4
$\gamma$	specific-heat ratio
$\zeta$	coefficient in stream-function equation, defined in eq. (A3)
$\theta$	relative angular coordinate, rad; see fig. 4
$\lambda$	prerotation, $(rV_{\theta})_i$ , meters <sup>2</sup> /sec
$\xi$	coefficient in stream-function equation, defined in eq. (A2)
$\rho$	density, kg/meter <sup>3</sup>
$\varphi$	angle between s-distance line and axis of rotation, rad; see fig. 3
$\psi$	stream function, kg/sec
$\omega$	rotational speed, rad/sec; see fig. 4

Subscripts:

av	average blade-to-blade
b	blade
bf	blade flow
cr	critical
fs	free stream
h	hub
i	inlet
l	blade surface facing direction of positive rotation
m	component in direction of meridional streamline
mid	midchannel blade-to-blade
o	outlet
r	component in radial direction
s	component in s-direction
t	tip, or component in t-direction
tr	blade surface facing direction of negative rotation

$z$       component in axial direction  
 $\theta$       component in tangential direction

Superscripts:

'      absolute stagnation condition  
"      relative stagnation condition

## REFERENCES

1. Wu, Chung-Hua: A General Theory of Three-Dimensional Flow in Subsonic and Supersonic Turbomachines of Axial-, Radial-, and Mixed-Flow Types. NACA TN 2604, 1952.
2. Katsanis, Theodore: Use of Arbitrary Quasi-Orthogonals for Calculating Flow Distribution in the Meridional Plane of a Turbomachine. NASA TN D-2546, 1964.
3. Katsanis, Theodore: FORTRAN Program for Calculating Transonic Velocities on a Blade-to-Blade Stream Surface of a Turbomachine. NASA TN D-5427, 1969.
4. Katsanis, Theodore; and McNally, William D.: FORTRAN Program for Calculating Velocities and Streamlines on the Hub-Shroud Mid-Channel Flow Surface of an Axial- or Mixed-Flow Turbomachine. I - User's Manual. NASA TN D-7343, 1973.
5. Katsanis, Theodore; and McNally, William D.: FORTRAN Program for Calculating Velocities and Streamlines on the Hub-Shroud Mid-Channel Flow Surface of an Axial- or Mixed-Flow Turbomachine. II - Programmer's Manual. NASA TN D-7344, 1974.
6. Katsanis, Theodore; and McNally, William D.: Revised FORTRAN Program for Calculating Velocities and Streamlines on the Hub-Shroud Midchannel Stream Surface of Axial-, Radial-, or Mixed-Flow Turbomachine or Annular Duct. II - Programmer's Manual. NASA TN D-8431, 1977.
7. McNally, William D.: FORTRAN Program for Generating a Two-Dimensional Orthogonal Mesh Between Two Arbitrary Boundaries. NASA TN D-6766, 1972.
8. McCracken, Daniel D.; and Dorn, William S.: Numerical Methods and FORTRAN Programming. John Wiley & Sons, Inc., 1964.
9. Varga, Richard S.: Matrix Iterative Analysis. Prentice-Hall, Inc., 1962.
10. Shapiro, Ascher H.: The Dynamics and Thermodynamics of Compressible Fluid Flow. Vol. I, Ronald Press Co., 1953.
11. Crouse, James: Computer Program for the Definition of Transonic Axial-Flow Compressor Blade Rows. NASA TN D-7345, 1973.
12. Johnsen, Irving A.; and Bullock, Robert O., eds.: Aerodynamic Design of Axial-Flow Compressors. NASA SP-36, 1965.
13. Katsanis, Theodore: FORTRAN Program for Quasi-Three-Dimensional Calculation of Surface Velocities and Choking Flow for Turbomachine Blade Rows. NASA TN D-6177, 1971.

14. Mechtly, E. A.: The International System of Units: Physical Constants and Conversion Factors (Second Revision). NASA SP-7012, 1973.
15. Walsh, J. L.; Ahlberg, J. H.; and Nilson, E. N.: Best Approximation Properties of the Spline Fit. J. Math. Mech., vol. 11, no. 2, 1962, pp. 225-234.
16. Stanitz, John D.; and Prian, Vasily D.: A Rapid Approximate Method for Determining Velocity Distribution on Impeller Blades of Centrifugal Compressors. NACA TN 2421, 1951.







